THESIS FOR THE DEGREE OF LICENTIATE OF ENGINEERING

Random Fatigue Analysis of Container Ship Structures

Wengang Mao

CHALMERS | UNIVERSITY OF GOTHENBURG

Department of Mathematical Sciences
Division of Mathematical *Statistics*
Chalmers University of Technology and University of Gothenburg

Göteborg, Sweden 2009

Random Fatigue Analysis of Container Ship Structures

Wengang Mao

ISSN 1652-9715 /NO 2009:22

Department of Mathematical Sciences
Division of Mathematical Statistics
Chalmers University of Technology and University of Gothenburg
SE-412 96 Göteborg, Sweden
Telephone: +46 (0) 31 772 1000

Author e-mail: wengang@chalmers.se

Printed in Göteborg, Sweden, 2009

Random Fatigue Analysis of Container Ship Structures

Wengang Mao

Department of Mathematical Sciences
Division of Mathematical Statistics
Chalmers University of Technology and University of Gothenburg

Abstract

The work presented in this thesis concerns the fatigue estimation model and the corresponding uncertainties for container vessels based on both onboard measurement and theoretical analysis. The fatigue model developed is based on the generalized narrow band approximation, where the significant response height is shown to have a linear relation with the corresponding significant wave height H_s, and the zero up-crossing response frequency, f_z, is represented by the encountered wave frequency also in terms of H_s. It is then validated by the measurement from the onboard hull monitoring system of a 2800 TEU container vessel operated in the North Atlantic. Considering that the model is strongly dependent on the H_s, we also calibrated the H_s measurement from onboard system using different types of satellite measurement. It shows that there is about a 25% overestimation from the onboard measurement system, which coincided well with the captain's report. Based on such calibration, the fatigue model is then improved with a less than 10% bias with regard to the "accurate" rainflow estimation for all 14 voyages measured during 2008.

The uncertainty in using the proposed fatigue model, as well as the other general uncertainty sources, i.e. S-N curve, failure criterion, etc, is investigated through the so called safety index. In the computation of such an index, the variation coefficient for the accumulated damage is required. Firstly, the expected fatigue damage and its coefficient of variation are estimated from measured stresses referred to above. Secondly, when suitable stress measurements are not available, these are computed from models for damage accumulation and sea states variability. The space time variability of significant wave height is modeled as a lognormal field with parameters estimated from the satellite measurements. The proposed methods for estimating uncertainties in the damage accumulation process are finally validated using the onboard time series of stresses measurement of the same voyages during 2008, as described above.

Keywords: RAOs, rainflow counting, narrow band approximation, zero up-crossing response frequency, significant wave height, ship structure response, S-N curve, spatio-temporal model, safety index.

Acknowledgements

When I sit here looking back the whole process of writing this thesis, there are a lot people that immediately come into my mind. It is your nice guidance, encouragement and company that makes the thesis look like what it is now.

First of all, I would like to express my utmost gratitude to my supervisor Igor Rychlik for giving me this opportunity and helping me further continue this interesting research topic. Your inspiring, experience and intelligence are extremely beneficial to my research here. I have never felt so confident about my research, since I know you are always walking with me and sharing your creative mind with me. I am very proud of being one of your students. Beside the scientific guidance, your encouragement and care about my life also makes my stay in Sweden full of warmth. Also, many thanks for your positive company in the early morning flights to many meetings. Thank you!

My next sincere appreciation goes to my associate advisor Jonas Ringsberg; you should know I am very grateful for your beneficial discussions, being the co-author of appended papers and working with all the contents in this thesis. Whenever I encounter any problems, not only on the research but also in my daily life, you are the person who can always encourage me and supply the most immediate help. Thank you my dear friend! I also want to thank my co-advisor Gaute Storhaug, for sharing the practical engineering ideas, and setting up this PhD project. Grateful acknowledgement is also made to the EU SEAMOCS fund for supporting my PhD studies in Sweden.

I would like to thank all my colleagues in the Department of Mathematical Sciences, Thomas, Anastassia, Frank, Ottmar, Emilio, Oscar, Daniel, Fardin… for nice chats and communications with different kinds of topics, as well as my friends in the other department: Zhiyuan, Per, Martin… Also I thank all the administrators in the department; your work makes my studying here more convenient.

Finally, I want to show my gratitude towards my family, specially my dear Tiantian, for your enduring support and love, as well as your appropriate encouragement and push that made me full of energy.

Göteborg, April, 2009

Wengang Mao

List of Papers

The licentiate thesis includes the following papers.

Paper I. **Mao, W.**, Ringsberg, J.W., Rychlik, I. and Storhaug, G., (2009). "Comparison between a Fatigue Model for Voyage Planning and Measurements of a Container Vessel". 28th International Conference on Ocean, Offshore and Arctic Engineering, in Hawaii USA, 31st May to 5th June, 2009.

Paper II. **Mao, W.**, Ringsberg, J.W., Rychlik, I. and Storhaug, G., (2009). "Estimation of Fatigue Damage Accumulation in Ships during Variable Sea State Conditions". *Submitted.*

Paper III. **Mao, W.**, Rychlik, I. and Storhaug, G., (2009). "Safety index of fatigue failure for ship structure details". *Submitted.*

Contents

Appended Papers

1 Introduction

In materials science, fatigue is the progressive and localized structural damage that occurs when a material is subjected to cyclic loading. Fatigue failure can happen when the maximum stress value is less than the ultimate tensile stress limit or possibly even below the yield stress limit. The accidents caused by fatigue failure have been documented and researched for over 150 years, but the unexpected failures are still occurring for different engineering structures. Fatigue damage is a stochastic accumulation process that results in considerable variability in the durability of all structures and components. Sources of this variability include geometry, size of the structure, surface smoothness, surface coating, residual stress, material grain size and defects and manufacturing processes. Further, the nature of the load process is also an important factor. The complex dependence between these factors and fatigue life makes predictions uncertain and even for controlled laboratory experiments the results from fatigue life tests exhibit a considerable scatter.

1.1 Fatigue problems of commercial vessels

The ocean-going commercial vessels, mainly composed of steel beam and plate, can be assumed to be of a simple rigid/flexible hull beam model. As a ship moves along the waves, the wave induced stress can result in the center of the ship keel bending upwards and downwards, known as hogging and sagging, respectively, shown in Fig. 1.1. The dynamic hogging is caused due to the fact that the crest of the wave is amidships. Otherwise, when the trough of the wave is amidships sagging will occur. When the vessel is operated in the ocean, the interlaced hogging and sagging will lead to vibrations of the ship structure. In such situations, the stresses acting on the ship structural details vary in time (dynamic stress), which may cause fatigue problems. Modern commercial vessels are, almost without exception, built of steel (often the high tensile strength steel) using welding technology. Hence, fatigue problems due to the wave induced ship vibration become more and more serious in ship industry. They may destroy the integrity of the ship structure, which results in fatigue failure. (Note, the vibrations caused by hull, machinery and cargo loading are not within the scope of this thesis.) As the development of marine technology makes it possible to construct much larger ships and they can survive (ultimate strength is enough) encountering even more severe ocean environment, as well as optimized ship structures, the fatigue problems become an increasingly important issue for both industry and research.

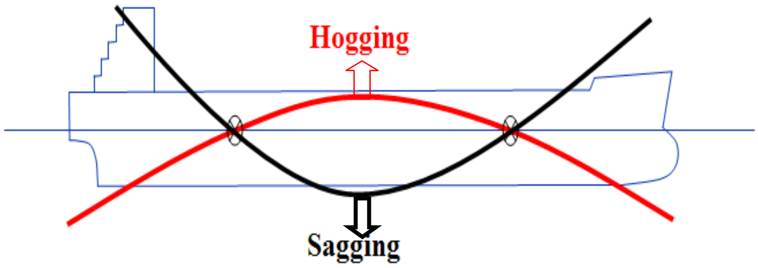

Figure 1.1, Vertical 2-node vibration of ship structure

Furthermore, every year large numbers of new ships are launched into the shipping market, which makes current shipping traffic so crowded that some of them have to change their original ship routes. On the other hand, when global economy slowdown hits the shipping market, some vessels may be adjusted to operate in the flexible routes. Sometimes these ships may be chosen to operate in a more severe sea climate. Hence, the fatigue damage accumulation rate increases much higher than designed, which results in a considerable ship service time decrease. Especially for the ships operated in the North Atlantic, which is considered as being one of the worst areas with respect to wave loading, fatigue cracks in vessels are found much earlier than elsewhere, seen *Moe et al. (2005)* and *Storhaug et al. (2007).*

Figure 1.2, Fatigue cracks found in one vessel after only 5 years service

In Fig. 1.2, some fatigue cracks are observed in the vessel after only 5 years of service (In general the ship design life is about 20 - 25 years). These fatigue problems cause great threats to ship safety. As a consequence, special attention is paid to the risk and safety margin of vessels operating in the North Atlantic. For ship owners and operators, the economic aspect is of equal importance as safety, and their concern about ship fatigue is related to maintenance, repair costs and reputation.

1.2 General fatigue estimation methods

The micro physical mechanism of the material fatigue was known about 100 years ago, first demonstrated by *Ewing (1899)* with the invention of the atomic force microscope. There are already some general methods available for estimating the fatigue damage due to variable loads for different structures, although there are many uncertainties also inside these models and probably these uncertainties will never disappear. Historically, the greatest attention was focused on situations that require more than 10^4 cycles to failure. In such cases, the stress is low and deformation primarily elastic, known as the high-cycle fatigue damage and mainly carried out based on the structure (material) stress. When the stress is high enough for plastic deformation to occur, the account in terms of stress is less useful and the strain in the material governs fatigue life. In such case, the fatigue model, known as the low-cycle fatigue, is usually characterized by the Coffin-Manson relation (published independently by *Coffin (1954) and Manson (1953)*). However, the stress of ship structure is mainly within material elastic range during the service period, the fatigue damage thus belonging to the high-cycle fatigue accumulation process. Therefore, we will mainly focus on the high-cycle fatigue estimation in the following sections.

1.2.1 Rainflow fatigue analysis

For high-cycle fatigue estimations, material performance is commonly characterized by the relevant *S-N curve*, also known as *Wöhler curve,* with a log-linear dependence between the number of cycles to failure *N*, and the stress cycle range *S*,

$$\log(N) = \alpha - mlog(S) + e \quad , \tag{1}$$

where parameters $\alpha > 0$ and $m \geq 1$ depend on the properties of material, structural details and the stress ratio *R*; and e is a random "error". When studying the fatigue of welded ship structures, the parameters *a, m* are usually categorized into different types based on the properties of structural details. They are derived from tests on samples of the material to be characterized (often called *coupons*) where a regular sinusoidal stress is applied by a testing machine which also counts the number of cycles to failure. This process is sometimes known as coupon testing. Each coupon test generates a point on the plot, though in some cases there is a run-out where the time to failure exceeds that which is available for the test. Analysis of fatigue data requires techniques from statistics, especially survival analysis and linear regression. The S-N curves directing the ship fatigue design are provided in the ship classification rules. Fig. 1.3 shows S-N curves used in the DNV guidelines, i.e. *DNV (2005),* for different types of ship structural details, and the magnitude of a cyclical stress range (S) vs. the logarithmic scale of cycles to failure (N).

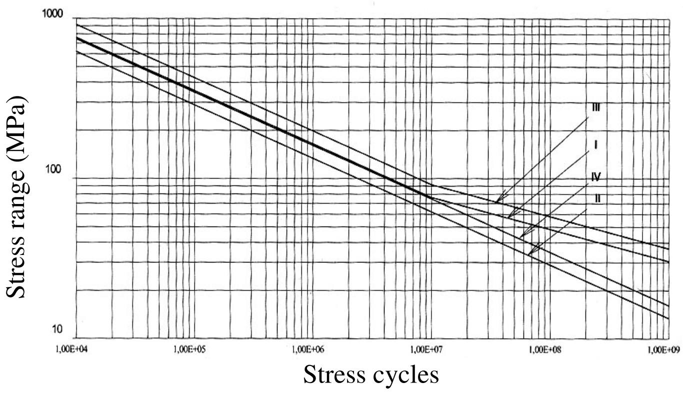

Figure 1.3, S-N curves for ship fatigue design of different types of structures (denoted as I, II, III and IV) provided in DNV guidelines.

A mechanical part is, in general, exposed to a complex, often random, sequence of loads, large and small. In order to assess the safe life of such a part, we should first reduce the complex loading to a series of simple cyclic loadings using a technique, such as rainflow cycle counting, min-max cycle counting, etc, where the former is recognized as the relatively most "accurate" approach. Then for each stress level, one calculates the degree of cumulative damage with respect to the S-N curve and combines the individual contributions using an algorithm such as the linear fatigue damage law, i.e. Palmgren–Miner's rule, or some other non-linear fatigue accumulation laws. An overview of different fatigue cumulative laws can be seen in *Fatemi and Yang (1998).* On account of the simple form of Palmgren–Miner's rule, it is widely used for engineering applications.

Rainflow cycle counting was first introduced by *Matsuishi and Endo (1968)*, and then improved for different practical applications; for further discussion, see *Rychlik (1993a)* and *ASTM (2005)*. The algorithm to get the fatigue cycles using rainflow counting, namely rainflow cycles, is carried out for the sequence of peaks and troughs. In the following, a sequence of peaks with typical stress characters, shown in Fig. 1.4, is employed to explain the rainflow counting. One can imagine, in Fig. 1.4, that the time history is a template for a rigid sheet (pagoda roof), and then one turns the sheet clockwise 90° (earliest time to the top). Each tensile peak is imagined as a source of water that "drips" down the pagoda. One counts the number of half-cycles by looking for terminations in the flow occurring when either:

- It reaches the end of the time history;
- It merges with a flow that started at an earlier tensile peak; or
- It flows opposite a tensile peak of greater magnitude.

Repeating the above steps for compressive troughs, one gets all the possible cycles. In Fig. 1.4, half-cycle (A) starts at tensile peak ① and terminates opposite a greater tensile stress, peak ②; Half-cycle (B) starts at tensile peak④ and terminates where it is interrupted by a flow from an earlier peak ③; Half-cycle (C) starts at tensile peak ⑤ and terminates at the end of the time history. One assigns a magnitude to each cycle range equal to the stress difference between its start and termination, denoted as S_i here and then pairs up these cycles of identical magnitude (but in the opposite sense) in order to count the number of corresponding cycles, denoted as N_i.

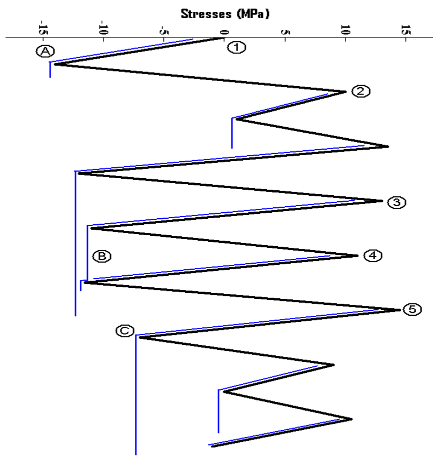

Figure 1.4, Rainflow cycle counting for tensile peaks

In this thesis, an alternative mathematical definition of the rainflow counting method given by *Rychlik (1987)* will be employed for investigation. It is possible to consider closed-form computations from the statistical properties of the load signal. For any measured stress (for example a time series of stresses), each maximum of the stress signal, v_i, is paired with one particular local minimum u_i^{rfc}. The pair, (u_i^{rfc}, v_i), is called the rainflow cycle, and the cycle stress range, $S_i = v_i - u_i^{\mathrm{rfc}}$, is then applicable for fatigue analysis. The corresponding minimum of the cycle, u_i^{rfc}, is determined as follows:

- From the i-th local maximum v_i, one determines the lowest values, u_i^{back} and

$u_i^{forward}$, respectively, in backward and forward directions between the time point of local maximum v_i, and the nearest crossing points of level v_i along the time series of stress in the left-hand plot of Fig. 1.5.

- The larger value of those two points, denoted by u_i^{rfc}, is the rainflow minimum paired with v_i, i.e. u_i^{rfc} is the least drop before reaching the value v_i again between both sides. In the situation of Fig. 1.5 (left-hand plot), $u_i^{rfc} = u_i^{forward}$.
- Thus, the i-th rainflow pair is (u_i^{rfc}, v_i), and S_i is the stress range of this rainflow cycle.

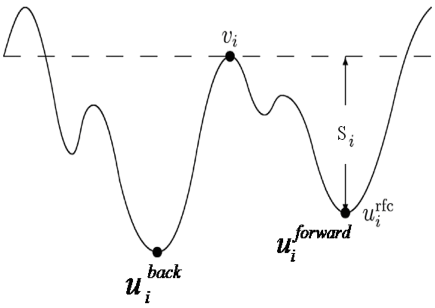

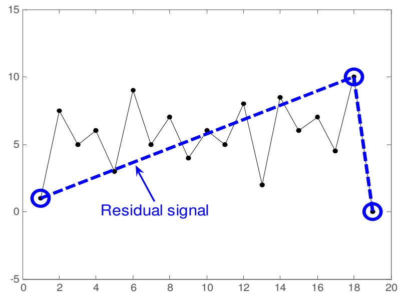

Figure 1.5: (Left): definition of a rainflow cycle; (Right): residual signal after rainflow counting

Note that for some local maxima the corresponding rainflow minima could lie outside the measured or caring load sequence. In such situations, the incomplete rainflow cycles constitute the so called residual (see the dashed lines in the right-hand plot of Fig. 1.5) and have to be handled separately. In this approach, we assume that, in the residual, the maxima form cycles with the preceding minima.

After getting all the cycles during the time period t, we can use the accumulation rule to estimate the relevant fatigue damage. In 1945, Miner popularized a rule that had first been proposed by Palmgren in 1924. The rule, alternatively called Miner's rule or the Palmgren-Miner linear damage hypothesis, states that where there are k different stress magnitudes in a spectrum, S_i $(1 \leq i \leq k)$, each contributing $n_i(S_i)$ cycles, then the fatigue damage accumulation $D(T)$ can be estimated by Eq. (2) in combination with the relevant S-N curve,

$$D(T) = \sum_i \frac{n_i \cdot S_i^m}{\alpha} \tag{2}$$

where D is experimentally found between 0.7 and 2.2 when the failure occurs, but for design purposes, D is assumed to be 1; and α ,m are the related S-N curve parameters.

1.2.2 Narrow Band Approximation

For a random load, the stress cycle range S_i is a random variable, and thus the damage *D(T)* is also a random variable. Then the related fatigue failure criterion is reformulated so that $E[D(T)] = 1$. The expected damage can be computed if the distribution of cycle ranges is known. Here, the distribution describes variability of the range of a cycle taken at random. It can be estimated if the measurement of stresses is available and computed for special classes of loads, for example the Markov or Gaussian load. However, if the distribution of the rainflow cycle range S_i in Eq. (2) cannot be found, one can use other approximations, such as the so called narrow band approximation proposed first by *Bendat (1964)*, where the expected fatigue damage during time interval *[0,T]* under the symmetric load is estimated in Eq.(3),

$$E[D^{nb}(T)] = \frac{1}{\alpha}\int_0^{+\infty} 2m(2u)^{m-1}E[N_T^+(u)]du, \tag{3}$$

where α, *m* are parameters of the relevant *S-N* curve, and $\mathrm{E}[N_T^+(\mathrm{u})]$ is the expected up-crossing number of level *u* in the time interval *[0, T]*. If the (response) stress *x(t)* is a stationary Gaussian process, then by Rice's formula, see *Rice (1944)*, the expected up-crossing intensity of level *u* ($E[N^+(u)] = E[N_T^+(u)]/T$ for stationary process), is given as follows:

$$E[N^+(u)] = \frac{1}{2\pi}\sqrt{\frac{Var(\dot{x}(0))}{Var(x(0))}}\exp\left[-\frac{u^2}{2Var(x(0))}\right] = \frac{1}{2\pi}\sqrt{\lambda_2/\lambda_0}\,\mathrm{e}^{-\frac{u^2}{2\lambda_0}}, \tag{4}$$

where λ_0 and λ_2 are, respectively, the zero and second-order spectral moments of the stress *x(t)*. If one denotes the spectrum of response stress *x(t)* as $S(\omega)$, then the corresponding spectral moments are computed as $\lambda_i = \int_0^{+\infty} \omega^i S(\omega)d\omega$. In general the response spectrum can be directly obtained through the frequency domain analysis of relevant structures, for example in the following section 1.3. Hence, the fatigue estimation model in Eq. (3) for a stationary Gaussian stress process is then represented by Eq. (5):

$$E[D^{nb}(T)] = \frac{1}{\alpha}Tf_z h_s^m 2^{-m/2}\Gamma(1 + \mathrm{m}/2), \tag{5}$$

where $\Gamma(x)$ is the gamma function, the so called significant response h_s is 4 times the standard deviation of stress $x(t)$, and the zero up-crossing response f_z as well as the significant response height h_s for a Gaussian stress process can be computed through the spectral moments of the (response) stress $x(t)$ in Eq. (6); for a detailed discussion, see *Rychlik (1993b)*,

$$h_s = 4\sqrt{\lambda_0}\ , \quad f_z = \frac{1}{2\pi}\sqrt{\lambda_2/\lambda_0} \tag{6}$$

This model in Eqs (5 and 6), also known as the Narrow Band Approximation, works quite well for the narrow band stationary Gaussian load, which is uniquely defined by its load spectrum.

However, the response process is not always stationary through the whole period *T*, such as 1 year. For such non-stationary cases, one can divide the whole process into many stationary periods of length t_i. Hence, the expected up-crossing of level u in the whole time interval $[0, T]$ is the summation of the expected up-crossing of all these stationary periods, expressed in Eq. (7),

$$E[N_T^+(u)] = \sum_i E[N_{t_i}^+(u)] = \sum_i t_i E[N_i^+(u)], \tag{7}$$

in which $N_{t_i}^+(u)$ is the up-crossing number of level u during a stationary time period of length t_i, and $\mathrm{E}[N_i^+(u)]$ is the up-crossing intensity of the same. Sometimes $E[N_T^+(u)]$ computed by this approach is not unimodal and symmetrical, hence *Bendat*'s model in Eq. (3) is not appreciated and one needs to use some other model instead, see *Rychlik (1993a)*. These problems were further discussed in *Bogsjö and Rychlik (2007)* for vehicle fatigue estimation.

For ship fatigue estimations, it is often assumed that its stress response is a stationary Gaussian process during each short period, such as one sea state lasting about 15-30 minutes. Further, $E[N_T^+(u)]$ of long period *T* for ship response can be assumed to be unimodal and symmetrical, see Papers I and II, which means that it is reasonable to sum the expected fatigue during all the stationary periods as the expected fatigue damage during the whole period *T*. And for each stationary period (assuming the Gaussian process), the up-crossing intensity can be computed by Eq. (4). Hence, the Narrow Band Approximation in Eq. (5) is then employed to compute the expected fatigue damage during such periods. This approach is also used in some commercial software, such as SESAM/Postresp, see *DNV (2004).*

With respect to the responses of practical engineering structures, they are in general not exactly narrow band Gaussian. The wide band properties of such responses make the original model too conservative. In such situations, the Narrow Band Approximation model can be improved by adding some correction factors based on the detailed structure responses. For the general wide-band stationary Gaussian processes, different methods are proposed, respectively, by *Krenk (1978)*, *Wirsching and Light (1980)*, *Gall and Hancock (1985), Zhao and Baker (1990), Larsen and Lutes (1991), Naboishikov (1991)*, etc. It should be noted that estimation by different models may be only acceptable for those specific structure responses. Therefore, the responses of practical marine structures, dependent on specific structural details, are usually divided into bimodal or trimodal spectra in a frequency domain with both Gaussian and non-Gaussian properties for fatigue estimation; for a detailed discussion, see *Jiao and Moan (1990), Benasciutti and Tovo (2005), Gao and Moan (2007)* and *(2008).*

1.3 Ship fatigue design guidelines

After several decades of investigation, there are already some guidelines available for fatigue design of ship structures from the early 1990s. In particular during the last decade, under a large amount of joint work, the state-of-the-art fatigue design guidelines for different types of vessels are published and adopted by all the big ship classification societies within the International Association of Classification Society (IACS), known as the Common Structure Rule (CSR) through the Joint Tanker Project (JTP) and Joint Bulk Project (JBP).

1.3.1 Fatigue design based on empirical formula

The guidelines for ship fatigue design are based on the S-N curve and Miner's accumulative law, the mainly interesting part in which is how to determine the distribution of stress ranges during different service periods. There are two approaches to estimate such a distribution, i.e. short-term and long-term calculation based on the so-called empirical formulas.

The stress ranges during a short-term period, for example a sea state lasting about 15-30 minutes, are often assumed to be Rayleigh distributed. Then the fatigue damage during the design period, for example 20 years, is the sum of fatigue damage during all the encountered sea states. Alternatively, one can directly define the distribution of ship stress ranges during the long-term period. Often, the Weibull distribution is fitted to the data. The shape and scale parameters of the Weibull distribution are dependent on the detailed structural details and encountered wave environments, as well as the cycle intensity during the design life for fatigue analysis.

The values of parameters of both short-term Rayleigh distribution and long-term Weibull distribution, as well as the cycle intensity, can be determined by the empirical formulas in *IACS CSR (2006)*. These empirical formulas may be a good approximation for the average fatigue estimation of all kinds of vessels, and are also simple for application during the design period. But a direct calculation based on the specific ship structures is obviously a better choice as it gives more precise predictions.

1.3.2 Fatigue design based on direct calculation

Another approach for fatigue assessment is carried out by a direct load analysis. The loads computed by direct calculation are mainly intended for use in combination with the finite element analysis. For each sea state vessel operated, the corresponding ship response will be estimated by a linear modeling, which is in general sufficient for fatigue assessment purposes. Subsequently, the fatigue damage during such a sea state is estimated by the so called Narrow Band Approximation. The fatigue accumulation during the whole service period is simply assumed to be the sum of all the encountered sea states having caused fatigue damages, which is obviously dependent on the detailed design routes.

1.3.2.1 Sea states description

One sea state, describing the wave environment in some area with about 15-30 minutes for marine engineering application, is characterized by the wave spectrum $S(\omega)$ in terms of the significant wave height H_s, and zero crossing wave period T_z. The wave spectrum obtained from wave measurement is always referred to as a short-term description of the sea. There are many different classical spectrum models to express the practical sea states for engineering applications, such as the Pierson-Moskowitz wave spectrum, which can be determined by a significant wave height H_s and zero crossing wave period T_z, proposed by *Pierson and Moskowitz (1964)* as follows,

$$S(\omega|H_s, T_z) = \frac{4\pi^3 H_s^2}{T_z^4 \omega^5} \exp\left[-\frac{1}{\pi}\left(\frac{\omega T_z}{2\pi}\right)^{-4}\right]. \tag{8}$$

It is used to describe the fully developed sea, which perhaps is the simplest wave model available for applications and also used in this thesis. However, the wave spectrum is never fully developed, and it continues to develop through non-linear wave-wave interactions even for very long times and distances. Therefore, there are also some complicated models, such as Jonswap, Ochi spectrum, etc., as seen in the *WAFO-group (2000).*

1.3.2.2 Response amplitude operators (RAOs)

As a vessel operating in such a sea state with a forward speed U_0 and heading angle β, the wave induced load can be described in a frequency domain by the response amplitude operators (RAOs), $H(\omega|U_0, \beta)$, also known as the transfer function, where for each unit amplitude regular wave ω_i, the hydrodynamic load is denoted as $H(\omega_i|U_0, \beta)$. We use the linear hydrodynamic code to compute this transfer function. It should be noted that $H(\omega_i|U_0, \beta)$ is a complex value, but here we use its absolute value instead in order to simplify description. For practical ship structures, they are in general impacted by three different hydrodynamic loads, i.e. three types of transfer functions for the vertical bending moment denoted as $H_v(\omega|U_0, \beta)$, the horizontal bending moment denoted as $H_h(\omega|U_0, \beta)$, and the torsion bending moment denoted as $H_t(\omega|U_0, \beta)$.

Based on the linear hydrodynamic theory, the transfer function of all wave induced response components can be computed by adding them together. Hence, the transfer function (RAOs) of ship structure stress response, $H_\sigma(\omega|U_0, \beta)$, can be computed by Eq. (9),

$$H_\sigma(\omega_e|U_0,\beta) = A_1 H_v(\omega_e|U_0,\beta) + A_2 H_h(\omega_e|U_0,\beta) + A_3 H_t(\omega_e|U_0,\beta). \quad (9)$$

A_i, (i = 1, 2, 3) – the structure stress caused by unit applied load,

H_v – transfer function for a vertical bending moment,

H_h – transfer function for a horizontal bending moment,

H_t – transfer function for a torsion bending moment,

U_0 – ship forward speed,

β – heading angle, i.e. angle between a ship's direction and wave moving direction.

Here, A_i, is usually computed by the finite element method based on the following two steps: first by applying the hydrodynamic load on the global ship structure model with crude elements of big size, shown in Fig.1.6 (left), to get the global response; in the following by refining the element with small size for the local structure model to consider the stress concentration factor (SCF) and getting the local stress, shown in Fig. 1.6 (right), for example; for a detailed description, see *IACS CSR (2006)* and *DNV (2005).*

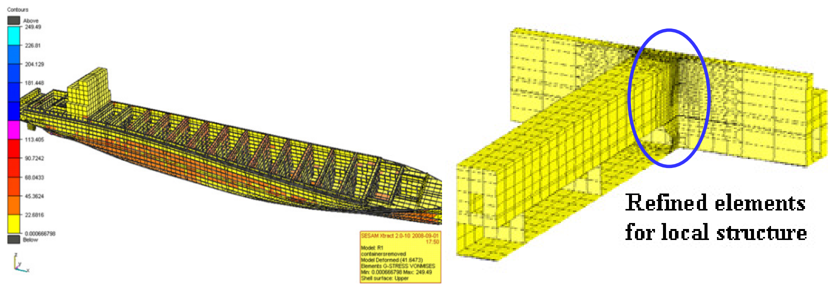

Figure 1.6, (Left): global finite element (FE) model of a container vessel; (Right): refined finite element FE model of local structure.

1.3.2.3 Structure stress response analysis

Ship structure response, described as the response spectrum S_σ, is then calculated by combining the RAOs computed above and the wave spectrum used to describe the encountered sea state as follows:

$$S_\sigma(\omega_e|U_0,\beta,H_s,T_z) = |H_\sigma(\omega_e|U_0,\beta)|^2 S(\omega_e|H_s,T_z), \quad (10)$$

where it should be noted that in Eq. (10) we should use the encountered wave spectrum $S(\omega_e|H_s,T_z)$, which also depends on the ship speed U_0 and heading angle β; for a detailed discussion, see *Lindgren, Rychlik and Prevosto (1999).*

Notes: the sea states above, for simplification, are described as the long-crested sea, but the practical sea states are usually known as the short-crested sea, which can be determined by adding some type of spreading functions to the corresponding long-crested sea. There are many literature references to model the short-crested sea; for a detailed description, see *Lewis (1989)* and *Brodtkorb at el. (2000)*. Also, when a ship operates in a severe storm, with high significant wave height, it may result in its speed reduction and then have a big influence on the stress response. However, for the preliminary investigation, its influence lies outside the scope of this thesis.

1.3.2.4 Fatigue estimation by Narrow Band Approximation

The expected fatigue damage during each of the sea states can be estimated by the Narrow Band Approximation in Eq. (5), where the spectral moments with order *n*, denoted as λ_n, can be easily calculated from ship structure response, which is written as:

$$\lambda_n = \int_0^{+\infty} |\omega + (\omega^2 U_0/g)cos\beta|^n \, H_\sigma^2(\omega|U_0,\beta)S(\omega|H_s,T_z)d\omega \tag{11}$$

The fatigue damage estimated above is the cumulative damage during each sea state. The frequency of the occurrence of different sea states (H_s, T_z) in different nautical zones can be obtained from the scatter diagram, for example *DNV (2007)*, and Pierson-Moskowitz spectrum $S(\omega|H_s,T_z)$ in Eq. (8), can be also employed to describe the sea states. When designing a ship with a specific route, one estimates the fractions f_i $(0 \le f_i \le 1)$ of the design life the ship will operate in for each of the nautical zones. Hence, the design fatigue damage is computed by adding the cumulative damages in all different nautical zones, i.e. $\sum_i f_i \cdot E[D_i]$, where $E[D_i]$ is the expected damage estimated for a ship that would sail only in the nautical zone *i* for the whole design period. Furthermore, if all the operation conditions, i.e. the encountered sea states with corresponding ship forward speed and heading angles, are recorded after the ship has been launched, we can also use them in order to estimate the accumulated fatigue damage to understand the fatigue status of different ship structures. This is also beneficial for the ship inspection in finding some tool for decreasing fatigue damage and increasing the efficiency of ship operation.

1.4 Spatio-temporal wave model

For marine engineering, the significant wave height H_s is the most important weather information used for different purposes. In order to compute the expected fatigue damage for any voyages, one needs to find the distribution of H_s at different positions and time along these voyages. Such a model $H_s(\boldsymbol{s},t)$ has been proposed and parametrically fitted using satellite and buoy data by *Baxevani et al. (2009),* where the significant wave height H_s at position $\boldsymbol{s}$ and time t is accurately modeled by means of a lognormal cumulative distribution function (cdf). Based on the satellite measurement used to model the spatial H_s model and buoys to model the temporal model, the marginal distribution over space of the random field of *log*(H_s) is fitted by estimating its mean and covariance function under some assumptions, see *Baxevani et al. (2005)*. In this model, $X_t(\boldsymbol{s})$ denotes the logarithm of H_s in the stationary Gaussian field (one sea state for example), where t represents time and $\boldsymbol{s}$ = *(s1, s2)* represents location in space. The Gaussian field $X_t(\boldsymbol{s})$ is assumed to have a mean that varies annually due to the periodicity of the climate. For the mean, it assumes the following model:

$$\mu(t) = E[X_t(\boldsymbol{s})] = \beta_0 + \beta_1 \cos(\phi t) + \beta_2 \cos(\phi t) + \alpha t \tag{12}$$

where $\phi = 2\pi / 365.2$ is chosen to give an annual cycle for time in days.

However, if the variance of the accumulated damage during a voyage is needed, the covariance between $X_{t_1}(\boldsymbol{s}_1)$ and $X_{t_2}(\boldsymbol{s}_2)$ is also needed to compute the covariance of fatigue damages between different sea states in one voyage. One example of such a model is shown in Fig. 1.7, where the left-hand plot shows the median value of H_s in February, and the right-hand plot shows the small scale correlation length in the same month. For a further description and validation of this model, see *Baxevani et al. (2007a)* and *Baxevani et al. (2009)*. Further, *Baxevani and Rychlik (2007b)* also present a simple example about how to use this model for ship fatigue estimation.

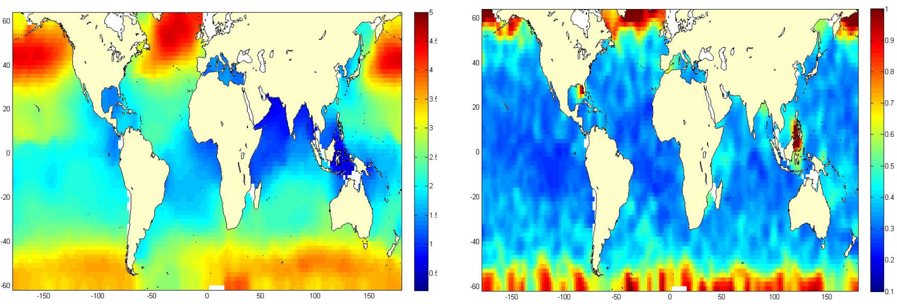

Figure 1.7, (Left): the median value of H_s (in meters) in February, (Right): the small scale correlation length in February (in degrees)

1.5 Objectives of research project and thesis

The long-term fatigue estimation guidelines for ship structure fatigue design, in *IACS CSR (2006)*, are developed mainly based on the large amount of statistical work for different types of structural details. These crude guidelines may be suitable enough for the fatigue design of some typical ship types, but sometimes are not so precise for special ships. Especially nowadays, the size of vessels becomes increasingly larger; there is an extreme lack of experience for their fatigue design, which means that the current guidelines are not applicable for those structures. More seriously, the fatigue cracks can be observed on launched ocean-going vessels with a design based on the older fatigue guidelines and with no more than only five years of service, some of them even having only one year in operation. It also demonstrates the huge uncertainties due to these fatigue guidelines. The short-term fatigue estimation, which may consider the detailed structure properties by finite element analysis, is based on the narrow band approximation. The Narrow Band Approximation model, described in Eqs (5 and 6), is developed preliminarily for the Gaussian process with a constant mean, but the practical ship structure response is often known as the non-Gaussian process. This non-Gaussian property may result in underestimation of fatigue damage from that Gaussian model.

Hence, there is an increasing demand to develop a simple but precise enough fatigue model for practical application. Currently, some vessels have installed the hull monitoring system, such as *Storhaug et al. (2007)*, in order to investigate the response characters of those ship structures under different operating conditions. These measurements can be used to calibrate the developed fatigue models. After the fatigue model is established, we can apply it for the scheduling of a ship route with minimum fatigue damage, namely routing design. Nowadays, most of the available commercial routing tools are based on the weather forecast information updated every 6 to 24 hours, and they should also be the main input of the fatigue model for considering the fatigue influence when designing the routings. This fatigue model is also applicable for the ship fatigue design, through a combination with the encountered significant wave height from the scatter diagram of the regions where vessel will be operated.

However, for all available fatigue estimation models, there are a lot of uncertainties even for the most precise approach. It also attracts a lot of attention to investigate and calibrate these uncertainties, namely fatigue reliability analysis. Through such an approach, people can describe the inputs of the fatigue model as the random variables, with specific distributions. A detailed description of the so called fatigue reliability approach is presented in *Ditlevsen and Madsen (1996)*. With regard to the fatigue problems of ship structures, the uncertainties for any different models mainly come from the material S-N curve, fatigue failure criterion and environment load. By combining the developed model with the spatio-temporal wave model, we will present a simplified safety analysis showing how the different sources of uncertainties can be combined into a safety index using a Bayesian approach with material and structural details dependent parameters modelled as random variables. We will particularly focus on the variability of the loads a ship may encounter in a specified period of time. The other types of uncertainties from the material fatigue experiments, i.e. S-N curve and fatigue failure criterion, are directly referenced from the other researches by *Johannesson, Svensson and Maré (2005a)* and *(2005b)*.

2 Summary of appended papers

2.1 Workflow

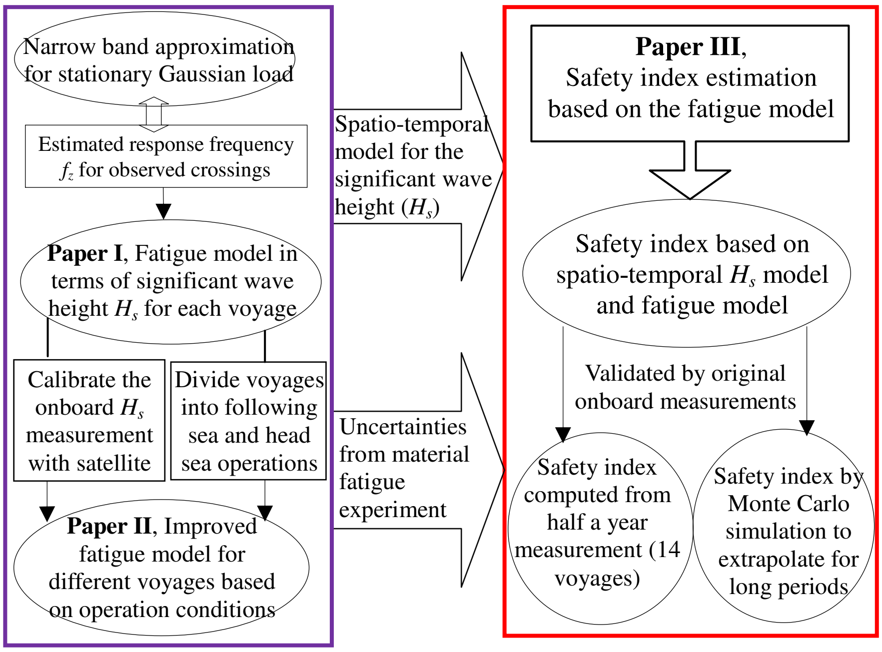

Figure 2.1, Organization of the papers

The objective of this research project was to develop a fatigue model to be used for ship routing design. Such a model should simply depend on the encountered wave environment that is available in the Operation Bridge of ocean-going commercial vessels. The validation and further improvement of such a model was then carried out by the onboard measurement, i.e. the time series of stresses and wave environments calibrated by satellite wave measurements. These were done in Papers I and II, shown in the workflow in Fig. 2.1. Consequently, in Paper III, the fatigue model was combined with variable material fatigue properties and encountered environment, i.e. spatio-temporal wave model development by *Baxevani and Rychlik (2005)*, in order to investigate the uncertainties by means of the safety index.

2.2 Fatigue model in terms of H_s (Paper I & II)

In the first two papers of this thesis, a fatigue model was developed to be able to use only the encountered significant wave height for fatigue estimation. The preliminary objective of proposing such a model is to design a ship routing with the minimum fatigue damage. It can be used to predict ship fatigue accumulation during a voyage. The formulation of the model is developed based on the Narrow Band Approximation in Eq. (3). The significant response height, h_s, is shown to have a linear relationship with its encountered significant wave height, H_s, in Eq. (14) as follows,

$$C = \frac{h_s}{H_s} = 4\sqrt{\int_0^\infty H_\sigma^2(\omega|U_0,\beta)\frac{4\pi^3}{T_z^4\omega^5}\exp\left[-\frac{1}{\pi}\left(\frac{\omega T_z}{2\pi}\right)^{-4}\right]d\omega} \quad , \tag{14}$$

where the wave spectrum is modelled by the Pierson-Moskowitz spectrum in terms of H_s and T_z, since the wave spectrum measurement in general is not available. C is thus dependent on ship forward speed U_0, heading angle β, and wave period T_z for a short-term fatigue estimation. The narrow band method in Eq. (5) can be employed for fatigue estimation if the observed up-crossings can be well modelled. For example, in Fig. 2.2, the irregular lines are the observed up-crossing numbers of measured stresses for a container vessel operated in 4 typical sea states, i.e. H_s =1.1m, 3.3m, 4.9m and 7.7m. The dash-dotted lines represent the up-crossings computed using Gaussian model for stationary stresses by means of Rice's formula, $E[N_t^+(u)] = tf_z\exp\left(-\frac{8u^2}{h_s^2}\right)$, where $t = 1800\ [s]$ for one sea state. It is easy to see that the zero up-crossing response frequency f_z for a Gaussian model in Eq. (6) is too large. This will lead to very conservative fatigue predictions, hence an alternative mean of estimating f_z was proposed. Since the value of the zero up-crossing response frequency is, in general, related to the encountered dominant wave frequency, we proposed another simple estimate for f_z, viz.

$$f_z = |1/T_z + (2\pi U_0 cos\beta)/(gT_z^2)|. \quad (15)$$

Using f_z given in Eq. (15), we estimated the expected numbers of up-crossings during the sea states, see the dashed lines in Fig. 2.2, which agree very well with the observed ones.

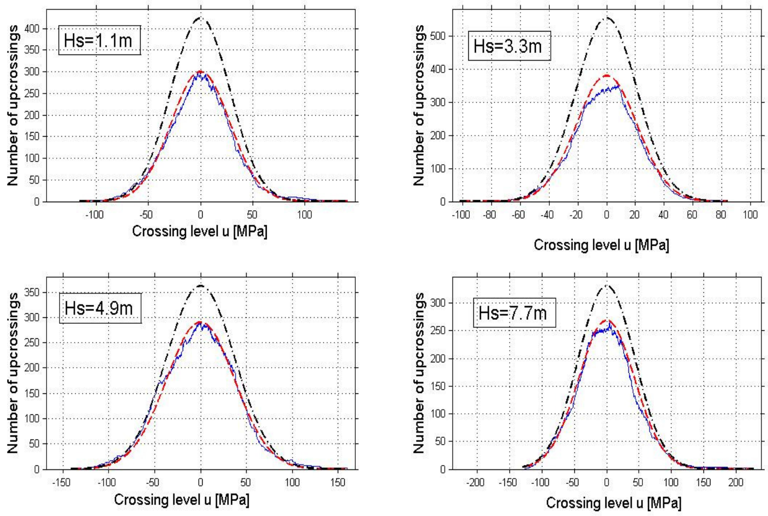

Figure 2.2, Observed numbers of up-crossing (from response measurements) during four typical sea states represented by the irregular curves, theoretical crossings based on Gaussian model represented by dash-dotted curves, and the crossings in Eq. (4) with estimated f_z instead represented by the dashed curves.

Furthermore, by investigating the properties of long-term wave statistics for the real vessel operation conditions, we divided the ship operations into two groups, i.e. following sea and head sea. Hence, the fatigue model for each operation group, based on Eq. (14) and Eq. (15), are further simplified as only dependent on encountered sea states (H_s) and the estimated structural details using the FEM model (hence it can be extended to other structural details). The capacity and accuracy of the approach is illustrated by comparison with the observed fatigue damage computed using the rainflow method for different voyages from one container vessel, operating in the North Atlantic during 2008.

The constant C defined in Eq. (14) did not agreed with the statistically estimated relation between h_s and H_s from the time series of stresses and the significant wave height from the onboard monitoring system. We investigated the reasons for the disagreement. It was reported by both the captain of the vessel and other researchers, (*Storhaug et al. (2007)*), that the waves seem to be overestimated about 20-30% by the wave measurement from the onboard system. Hence, we calibrated the onboard wave measurement using different types of satellite measurements, i.e. GFO-1, JASON-1 and ERS-2, shown in the left-hand plot of Fig. 2.3. It also indicates a 25% overestimation from the onboard system with respect to the satellite measurements shown as the thick line. In such situations, the modified constant C based on the measurements (calibrated wave measurements and time series of stress) is quite consistent with the one computed by Waveship as Eq. (14). Thus based on the wave calibration and real ship operations, the fatigue model is improved to be applied without the measurement of time series of stresses. The results from the improved fatigue model are compared with the well-known and “accurate” rainflow analysis shown in the right-hand plot of Fig. 2.3. It tells us that the discrepancy of estimations using the improved fatigue model is under 10%.

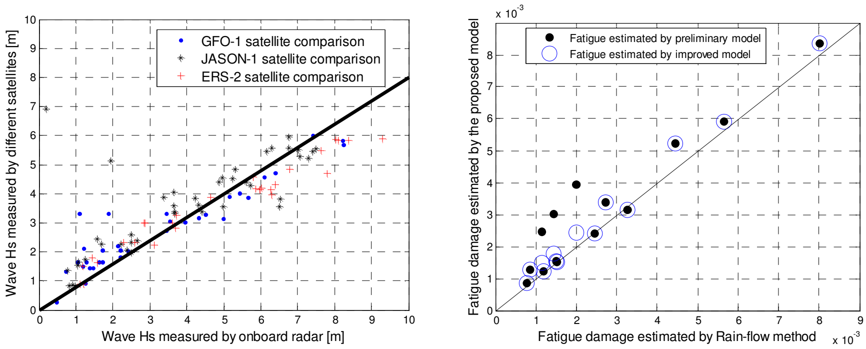

Figure 2.3, (Left): Significant wave height (H_s) measured by the onboard system, compared with H_s measured by three different satellite measurements; (Right): Fatigue damage estimated by the preliminarily proposed fatigue model (dots), and the improved model (circles) *vs.* “accurate” rainflow estimation.

2.3 Uncertainty of fatigue model (Paper III)

As it is known that the fatigue accumulation is a random process, the relevant parameters needed for fatigue estimation are random variables, such as the parameters of S-N curve, fatigue failure criterion, etc., as well as the proposed fatigue model itself. One way to assess these uncertainties in fatigue damage analysis is to use the so-called safety index. In the computation of such an index the variation coefficient for the accumulated damage is required.

In Paper III, the expected fatigue damage and its coefficient of variation is first estimated from measured stresses, which, in this paper, are obtained from the onboard monitoring system of a 2800 TEU container vessel operated in the North Atlantic. Its detailed measured passages are shown in Fig. 2.4. Secondly, when suitable stress measurements are not available these are computed from models for damage accumulation and variability of sea states. Stresses during the ship sailing period are known as the non-stationary, slowly changing, Gaussian processes and hence damage accumulation, during an encountered sea state, can be approximated by an algebraic function of significant wave height, ship speed and heading angle. Further the space time variability of the significant wave height is modelled as a lognormal field with parameters estimated from the satellite measurements. Such a spatio-temporal model can give us the expected value of H_s for specific time and location, as well as the correlation between different time and locations if needed.

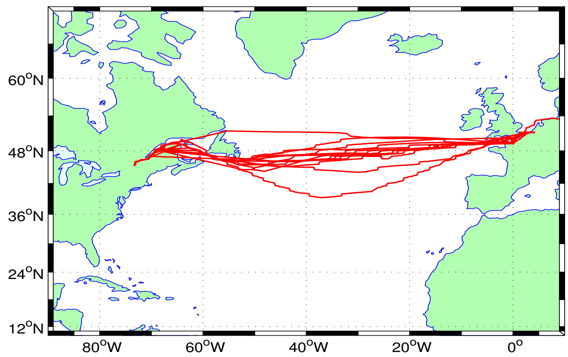

Figure 2.4, The operated routes of 14 measured voyages for the 2800TEU container ship operating in the North Atlantic during the first six months of 2008.

Finally, the proposed methods of estimating uncertainties in the damage accumulation process are validated using full scale measurements carried out for the container vessel described above. For each sea state with a specific time and location measured in Fig. 2.4, we compute the expected fatigue damage using the developed fatigue model, where the encountered expected H_s from the spatio-temporal model and the constant C (dependent on ship speed and heading angle) in the fatigue model is calculated from the hydrodynamic code Waveship. In this paper, we assume that different voyages are mutually independent. Furthermore, the uncertainty from the material fatigue experiment, i.e. S-N curve and fatigue failure criterion, is employed from the work by *Johannesson et al. (2005a and b)*. The approach seems to provide us with a very accurate approximation of the damage accumulation process. It has a clear advantage that no measurements of stresses or significant wave height are explicitly needed and could be applied to any route and ship.

3 Future work

The proposed model for the fatigue damage accumulation predicted surprisingly well with the observed damage computed using the rainflow algorithm from the measurements of stresses in some structural details of a container vessel. The model relies on the assumption that stresses vary as local stationary Gaussian processes. However, it is well known that the stresses are non-Gaussian, mainly due to whippings (and other nonlinear responses) which may increase the damage by up to 40%. This apparent contradiction needs further investigations. Possible explanations could be that the ship was operated to avoid the occurrence of whippings during the measurement period and/or that the conservatism of the narrow-band approximation is larger than the damage increase due to whippings.

Whether the model can be used for predictions of the fatigue damage for other ship details, types of routes, different operators, or other ship structures, still needs to be checked. In particular, the impact on fatigue of the non-linear responses like whippings (not included in the model) should be carefully investigated and lead, if necessary, to improvements of the proposed fatigue model. The final goal is to have a simple robust model for the fatigue damage accumulation that can be used for the construction of fatigue routing program.

3.1 Whipping contribution to fatigue

Springing is a stationary or apparently stationary resonant vibration due to oscillating wave loads and wave impacts that excite the vertical 2-node mode, sketched in the left-hand plot of Fig. 3.1. This includes nonlinear forces that may oscillate more locally, and small wave impacts due to low damping. Whipping is the detectable transient vibration due to wave impacts. A whipping vibration may be identified by the presence of higher vibration modes, but the vertical 2-node mode is normally dominant amidships, see the right-hand plot of Fig. 3.1.

The springing response of a ship structure is not so important for fatigue damage accumulation, since it does not increase so much by the stress range. But the whipping response, dependent on the pressure time history of the impact, and the natural periods of the structure, may result in a 40% increase of the stress range shown in Fig. 3.2, as seen in *Storhaug et al. (2007)*. It may contribute to large fatigue damage to the ship structure, but such a property is not accounted for when developing the present fatigue model.

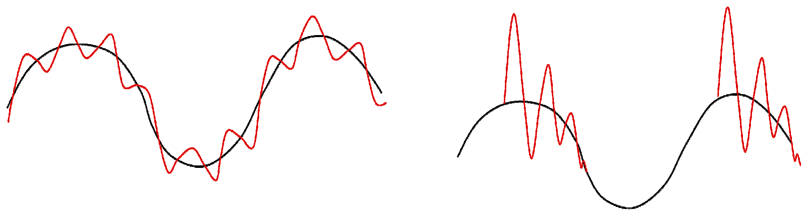

Figure 3.1, sketch of springing (left-hand plot) and whipping signal (right-hand plot)

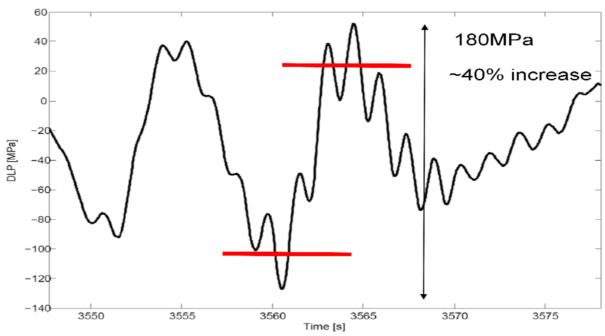

Figure 3.2, whipping contributes to the increase of stress cycle range

In order to consider the whipping contribution to fatigue damage, one needs to find an available way to distinguish it from the normal wave induced response. Furthermore, the following problems should also be clarified in order to take into account the detailed whipping influence:

✧ How to describe the fatigue effect of whipping response in mathematical form?

- ✧ What are the relationships between the whipping response and ship speed, heading angle and encountered significant wave height, respectively?
- ✧ For different sea states, how much fatigue damage is contributed by the whipping response?

3.2 Torsion and Nonlinear effects

Container ship structures are characterized by large hatch openings. Due to this structural property, they are subject to large diagonal deformations of hatch openings and warping stresses under complex torsion moments in waves. This necessitates torsion strength assessment of hull girders in container ships at their structural design stage, which is not well clarified in the main classification rules. The torsion stress becomes increasingly important, especially in the areas of transversal stiff structures, for example the bulkhead of engine room, and frames of openings, etc. The additive stress due to the torsion may also increase the fatigue damage. In order to consider the torsion contribution in the proposed fatigue model, we also need to investigate the following items:

- ✧ How to calculate the torsion induced response under specific sea states and operational conditions, i.e. ship speed and heading angle?
- ✧ How does torsion influence the fatigue damage?
- ✧ Is there a relationship between the ship operational environment and fatigue damage caused by the torsion in such an environment? What is such a relation?

For engineering applications, one can, in general, use the hydrodynamic code to compute the wave induced load, which is then applied on the ship structure Finite Element (FE) model to compute the corresponding stresses. Hence, the torsion moments can be calculated by the hydrodynamic code. It is often assumed that the linear code is enough for fatigue estimation. The proposed fatigue model in this thesis was also established, based on the linear code, i.e. Waveship using a two-dimensional strip theory, which cannot consider the torsion influence, see *DNV (2004)*. To make the fatigue estimation more precise, it is also worthwhile to validate and improve the fatigue model based on a three-dimensional nonlinear codes stress analysis.

3.3 Fatigue model for other vessels

The present fatigue model in this thesis is proposed for the container vessel, and calibrated by a 2800 TEU container ship operated in the North Atlantic. Whenever going from one port to another or back, the container vessel is, in general, fully loaded to increase efficiency. Hence it is enough to develop the fatigue model only based on one loading condition, i.e. full load condition. But for some other types of vessels, such as the bulk carriers, tankers, they are operated with many different loading conditions because of their one-directional transport and operation environment. However, it is often assumed that two loading conditions, i.e. ballast condition and full loading condition, are enough to be chosen for fatigue estimations. To make the fatigue model more widely applicable, we also need to investigate the other loading conditions for the other types of vessels. The problems needed to be analyzed are listed as followings:

- ✧ What are the parameters in the proposed model for other sizes of container vessels, e.g. 4400 TEU, or 10000 TEU?
- ✧ Is the model suitable for other types of vessels, e.g. tankers, bulk carriers?
- ✧ How does one determine the parameters in the model for other loading conditions?

4 Bibliography

ASTM E1049-85, (2005), "*Standard Practices for Cycle Counting in Fatigue Analysis*", ASTM International.

Baxevani, A., Rychlik, I. and Caires, S., (2005), "*A new method for modelling the space variability of significant wave height*", Extremes (2005) 8: 267–294

Baxevani, A., Borgel, C., and Rychlik, I. (2007a), "*Spatial models for the variability of the significant wave height on the world oceans*", Proceedings of the 16th International Offshore and Polar Engineering Conference, Lisbon, Portugal, July 1-6.

Baxevani, A., Rychlik, I. (2007b), "*Fatigue life prediction for a vessel sailing the North Atlantic route*", Probabilistic Engineering Mechanics, Volume 22, Issue 2, April 2007, Pages 159-169.

Baxevani, A., Caires, S., and Rychlik, I. (2009), "*Spatio-temporal statistical modelling of significant wave height*", *Environmetrics*; **20**: 14–31.

Benasciutti, D., and Tovo, R., 2005, "*Comparison of Spectral Methods for Fatigue Damage Assessment in Bimodal Random Process*", Proceedings of the 9th International Conference on Structural Safety and Reliability, Rome, Italy, pp. 3181-3188.

Bendat, J.S. (1964) "*Probability functions for random responses: Predictions of peaks, fatigue damage and catastrophic failures*", Technical report, NASA.

Brodtkorb, P.A., Johannesson, P., Lindgren, G., Rychlik, I. Ryden, J. And Sjö, E. (2000), "*WAFO: A matlab toolbox for analysis of random waves and loads*", ISOPE

2000, vol. 3, pp. 343-350

Bogsjö, K., and Rychlik, I., (2007), "V*ehicle Fatigue Damage Caused by Road Irregularities*", Fatigue and Fracture of Engineering Materials & Structures, In Press (LUTFMS-5067-2007).

Bouyssy, V., Naboishikov, S.M, and Rackwitz, R. (1993), "*Comparison of analytical counting methods for Gaussian processes"*. Structure Safety; 12:35–57.

Coffin, L. F. (1954), "*A study of the effects of cyclic thermal stresses on a ductile metal*", Trans, ASME, 76:931-50, 1954.

Ditlevsen, O. and Madsen, H.O. (1996), "*Structural Reliability Methods*", ISJohan Wiley & Sons Ltd, England.

DNV SESAM User Manual Postresp (2004) "*Interactive Postprocessor for General Response Analysis*" , 15th November.

DNV CN 30.7 (2005) "*Fatigue Assessment of Ship Structures, Classification Note 30.7*" July 2005.

DNV-RP-C205 (2007) "*Environmental conditions and environmental loads, Recommended Practice*", April, 2007.

Ewing, J. A. (1899), *"The Strength of Materials",* Cambridge, The University Press.

Fatemi, A. and Yang, L. (1998) "Cumulative fatigue damage and life prediction theories: a survey of the state of the art for homogeneous materials" , Int. J Fatigue Vol. 20. No. I, pp. Y-34.

Gall, D.S., and Hancock, J.W. (1985) "*Fatigue crack growth under narrow and broad band stationary loading*", Glasgow University, Marine Technology Centre.

Gao, Z., and Moan, T., 2007, "*Fatigue Damage Induced by non Gaussian Bimodal Wave Loading in Mooring Lines*", Applied Ocean Research, 29, pp. 45-54.

Gao, Z. and Moan, T. (2008) "*Frequency-domain fatigue analysis of wide-band stationary Gaussian processes using a trimodal spectral formulation*", International Journal of Fatigue, Volume 30, Issues 10-11, Pages 1944-1955

IACS CSR (2006), "*Common Structure Rule for Bulk Carriers" & "Common Structure Rule for Oil Tanker*", 15 Jan.

Jiao. G, and Moan. T., (1990) "*Probabilistic analysis of fatigue due to Gaussian load processes*", Probability Engineering Mechanics, 5(2):76–83.

Johannesson, P., Svensson, T. and Maré, J. de., (2005a), "*Fatigue life prediction based on variable amplitude tests – methodology*", International Journal of Fatigue, **27,** 954–965.

Johannesson, P., Svensson, T., and Maré, J. de., (2005b), "*Fatigue life prediction based on variable amplitude tests - specific applications*", International Journal of Fatigue, **27,** 966–973.

Krenk, S. (1978) "*A double envelope for stochastic processes*", Report No. 134, Danish Centre for Applied Mathematics and Mechanics.

Larsen, C.E., and Lutes, L.D. (1991) "*Predicting the fatigue life of offshore structures by the single-moment spectral method"*, Probab Eng Mech, 6(2):96–108.

Lewis, E.V., (1989), "*Principles of Naval Architecture: Volume III - Motions in Waves and Controllability, Society of Naval Architects and Marine Engineers*", Jersey City, NJ, USA.

Lindgren, G., Rychlik, I. and Prevosto, M. (1998), "*Stochastic Doppler shift and encountered wave period distributions in Gaussian waves*", Ocean Engineering 26: 507–518

Manson S. S, (1953) "*NACA TN 2933*", 1953.

Matsuishi, M., and Endo, T., (1968), "*Fatigue of Metals Subjected to Varying Stress*", Proceedings of the Kyushu Branch of Japan Society of Mechanics Engineering, Fukuoka, Japan, pp. 37-40.

Moe, E., Holtsmark, G., and Storhaug, G., (2005). "*Full Scale Measurements of the Wave Induced Hull Girder Vibrations of an Ore Carrier Trading in the North Atlantic*", RINA, 18-19th of October 2005, London, UK, pp. 57-85.

Naboishikov, S. (1991), "*On the distribution of local extremes, ranges and means of Gaussian processes*", Proceedings of the 4th IFIP WG 7.5 Conference, Munich 1991; p. 305–12.

Pierson, W. J., Jr., and Moskowitz, L. (1964), "*A Proposed Spectral Form for Fully Developed Wind Seas Based on the Similarity Theory of S. A. Kitaigorodskii*", J. Geophys. Res., 69(24), 5181–5190.

Rice, S. O. (1944). "*Mathematical analysis of random noise*", Bell Syst. Tech. J., **23**(3), 282–332.

Rychlik, I., (1987), "*A New Definition of the Rainflow Cycle Counting Method*", International Journal of Fatigue, 9(2), pp. 119-121.

Rychlik, I., (1993a), “*Note on cycle counts in irregular loads*”, Fatigue Frac. Engng Mater. and Struc., 377-390.

Rychlik, I., (1993b), “*On the "Narrow-band" Approximation for Expected Fatigue Damage*”, Probabilistic Engineering Mechanics, 8, pp. 1-4.

Rychlik, I., (2000), “On Some Reliability Applications of Rice's Formula for the Intensity of Level Crossings”, Extremes, 3:4, 331-348.

Storhaug, G., Moe, E., and Piedras Lopes, T.A., (2007). “*Whipping Measurements Onboard a Midsize Container Vessel Operating in the North Atlantic*”, Marintec China Proceedings (RINA, CMP and SNAME), International Symposium on Ship Design and Construction, 28-29th of November, Shanghai, China, pp. 55-70.

Wirsching, P.H., (1980) “*Light MC. Fatigue under wide-band random stresses*”, Proc ASCE J Struct Div; 106(ST7):1593–607.

WAFO-group, (2000), “*WAFO - a Matlab Toolbox for Analysis of Random Waves and Loads - A Tutorial*”, Department of Mathematical Statistics, Centre for Mathematical Sciences, Lund University, Lund, Sweden.

Zhao, W., and Baker, M.J. (1990), “*A new stress range distribution model for fatigue analysis under wave loading*”, Environmental Forces of Offshore Structures and their Prediction, Kluwer Academic Publishers. p. 271–91.

Paper I

Proceedings of the ASME 28th International Conference on Ocean, Offshore and Arctic Engineering (OMAE2009)

May 31 - June 5, 2009, Honolulu, Hawaii

OMAE2009-79235

COMPARISON BETWEEN A FATIGUE MODEL FOR VOYAGE PLANNING AND MEASUREMENTS OF A CONTAINER VESSEL

Wengang Mao
Department of Mathematical Sciences,
Chalmers University of Technology
SE-412 96 Gothenburg, Sweden

Jonas W Ringsberg
Department of Shipping and Marine Technology,
Chalmers University of Technology
SE-412 96 Gothenburg, Sweden

Igor Rychlik
Department of Mathematical Sciences,
Chalmers University of Technology
SE-412 96 Gothenburg, Sweden

Gaute Storhaug
Det Norske Veritas,
Maritime Technical Consultancy
1322 Høvik, Norway

ABSTRACT

This paper presents results from an ongoing research project which aims at developing a numerical tool for route planning of container ships. The objective with the tool is to be able to schedule a route that causes minimum fatigue damage to a vessel before it leaves port. Therefore a new simple fatigue estimation model, only using encountered significant wave height, is proposed for predicting fatigue accumulation of a vessel during a voyage. The formulation of the model is developed based on narrow-band approximation. The significant response height h_s, is shown to have a linear relationship with its encountered significant wave height H_s. The zero up-crossing response frequency f_z, is represented as the corresponding encountered wave frequency and is expressed as a function of H_s. The capacity and accuracy of the model is illustrated by application on one container vessel's fatigue damage accumulation, for different voyages, operating in the North Atlantic during 2008. For this vessel, all the necessary data needed in the fatigue model, and for verification of it, was obtained by measurements. The results from the proposed fatigue model are compared with the well-known and accurate rain-flow estimation. The conclusion is that the estimations made using the current fatigue model agree well with the rain-flow method for almost all of the voyages.

Keywords: Fatigue ship routing; rain-flow analysis; narrow-band approximation; significant response height; zero up-crossing response frequency; encountered wave frequency.

1. INTRODUCTION

The accumulation of fatigue damage in a vessel is a continuous process during the whole operational period, where the rate of damage is related to encountered sea state, ship's forward speed, heading angle and loading condition, etc. The variable encountered sea state is characterised by the significant wave height and wave period. It is the major cause of fatigue damage in ship structures. In general, the North Atlantic is considered to be one of the worst areas with respect to wave loading. Here, fatigue cracks in vessels are found earlier than elsewhere [1, 2]. As a consequence, special attention is paid to the risk and safety margin of vessels operating in the North Atlantic. For ship owners and operators, the economic aspect is of equal importance as safety, and their concern about ship fatigue is related to maintenance, repair costs and reputation. However, these fatigue-caused problems can be lowered by means of ship routing, i.e. scheduling a ship's route which causes the lowest possible fatigue damage to a vessel. There are already some routing tools commercially available. For example, WRI fleet routing is targeted to provide the time-optimised route [3]. SeaWare routing aims at predicting an intended route with minimum fuel consumption and accurate ETA (estimated time of arrival) [4], and Amarcon OCTOPUS intends to supply the response-based route by installing an onboard hull monitoring and decision support system [5], etc. Most of these routing tools are based on the weather forecast information updated every 6 to 24 hours, but fatigue problems have so far not been considered.

In this paper, we propose a new simplified fatigue estimation model, using only significant wave height H_s. This model will then be applied to develop a routing tool, which should minimize fatigue damage during ship operation from harbour to harbour. In Section 2, two different estimation methods for fatigue damage during a whole ship voyage are introduced. Section 3 presents the detailed process to develop the fatigue estimation model based on the narrow-band approximation, where the significant response height h_s and zero up-crossing frequency f_z are deduced respectively in Sections 3.1 and 3.2, and its simple application to routing is introduced in Section 3.3. Finally, in Section 4, this model is validated by the measured data from a container ship with an onboard hull monitoring system [1]. For convenience, we will not differentiate between the true value of encountered significant wave height H_s and the onboard measurement.

2. ESTIMATION OF SHIP FATIGUE DAMAGE ACCUMULATED DURING ONE VOYAGE

The fatigue damage of a vessel can be estimated based on a time domain analysis (e.g. "accurate" rain-flow analysis [6-8]), or be based on a frequency domain analysis applicable for Gaussian loads (e.g. narrow-band approximation and its extensions [9-13]). Fatigue damage in a voyage is caused by the wave induced stress responses from all sea states (30-minute intervals in this paper). In order to evaluate it, the simplest way is to sum up the fatigue damage caused by all sea states. The simple summing of the damages, accumulated during stationary periods, gives always smaller damage than the one computed for the whole signal. However, if the variability of mean stresses (between sea states) is small then the method often gives accurate results, detailed discussion see [14]. For example, the wave induced structure response, i.e. time series of stress, during one voyage is shown in Fig. 1, the stresses in one typical sea state is shown in Fig. 2 and the mean stress values of each sea state (half-hour) in this voyage are shown in Fig. 3. In Fig. 3 we can see that the mean stresses are quite constant for the sea states when damage is mainly accumulated and hence the proposed method could be used. The detailed comparison is carried out by rain-flow analysis shown in Table 1, which lists the fatigue damage in both winter and summer voyages. Here fatigue damage is estimated based on rain-flow counting through two different approaches (columns 2 and 3) considering the influence mentioned above.

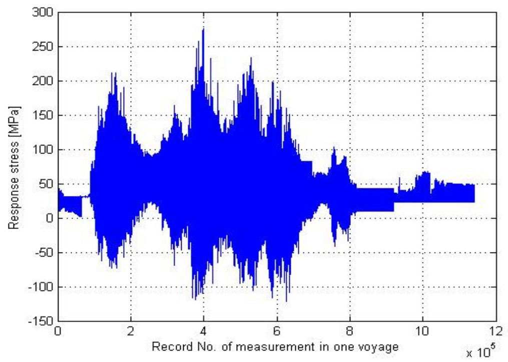

Fig. 1: Time series of stress for one whole winter voyage with large stress response, measured at the midship structure detail by a sensor relating to vertical bending-caused stress with SCF = 2.

In Table 1, the first column is the arrival time of six chosen voyages (3 in winter and 3 in summer) of a container ship operating in the North Atlantic [1]. In column 2, we use the rain-flow counting to get all cycles in one voyage based on the whole time series of stress for this voyage. In column 3, we split the time series of stress for one voyage into several parts. Each part represents the stress response for each half-hour (sea state), and then we use the same approach to get the cycles in each part, and collect all of them as the cycles in this voyage. The stress ranges directly from the above cycles in a voyage are used to compute fatigue damage, shown in columns 2 and 3, by using the Palmgren-Miner law.

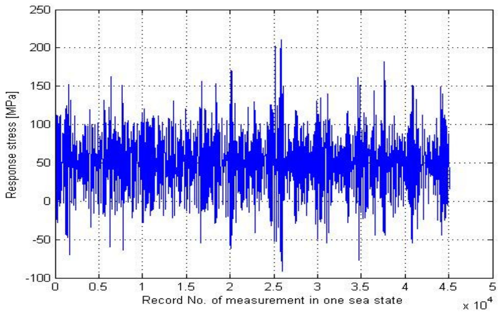

Fig. 2: Time series of stress for one typical sea state from the same measurement as Fig. 1 with SCF=2.

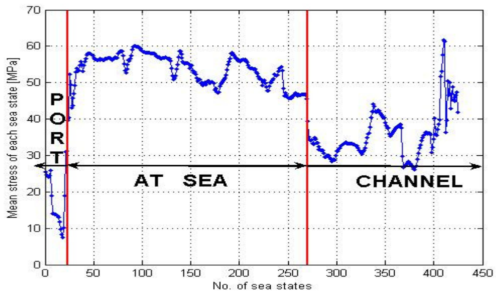

Fig. 3: Mean stress values of all different sea states during the same voyage measurement above.

It is observed that fatigue damage estimated by the two approaches in Table 1 are close to each other and the difference is less than 10%, which means it is reasonable to first estimate fatigue damage caused during all individual sea states, and then add them together as the fatigue damage during one voyage. The difference between the two approaches is mainly caused by variability of the mean stresses between the sea states. This should not be confused with "mean stress influence" which refers to the damage accumulation law for individual cycles. The narrow-band approximation used below is not taking this mean stress influence into account since the damage is a function of cycle range only. It is possible to modify the narrow-band approximation to include the more complex damage laws, see [15]. However for simplicity of presentation it is not done here.

Table 1: Fatigue damage estimated by rain-flow analysis based on different approaches.

Voyage Date	Whole voyage	Sum of all sea states
080106	0.00954	0.00936
080117	0.00163	0.00154
080129	0.00624	0.00612
080424	0.00320	0.00312
080504	0.00180	0.00177
080613	0.00169	0.00163

The fatigue damage accumulated during one sea state can be estimated assuming narrow-band approximation based on a time series of stress in Eq. (1); for a detailed discussion, see formulas (41) and (42) in the reference [16]:

$$E\left[D^{nb}(t)\right] \approx 0.47 t f_z h_s^3 / \alpha \qquad (1)$$

where f_z is the zero up-crossing response frequency, h_s is the significant response height (4 times standard deviation of the measured stress [16]) and α is the *S-N* curve parameter equal to $10^{12.76}$ and $m = 3$ refers to the inverse slope of the *S-N* curve used in this paper.

Alternatively, if the time series of stress is not available, one can also employ the frequency domain analysis to estimate fatigue damage in one sea state. First, one computes the transfer function of stress $H_\sigma(\omega|U_0, \theta)$ (frequency response function representing the response to a sinusoidal wave with a unit amplitude for different frequency ω under ship speed U_0 and heading angle θ) by a linear potential theory [12], and the encountered sea state is modelled as some type of wave spectrum $S(\omega|H_s, T_p)$ [17]. The stress response spectrum of ship structure detail is obtained by combining both of them as:

$$S_\sigma(\omega | U_0, \theta, H_s, T_p) = |H_\sigma(\omega | U_0, \theta)|^2 \cdot S(\omega | H_s, T_p) \qquad (2)$$

Finally, f_z and h_s in Eq. (1) can be calculated by spectral moments of vessel's response spectrum [12].

3. FATIGUE PREDICTION MODEL IN TERMS OF H_S

Rain-flow counting is a recognized tool for estimating fatigue damage based on a time series of stress. Frequency-domain fatigue analysis from measurement or numerical calculation is also widely applied in marine engineering [11, 12]. It can be used to predict fatigue damage by simulating the stress response under different operation environments. In this section, we will begin by investigating the narrow-band approximation, and then develop a simplified fatigue estimation model that can be applied as a model in a routing tool.

Significant response height, h_s

The significant response height h_s in Eq. (1) is expressed as 4 times the square root of the zero order spectral moment of the response spectrum [16]. The stress transfer function is dependent on the loading condition, ship forward speed U_0 and heading angle θ besides ω. Encountered sea states can be modelled as some type of wave spectrum $S(\omega|H_s, T_p)$ such as the P-M model used here. Finally, h_s is described as Eq. (3):

$$h_s = 4 \cdot \sqrt{\int_0^\infty H_\sigma^2(\omega | U_0, \theta) \frac{80\pi^4 H_s^2}{T_p^4 \omega^5} \exp\left[-\frac{5}{4} \left(\frac{\omega T_p}{2\pi} \right)^{-4} \right] d\omega} \tag{3}$$

From Eq. (3) it is observed that h_s and H_s have a linear relationship (when a linear transfer function is used), through constant C as follows:

$$C = h_s / H_s = 4 \cdot \sqrt{\int_0^\infty H_\sigma^2(\omega | U_0, \theta) \frac{80\pi^4}{T_p^4 \omega^5} \exp\left[-\frac{5}{4} \left(\frac{\omega T_p}{2\pi} \right)^{-4} \right] d\omega} \tag{4}$$

which is dependent on wave period T_p, ship forward speed U_0, and heading angle θ, as well as the loading condition.

When estimating fatigue damage accumulated during one voyage, the constant C for the whole voyage can be supposed as being only dependent on the distribution of ship speed U_0 and heading angle θ, since its loading condition is almost constant. The wave period T_p (4 to 20 seconds) of all its encountered sea states is also assumed with a fixed distribution.

Zero up-crossing response frequency

The zero up-crossing response frequency f_z of the vessel is related to the encountered wave frequency through transfer function, since the variable ship response is mainly caused by the wave induced load [17]. Initially, we presume that f_z is equal to the encountered wave frequency (assuming a constant transfer function) as:

$$f_z = 1/T_p + (2\pi U_0 \cos\theta)/(gT_p^2) \tag{5}$$

in which the wave period T_p of each sea state is evaluated as the value occurring most frequently for each h_s based on the long-term wave statistics [12], and simply described in Eq. (6):

$$T_p = 4.9\sqrt{H_s} \tag{6}$$

In Eq. (5) the zero up-crossing response frequency f_z is also dependent on the ship speed U_0 and heading angle θ, but it is less important when estimating fatigue damage in the whole voyage or for routing tool. In the model, U_0 is simplified as ship service speed, and θ equals to 0° (head sea), which may be a little conservative. Thus f_z is only determined by H_s. Finally, the new fatigue damage estimation model is expressed in Eq. (7):

$$D(T) \approx \frac{0.47TC^3}{\alpha} \cdot \left(\frac{H_s^{2.5}}{4.9} + \frac{2\pi V H_s^2}{4.9^2 g} \right) \tag{7}$$

where T is the time period of one sea state (1800 seconds here), H_s is the significant wave height during that period, V is the ship service speed and C is the constant relation between ship response h_s and H_s for each sea state discussed above.

Application in a decision support system for fatigue

It is known that most fatigue damage in one voyage is accumulated during storms with a short duration (big H_s), in which situation the vessel should be operated around a safe heading angle and the forward speed is also decreased involuntarily and voluntarily. Thus, the routing tool is needed to help the vessel operate with a minimum of fatigue damage. The proposed model in Eq. (7) can be used to estimate fatigue damage in each sea state, which is mainly dependent on the constant C. During the storm sailing period, this constant C is strongly dependent on the ship speed and heading angle, shown in Fig. 4. It can help the captain to choose suitable operation parameters with less fatigue damage (small C) under each sea state.

This model is also applicable when designing routing for the whole voyage with minimum fatigue damage. For example, a vessel is sailing in one sea state with significant wave height H_{si}. During the sea state, ship speed, heading angle and operation distance of the vessel is respectively equal to U_{0i}, θ_i and L_i. The constant C_i in the fatigue model is then determined by the operation parameters (U_{0i}, θ_i). For one sea state in a calm sea it may be large, but it can be controlled to be of relatively small value in severe sea states. Finally, the total fatigue damage for the voyage, estimated and based on Eq. (7), is then proportional to $\Sigma_i(C_i^3(H_{si}^{2.5}+H_{si}^2)L_i/U_{0i})$, which can be optimised to determine the route with a minimum of fatigue damage.

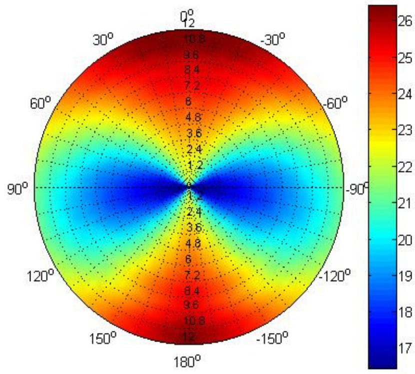

Fig. 4: Polar diagram of the constant *C* (linear relation between h_s and H_s) in terms of ship speed U_0 and heading angle *θ*, calculated by Waveship.

4. VALIDATION OF PROPOSED FATIGUE MODEL

One 2800 TEU container vessel operating between the EU and Canada is chosen for our application. Detailed dimensions and measurement locations are introduced in [1]. An onboard hull monitoring system has been installed to measure the time series of stress and encountered wave spectrum along the operation route. The measurement position chosen for our analysis here is approximately located amidships, and the stress mainly due to vertical bending measured by a strain sensor is used in this paper. The measurement considered is taken from the first half year of 2008, see Table 2.

In this paper, the numerical hydrodynamic simulation is performed by a linear strip theory program, Waveship [18], and the stress based on vertical bending is estimated by a simple ship beam model. The rain-flow analysis is carried out by WAFO [19, 20].

Before applying the narrow-band approximation to estimate the fatigue damage in the vessel, one needs to check if the vessel's response during each sea state is sufficiently stationary and Gaussian distributed. In Fig. 5, the measured stresses of 4 randomly chosen typical sea states (H_s is equal to 1.1, 3.3, 4.9 and 7.7 m, respectively) from one voyage are shown in a normal plot. They are approximately Gaussian distributed, which tells us that the narrow-band approximation is a suitable method to estimate these fatigue damages.

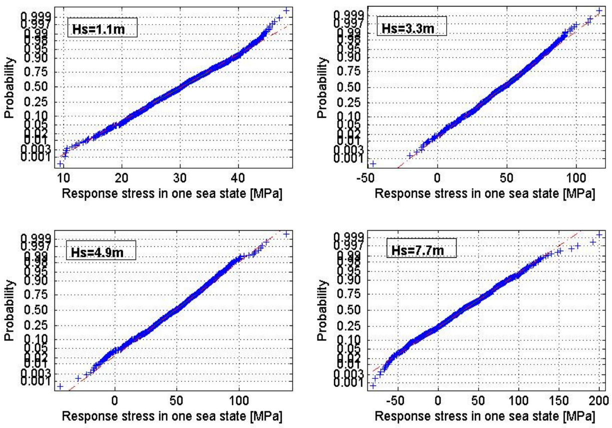

Fig. 5: Normal plot of measured stress response of 4 typical sea states in the same voyage as Fig. 1 (time interval of each sea state is half an hour).

Calculation and validation of constant C by two approaches

The constant C_i of one sea state, denoted as the linear relation between h_{si} and H_{si}, is calculated directly by Waveship [16] shown in Fig. 6. For the calculation of the constant C in Eq. (4), ship speed is assumed to be the ship service speed of 10 m/s. The encountered sea state is respectively modelled as JONSWAP with γ = 3.3 and γ = 5.0 for steep sea state, and Pierson-Moskowitz spectrum with spreading functions of $\mathrm{Cos}^2\alpha$ and $\mathrm{Cos}^8\alpha$ for the short-crested sea. Although for engineering applications, the $\mathrm{Cos}^2\alpha$ spreading function is often applied [21], one should observe that C changes greatly due to different wave spectra and spreading functions, see Fig. 6.

After getting the constant C_i for different heading angles of all encountered sea states during one voyage, we can use them to compute the constant C of the whole voyage based on the heading angle distribution of the voyage.

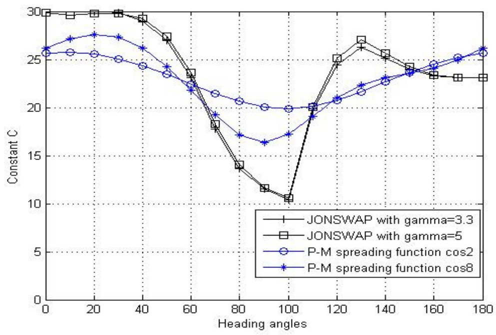

Fig. 6: The constant *C* in terms of heading angle with ship service speed *V* = 10m/s, under sea states modelled as JONSWAP with γ = 3.3 and 5.0 for steep sea state (line with pluses and squares, respectively), and P-M spectrum with spreading functions of $\mathrm{Cos}^2\alpha$ and $\mathrm{Cos}^8\alpha$ for the short-crested sea (line with circles and asterisks, respectively).

Table 2: Constant *C* calculated by least square method based on measured time series of stress for different voyages.

Voyage date	Constant C	Voyage date	Constant C
080106	18.4	080321	19.1
080117	13.9	080401	18.0
080129	17.2	080411	19.0
080209	13.2	080424	19.4
080218	20.2	080504	17.8
080301	13.8	080603	17.3
080312	16.7	080613	19.1

The constant *C* of the whole voyage can also be calculated by statistical analysis of the time series of stress. First, compute the significant response height h_{si} for all sea states with the significant wave height H_{si} during one voyage (h_{si}, H_{si}), and then we can employ the least square method to calculate the constant *C* for this voyage, which is listed in Table 2. For most voyages *C* is around 17 to 19, which is less than the one calculated from Waveship. The difference may be caused by overestimation of the wave heights measurement by wave radar. For lower wave heights, Storhaug [22] indicated a factor of 0.7 based on the comparison with buoys. If one multiplies H_{si} with 0.7, the constant *C* from measurements approaches the Waveship predicted C. It means we can use the Waveship to predict *C* also as a basis for the routing tool.

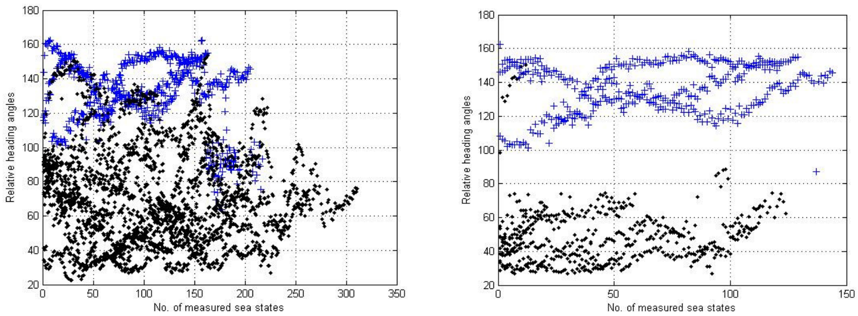

Fig. 7: (Left figure) Heading angles for all sea states of different voyages; (Right figure) heading angles for sea states $H_s \geq 5$ m of different voyages.

Note that the constant C in Table 2 for voyage 080117, 080209 and 080301 are even smaller than 19, about 13.5, which may be caused by different heading angle, obtained by measured directional wave spectrum for each sea state. If we assume the loading condition for all voyages as being fixed, the heading angle distribution of all voyages is shown in Fig. 7, where the left and right figures show a heading angle distribution for sea states with $H_s \geq 0$ m and $H_s \geq 5$ m, respectively, with the pluses representing the 3 special voyages with small constant C and dots representing the other voyages. These 3 special voyages are approximately operated in stern quartering, and the other voyages are bow quartering. Thus, from a statistical point of view, the constant C for stern quartering can be taken as 13.5 whereas 18.5 for others. This can be used for simple estimation of fatigue damage accumulated in one voyage. During bow quartering operation (i.e. the heading angle is between 30º and 60º), the estimated value of C using Waveship is between 22.5 and 27.5 for a P-M spectrum with $\mathrm{Cos}^8\alpha$ spreading. However, for stern quartering operation (i.e. the heading angle is between 100º and 140º) it is between 17 and 24, see Fig. 6. If we account for the correction factor 0.7 representing the overestimation of wave height during measurements [22], the values of C from the measurements in Table 2 agree well with the estimations using Waveship.

The comparison of the significant response height h_s from a statistical time series of stress analysis as the real response (x-axis) and our proposed model $C_i \cdot H_{sij}$ is shown in Fig. 8, where the constant C_i is constant for the same voyage, but different for different voyages based on Table 2. In Fig. 8, h_s from our model works quite well with real response results, but there are still some special cases, where the calm sea states (small measured H_s) caused a big vessel response, and measured moderate sea states caused small response, which may come from the error of wave spectrum measurement [22].

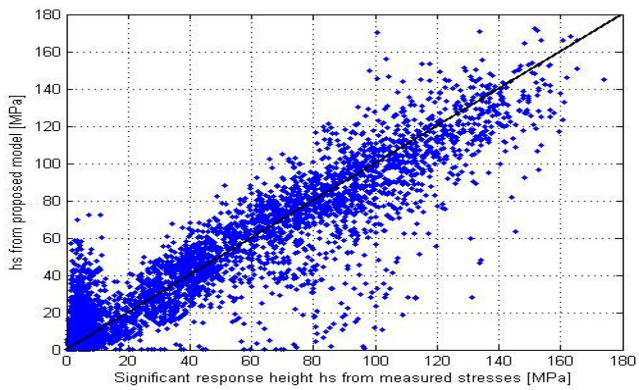

Fig. 8: Significant response height h_s calculated by statistical analysis of time series of stress (*x*-axis) and our proposed model (*y*-axis) for all measured sea states.

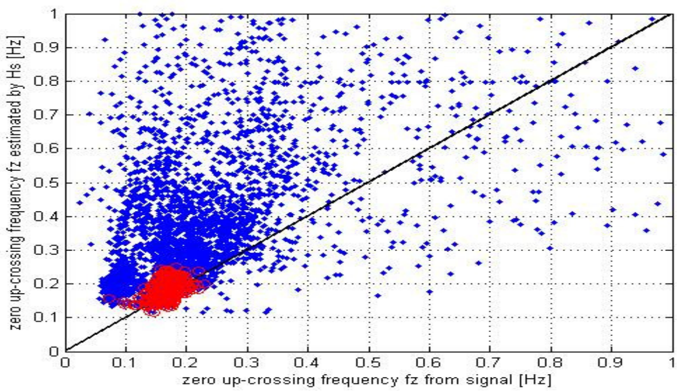

Fig. 9: Zero-crossing response frequency f_z comparison (real on the *x*-axis and our model on the *y*-axis) for all measured sea states from all voyages.

Investigation of f_z assumption

Inside our model, the zero crossing frequency f_z is expressed by a simple relation with H_s in Eqs. (5) and (6). In Fig. 9 the dots represent f_z for all measured sea states, where the *x*-axis represents a signal measurement analysis (real) and the *y*-axis is obtained from the assumption of our model. The f_z assumption inside the model is a little rough for the real condition. However, it is also somewhat reasonable for fatigue damage estimation, since their magnitude is satisfactory for the big sea states represented by the circles in Fig. 9, and most of the fatigue damage in one voyage is accumulated during the period with big sea states.

Estimation of each voyage accumulated fatigue damage

As mentioned above, the heading angle distribution during one voyage is a main factor of our proposed model for estimating the fatigue damage. In this section, all the measured voyages are divided into 2 parts: one is the voyage from the EU to Canada; the other is the opposite direction. The fatigue damage is estimated by rain-flow analysis, Waveship and our proposed model, respectively, and results are shown in Fig. 10. In Fig. 10, different voyages are separated by diamonds on a thick line, and only the sea states with both time series of stress and wave spectrum measurement are presented inside. The fatigue damage distribution of voyages from the EU to Canada is shown in the left figure, where squares, pluses and dots represent the 3 methods. The right figure presents the same results as the left figure, but for voyages from Canada to the EU. Meanwhile, the total fatigue damage caused by each voyage is listed in Table 3 for voyages from the EU to Canada, and Table 4 for voyages in the opposite direction. In order to compare with different estimation approaches, we only take into account the sea states with wave spectrum measurement for each voyage.

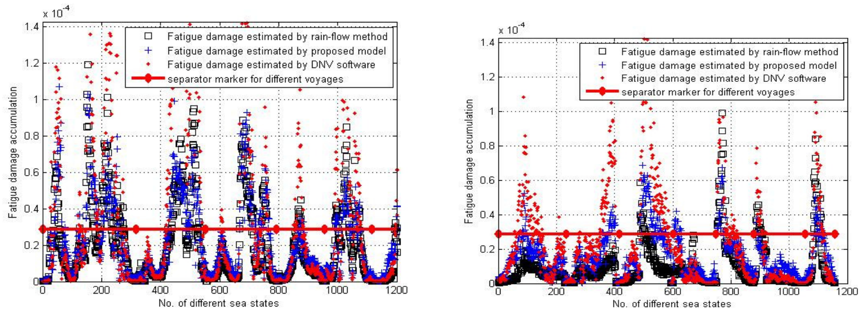

Fig. 10: (Left figure) Fatigue damage distribution of all measured voyages (the EU to Canada) estimated by the rain-flow method, Waveship and our proposed model, respectively; (Right figure) the same results as the left figure for voyages in the opposite direction.

The estimation by our proposed model is satisfactory for voyages from the EU to Canada. The pluses are close to the "accurate" evaluation represented by squares in the left figure of Fig. 10. The error of our proposed model is about 15% for the total fatigue damage caused by all voyages (from the EU to Canada). Note that the difference between our model and Waveship is related to the value of C. In our model, C is calculated by least square method using the results from the measurements of stresses and wave heights. It will eliminate the influence of overestimation of wave height measurements [22]. In Waveship, however, C is independent of H_s. As a consequence, the overestimation of wave height measurements yields that the fatigue estimation of Waveship is larger in contrast to our model.

However, the proposed model is less satisfactory for the estimation of voyages from Canada to the EU. The error of the first 3 voyages may result from the f_z assumption, which is not precise for the following sea with the constant C being approximately 13.5. There are also big errors in the fourth voyage (denoted as 080321), and we checked that this is caused by the wave spectrum measurement, since the measurement of H_s almost equals to 0 during the "storm" period with "big" response and fatigue damage. But, for the last 3 voyages, their estimations also agree well with the rain-flow analysis, and it is observed that the heading angle distribution of these voyages is about head sea with the constant C of 18 to 20.

Table 3: Total fatigue damage accumulated for different voyages (the EU to Canada).

Voyage date	RFC	Our model	Waveship
080106	0.0079	0.0086	0.0143
080129	0.0056	0.0061	0.0184
080218	0.0044	0.0057	0.0079
080312	0.0015	0.0017	0.0023
080401	0.0032	0.0032	0.0059
080424	0.0027	0.0038	0.0055
080603	0.0008	0.001	0.0014

Table 4: Total fatigue damage accumulated for different voyages (Canada to the EU).

Voyage date	RFC	Our model	Waveship
080117	0.0014	0.0033	0.0051
080209	0.0011	0.0027	0.0047
080301	0.002	0.0043	0.0078
080321	0.0008	0.0014	0.0008
080411	0.0024	0.0027	0.0044
080504	0.0012	0.0016	0.0015
080613	0.0015	0.0018	0.0025

Future improvement of our model

Although the proposed model works well for the head sea voyages, there is still room for improvement for following sea. The parameter f_z may not be good enough as seen in Fig. 9. In the future, we will investigate f_z more thoroughly. Meanwhile, the other parameter, the constant *C* of one voyage, is based on the heading angle distribution. We should establish a more detailed relation between them for use in a routing tool.

5. CONCLUSIONS

A simple model for estimating specific voyage fatigue damage is proposed based on the theory of narrow-band approximation. It is only in terms of significant wave height H_s and agrees well with the “accurate” rain-flow estimation, particularly in head sea. Inside the model, the constant *C* describing the relation between the significant response height h_s and H_s, is mainly based on the vessel’s heading angle distribution. This works satisfactorily and is validated against measurement from a 2800 TEU North Atlantic sailing container vessel. But the zero crossing response frequency f_z may need more improvements, especially for the estimation of following sea voyages.

As this preliminary model seems to be good enough for one voyage, it may be good enough also for a routing tool. For routing tool application, it can be combined with other parameters such as ship’s speed and course, in order to optimize a route for minimizing the fatigue damage. Meanwhile, this model can be used for simple estimation of fatigue damages caused during one voyage, thus the constant *C* inside this model can be approximated as 18.5 for head sea operation, and 13.5 for following sea. If provided with the heading angles along one voyage and the corresponding significant wave height, its fatigue damage can also be estimated more precisely by the model.

ACKNOWLEDGMENTS

The authors wish to acknowledge the support from EU project SEAMOCS and Gothenburg Stochastic Center and the Swedish foundation for Strategic Research through GMMC, Gothenburg Mathematical Modeling Center. Also many thanks to DNV, crews, management company and owner for providing data.

REFERENCES

[1] Storhaug, G., Moe, E., and Piedras Lopes, T.A., 2007, "Whipping Measurements Onboard a Midsize Container Vessel Operating in the North Atlantic", Marintec China Proceedings (RINA, CMP and SNAME), International Symposium on Ship Design and Construction, 28-29th of November, Shanghai, China, pp. 55-70.

[2] Moe, E., Holtsmark, G., and Storhaug, G., 2005, "Full Scale Measurements of the Wave Induced Hull Girder Vibrations of an Ore Carrier Trading in the North Atlantic", RINA, International Conference on Design and Operation of Bulk Carriers, 18-19th of October 2005, London, UK, pp. 57-85.

[3] WRI Fleet Routing, 2008-11-24, URL: http://www.wriwx.com/fleet_ routing.html.

[4] SeaWare Routing, 2008-11-24, URL: http://www.seaware.se/Routing.aspx.

[5] Amarcon Octopus, 2008-11-24, URL: http://www.amarcon.com/ products/index.html.

[6] Matsuishi, M., and Endo, T., 1968, "Fatigue of Metals Subjected to Varying Stress", Proceedings of the Kyushu Branch of Japan Society of Mechanics Engineering, Fukuoka, Japan, pp. 37-40.

[7] Rychlik, I., 1987, "A New Definition of the Rainflow Cycle Counting Method", International Journal of Fatigue, 9(2), pp. 119-121.

[8] ASTM E1049-85, 2005, "Standard Practices for Cycle Counting in Fatigue Analysis. ASTM International.

[9] Bendat, J.S., 1964, "Probability Functions for Random Responses: Prediction of Peaks", Fatigue Damage and Catastrophic Failures, NASA technical report 1964.

[10] Rychlik, I., 1993, "On the "Narrow-band" Approximation for Expected Fatigue Damage", Probabilistic Engineering Mechanics, 8, pp. 1-4.

[11] Benasciutti, D., and Tova, R., 2005, "Comparison of Spectral Methods for Fatigue Damage Assessment in Bimodal Random Process", Proceedings of the 9th International Conference on Structural Safety and Reliability, Rome, Italy, pp. 3181-3188.

[12] Det Norske Veritas, 2005, "Fatigue Assessment of Ship Structure", Classification Note No.30.7, July 2005.

[13] Gao, Z., and Moan, T., 2007, "Fatigue Damage Induced by non Gaussian Bimodal Wave Loading in Mooring Lines", Applied Ocean Research, 29, pp. 45-54.

[14] Bogsjö, K., and Rychlik, I., 2007, "Vehicle Fatigue Damage Caused by Road Irregularities", Fatigue and Fracture of Engineering Materials & Structures, In Press (LUTFMS-5067-2007).

[15] Rychlik, I., 1993, "Note on Cycle Counts in Irregular Loads". Fatigue and Fracture of Engineering Materials & Structures, 16, pp. 377-390.

[16] Bengtsson, A.K., and Rychlik, I., 2008, "Uncertainty in Fatigue Life Prediction of Structures Subject to Gaussian Loads", Probabilistic Engineering Mechanics, In Press.

[17] Lewis, E.V., 1989, Principles of Naval Architecture: Volume III - Motions in Waves and Controllability, Society of Naval Architects and Marine Engineers, Jersey City, NJ, USA.

[18] Det Norske Veritas, 1993, "Sesam User's Manual Waveship", DNV Sesam Report No.:93-7080/Rev.1, October 1993.

[19] Brodtkorb, P.A., Johannesson, P., Lindgren, G., Rychlik, I., Rydén, J., and Sjö, E., 2000, "WAFO - a Matlab Toolbox for Analysis of Random Waves and Loads", Proceedings of the 10th International Offshore and Polar Engineering Conference, Seattle, USA, Vol III, pp. 343-350.

[20] WAFO-group, 2000, "WAFO - a Matlab Toolbox for Analysis of Random Waves and Loads - A Tutorial". Department of Mathematical Statistics, Centre for Mathematical Sciences, Lund University, Lund, Sweden, 2008-11-24: URL http://www.maths.lth.se/matstat/wafo.

[21] Det Norske Veritas, 2007, "Environmental Conditions and Environmental Loads", Recommended practice DNV-RP-C205, April 2007.

[22] Storhaug, G., and Heggelund, S.E., 2008, "Measurements of Wave Induced Vibrations and Fatigue Loading Onboard Two Container Vessels Operating in Harsh Wave Environment", Proceedings of the International Conference on Design and Operation of Container Ships, 3-4th of July 2008, London, UK, pp. 81-100.

Paper II

Estimation of Fatigue Damage Accumulation in Ships during Variable Sea State Conditions

Wengang Mao,[*] **Jonas W Ringsberg,** [†] **Igor Rychlik**[*] and **Gaute Storhaug**[‡]

[*] Department of Mathematical Sciences,
Chalmers University of Technology, SE-412 96 Gothenburg, Sweden

[†] Department of Shipping and Marine Technology,
Chalmers University of Technology, SE-412 96 Gothenburg, Sweden

[‡] Det Norske Veritas, Maritime Technical Consultancy, 1322 Høvik, Norway

ABSTRACT

In this paper, a new simple fatigue estimation model, only using encountered significant wave height, is proposed for predicting fatigue accumulation of a vessel during a voyage. The formulation of the model is developed based on the generalized narrow-band approximation. The significant response height, hs, is shown to have a linear relationship with its encountered significant wave height, Hs. The zero up-crossing response frequency, fz, is represented by the corresponding encountered wave frequency and is expressed as a function of Hs. The capacity and accuracy of the model is illustrated by application on one container vessel's fatigue damage accumulation, for different voyages, operating in the North Atlantic during 2008. For this vessel, all the necessary data needed in the fatigue model, and for verification of it, was obtained by measurements. The results from the proposed fatigue model are compared with the well-known and accurate rainflow analysis. In the following, the onboard wave measurement is calibrated by satellite measurement, and hence, a further improved model is presented based on validation and wave calibration. The conclusion is that the estimations made using the proposed fatigue model agree well with the rainflow method for almost all of the voyages.

KEY WORDS: Rainflow analysis; narrow-band approximation; significant response height; zero up-crossing response frequency; encountered wave frequency.

1. INTRODUCTION

The accumulation of fatigue damage in a vessel is a continuous process during the whole operational period, where the rate of damage is related to encountered sea state, ship's forward speed, heading angle and loading condition, etc. The variable encountered sea state is characterized by the significant wave height and wave period. It is the major cause of fatigue damage in ship structures. In general, the North Atlantic is considered to be one of the worst areas with respect to wave loading. Here, fatigue cracks in vessels are found earlier than elsewhere [1, 2]. As a consequence, special attention is paid to the risk and safety margin of vessels operating in the North Atlantic (North Pacific is also regarded as the second harsh wave area). For ship owners and operators, the economic aspect is of equal importance to safety, and their concern about ship fatigue is related to maintenance, repair costs, off-hire and reputation. However, in order to decrease these fatigue-caused problems, one should first employ a suitable model to evaluate the fatigue status for the corresponding ship structural details. Ordinarily, there are two different approaches to estimate the fatigue damage for practical application, i.e. time-domain analysis and frequency-domain analysis. The time-domain analysis is based on the time series of structure response. One typical method, known as the rainflow counting analysis, was introduced by Matsuishi and Endo [3], and then improved for different practical applications; for further discussion see references [4, 5]. It is recognized to give the relatively "accurate" fatigue estimations. The frequency-domain analysis is based on the frequency response of structural detail. In such situations, the response is usually divided into Gaussian and non-Gaussian processes. Hence, some methods with specific formulations, such as narrow-band approximation [6], and its extensions [7-11], are employed for the corresponding estimations.

For fatigue assessment of ship structures, a more generalized narrow-band approximation is employed in this paper. It is preliminarily proposed for the Gaussian process, but improved also for the practical ship response. Based on this model, we propose a new simplified fatigue estimation model, using only significant wave height H_s. This model is initially developed for a routing tool, which should minimize fatigue damage during a ship operation from harbour to harbour. Beside that, it can be also used for other applications, see Section 5.3 for a detailed discussion. In Section 2, two different approaches, using rainflow counting analysis, to estimate fatigue damage during the whole ship voyage are compared, and their results agree well with each other. Section 3 presents the detailed process for developing the fatigue model based on the generalized narrow-band approximation, where the significant response height h_s and zero up-crossing frequency f_z are deduced, respectively, in Sections 3.1 and 3.2. In Section 4, this model is validated by the measured data from a container ship with an onboard hull monitoring system [1, 2, and 12]. For convenience, in Section 4, we do not differentiate between the true value of encountered significant wave height H_s and the onboard measurement. In the following Section 5, the onboard wave measurement is calibrated by three different satellite measurements, and hence, the improved model is proposed based on the validation in Section 4 and calibration in Section 5.1. Finally, some possible applications of this model, such as routing tool and fatigue reliability analysis, are introduced.

2. MEASURED FATIGUE IN ONE VOYAGE

Fatigue damage in a voyage is accumulated during all the encountered sea states (30-minute intervals in this paper). In general, for fatigue assessment, ship response in one sea state is assumed to be a Gaussian process. Thus one can use different approaches to estimate the induced fatigue damages for all sea states inside one voyage, and then add them together as the accumulated fatigue damage of such a voyage. It is known that ship response during one whole voyage is a non-stationary process, due to the variability of mean stress between sea states with reference to whole voyage: variability of mean stress as a function of time due to re-ballasting, speed changes and temperature effects and secondly due to non-linearity in the dynamic signal. The simple summing of the damages, accumulated during all sea states, always gives less damage than the one computed for the whole signal. However, if the variability of mean stresses is small, then the method often gives accurate results; for detailed discussion see [11].

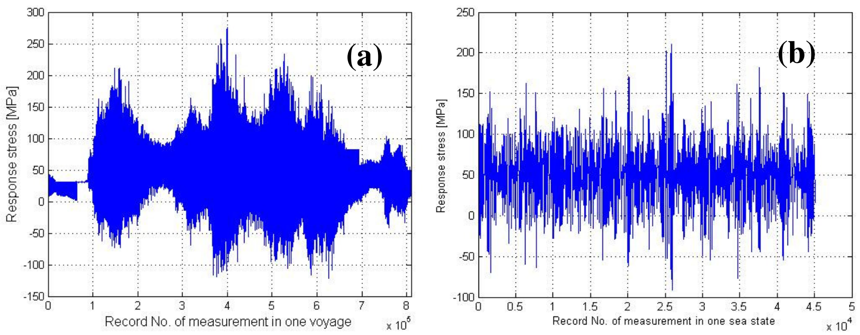

Fig. 1: Time series of stress measured at the midship structural detail by a sensor relating to vertical bending-caused stress with SCF = 2: (**a**) measurement of one whole winter voyage (denoted as "080106" in Table 1) with large stress response; (**b**) measurement of one typical sea state ($H_s = 5.2$ m, $T_z = 10.5$ s) inside the voyage.

In the following, we will check the preliminary conditions for the application of the above simple summing method, based on the measured stresses. One typical voyage during the winter is chosen for this investigation. Wave induced structure response, i.e. time series of stress, is measured by an onboard hull monitoring system; for detailed information see [1]. The time series of stress measured at the midship detail with a stress concentration factor (SCF) of 2 during this voyage is shown in Fig. 1a, and the corresponding response of one typical sea state inside this voyage is shown in Fig. 1b. Note that the signal contains a high frequency component due to vibration of the hull girder. This refers to whipping (transient impact response) and springing (resonance). The values of mean stress for each sea state (30-minute interval) are shown in Fig. 2 also with SCF=2. We can see from Fig. 2 that the mean stress distribution can be divided into 3 different parts, i.e. staying in port, operating at sea and in a channel. The mean stresses of each separate part change slightly, and thus the response of each part can be assumed to be stationary. Hence, the simple summing method is available for fatigue estimation of the whole voyage. Furthermore, the detailed comparison for voyages in both winter and summer is carried out by rainflow analysis; here we use an alternative definition given by

Rychlik [4], see appendix A. The results from the estimation using two rainflow counting approaches (whole and sum of half hours) are listed in the second and third columns of Table 1.

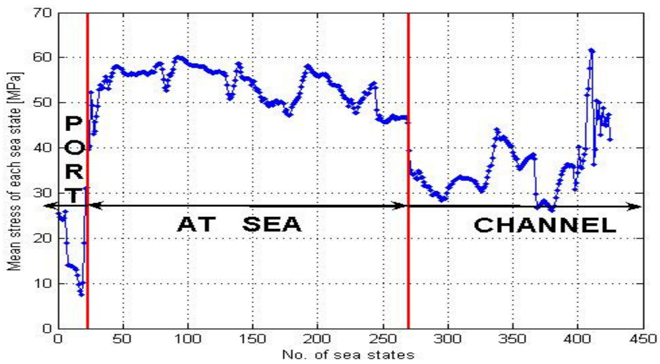

Fig. 2: Mean stress values of all sea states during the voyage presented in Fig. 1.

In Table 1, the first column is the arrival time of six chosen voyages (3 in winter and 3 in summer) of a container ship operating in the North Atlantic [1]. In column 2, rainflow counting was used to get all cycles in one voyage based on the time series of stress for this whole voyage. In column 3, the time series of stress for one voyage is split into several parts. Each part represents the stress response of each sea state (30-minute intervals), and then we use the same approach to get the cycles in each part, and collect all of them as the cycles in this voyage. Subsequently, these cycles can be used to compute the fatigue accumulation, using an *S*-*N* curve and the Palmgren-Miner law:

$$D(t) = \sum_i \frac{n_i S_i^k}{\alpha}, \tag{1}$$

where n_i is the number of stress cycles at stress range S_i, α and k are the related *S*-*N* curve parameters, see [9].

It is observed that fatigue damage estimated by the two approaches in Table 1 are close to each other and their difference is less than 6%, which means it is reasonable to first estimate fatigue damages caused during all individual sea states inside one voyage, and then add them together as the fatigue damage during this voyage. The difference between the two approaches is mainly caused by variability of the mean stresses between half hours. This should not be confused with "mean stress influence" which refers to the damage accumulation law for individual cycles. The narrow-band approximation used below does not take this mean stress influence into account, since the damage is a function of cycle range only. It is possible to modify the narrow-band approximation to include the more complex damage laws, see [11, 13]. However for simplicity of presentation it is not done here.

Table 1: Fatigue damage estimated by rainflow analysis based on different approaches.

Voyage date	Whole voyage	Sum of half hours
080106	0.00954	0.00936
080117	0.00163	0.00154
080129	0.00624	0.00612
080424	0.00320	0.00312
080504	0.00180	0.00177
080613	0.00169	0.00163

The narrow-band approximation [7, 14] is another method to estimate the fatigue damage during one sea state. For ship fatigue estimation, the inverse slope of the *S-N* curve used in the current paper is k = 3, thus the narrow-band approximation is expressed as follows:

$$E\left[D^{nb}(t)\right] \approx 0.47 t f_z h_s^3 / \alpha \,, \tag{2}$$

where f_z is the zero up-crossing response frequency, h_s is the significant response height, and α is the other parameter of the *S-N* curve equal to $10^{12.76}$. For a detailed discussion about this model, see the appendix B.
There are two approaches available for this approximation. First, if the structure response, i.e. time series of stress, is measured, the significant response height, h_s, is modelled as 4 times the standard deviation of the measured stresses; the zero up-crossing response frequency, f_z, is approximated as the up-crossing frequency of the mean stress level during this sea state. Alternatively, one can also employ the frequency domain analysis to calculate ship structure response spectrum $S(\omega)$ under different sea states. In such a situation, if the response of each sea state is assumed to be a stationary Gaussian process, h_s and f_z are calculated by the spectral moments of such a response; see Section 3 for further discussion.

3. A FATIGUE PREDICTION MODEL IN TERMS OF HS

Rainflow counting is a recognized tool for estimating fatigue damage based on a time series of stress of broad-band process. Frequency-domain fatigue analysis from measurement or numerical calculation is also widely applied in marine engineering [9, 10]. It can be used to predict fatigue damage by simulating the stress response under different operational environments. In this section, we will begin by investigating the generalized narrow-band approximation applicable for ship structure response of each sea state (30-minute interval), and then propose a simplified model using only the significant wave height, H_s, for estimating the fatigue damage during one voyage.

3.1. Linear Ship Response Spectrum

Ship structure response is usually known as the non-Gaussian process, especially when a vessel encounters a big storm. However, for fatigue assessment purposes here, such response is first assumed to be a Gaussian process [9]. Hence, a wave-induced load can be computed by the linear hydrodynamic analysis under a linear wave model, and the corresponding ship structure response is then calculated based on the linear stress response theory.

For linear ship structure stress called transfer function in hydrodynamics analysis, ship response under a series of regular waves is denoted as $H_\sigma(\omega|U,\beta)$ (frequency response function representing the response to a sinusoidal wave with a unit amplitude for different frequency ω under ship speed U and heading angle β), corresponding to different ship speed U and heading angle β. In general, it may be computed by the linear strip theory used in the current paper, expressed by the transfer function in Eq. (3),

$$H_\sigma(\omega | U, \beta) = \sum_i A_i H_i(\omega | U, \beta). \tag{3}$$

In Eq. (3), A_i is the stress caused by a unit wave-induced load, such as vertical bending moment, horizontal bending moment, torsional bending moment or axial force (not in strip theory) etc. It may be calculated by either a finite element analysis, or by simple ship beam model theory taking into account the stress concentration factor (used in this paper with SCF = 2). Additionally, H_i denotes the transfer function for the wave-induced load, for example, the transfer function for vertical bending moment, horizontal bending moment, etc. As referred above, the wave model is also assumed to be linear. Consequently, the complete stress transfer function is obtained by linearly summing the stress transfer functions of different components as Eq. (3).
When a vessel is operating in a sea state with wave spectrum $S(\omega)$, the corresponding encountered wave spectrum, $S(\omega_e)$, can be expressed as:

$$S(\omega_e) = S(\omega)/(1 + 2\omega U \cos\beta / g), \tag{4}$$

where $S(\omega)$ may be described by a spectrum model such as the Pierson-Moskowitz (P-M) or the JONSWAP model, in which the main parameters are the significant wave height, H_s, and wave period, T_z. U and β are the ship speed and heading angle during the sea state, respectively. Finally, the ship response spectrum is calculated by combining Eqs (3) and (4) as:

$$S_\sigma(\omega_e | U, \beta, H_s, T_z) = |H_\sigma(\omega_e | U, \beta)|^2 \, S(\omega_e | H_s, T_z). \tag{5}$$

The encountered wave spectrum is sometimes too complicated to be expressed in an analytical form [15]. In practice, however, only the response spectral moments are of interest for the narrow-band approximation. It can be computed as follows:

$$\lambda_n = \int_0^\infty \left|\omega_e + \omega_e^2 U \cos\beta / g\right|^n H_\sigma^2(\omega_e \mid U, \beta) S(\omega_e) d\omega_e \; . \tag{6}$$

Due to the assumption that the ship response during each sea state is a stationary Gaussian process, hence, the significant response height, h_s, and the zero up-crossing frequency, f_z, can be obtained as:

$$h_s = 4\sqrt{\lambda_0} \quad \text{and} \quad f_z = 2\pi\sqrt{\lambda_2/\lambda_0} \; . \tag{7}$$

where λ0, λ2 are, respectively, the zero and second-order spectral moments of the corresponding structure response. They are applicable for the narrow-band approximation in Eq. (2). Note that, as is shown in several references, the sea state is usually described as a short crested wave. A typical way to model this short crested sea is to use the spreading function f(α) or f(α,ω). The encountered wave spectrum S(ωe) is then replaced by its directional wave spectrum by S(ωe,α) = S(ωe)f(α), where α is the angle between the predominant wave direction (heading angle) and a wave component in one sea state. For marine engineering applications, the spreading function is often taken as Cos2α; see the references [15, 16] for a detailed discussion.

3.2. Significant Response Height, h_s

The significant response height h_s in Eq. (7) is expressed as 4 times the square root of zero-order spectral moment of the response spectrum. The stress transfer function is dependent on loading condition, ship forward speed U_0 and heading angle β, besides wave period characterized by ω. If we use the P-M model to express the encountered sea state, it can be modelled as follows:

$$S(\omega_e) = \frac{4\pi^3 H_s^2}{T_z^4 \omega^5} \exp\left[-\frac{1}{\pi}\left(\frac{\omega T_z}{2\pi}\right)^{-4}\right]. \tag{8}$$

If the encountered sea state wave spectrum $S(\omega_e)$ in Eq. (8) is put into Eq. (6), then the significant response height h_s in Eq. (7) can be formulated as:

$$h_s = 4 \cdot \sqrt{\int_0^\infty H_\sigma^2(\omega \mid U, \beta) \frac{4\pi^3 H_s^2}{T_z^4 \omega^5} \exp\left[-\frac{1}{\pi}\left(\frac{\omega T_z}{2\pi}\right)^{-4}\right] d\omega} \; . \tag{9}$$

It can be observed in Eq. (9) that h_s and H_s have a linear relationship (when a linear transfer function is used), through a “constant” C which is described as:

$$C = h_s / H_s = 4 \cdot \sqrt{\int_0^\infty H_\sigma^2(\omega \mid U, \beta) \frac{4\pi^3}{T_z^4 \omega^5} \exp\left[-\frac{1}{\pi} (\frac{\omega T_z}{2\pi})^{-4} \right] d\omega} \,. \tag{10}$$

This constant C is dependent on the wave period T_z, the ship forward speed U, the heading angle β, and the vessel's loading condition.

3.3. Zero Up-crossing Response Frequency, f_z

The zero up-crossing response frequency f_z expressed by Eq. (7) in the narrow-band approximation is developed for a stationary Gaussian process. However, for practical ship response it may cause about 20% overestimation of the fatigue damage; see appendix B for a detailed discussion. In the appendix, a generalized narrow-band approximation is proposed using an observed zero up-crossing response frequency $f_z = N^+(0)$. Since the variability in ship response is mainly caused by the wave induced load [15], the f_z of the vessel should be related to the encountered wave frequency through the transfer function. Initially, we presume that f_z is equal to the encountered wave frequency (assuming a constant transfer function) as:

$$f_z = 1/T_z + (2\pi U \cos\beta)/(gT_z^2)\,, \tag{11}$$

where the wave period T_z of each sea state is evaluated as the value occurring most frequently for each H_s based on the long-term wave statistics [16], and simplicity described by Eq. (12),

$$T_z = 3.75\sqrt{H_s}\ . \tag{12}$$

The simple model of f_z can be validated and improved when next based on the observed $N^+(0)$ for generalized narrow-band approximation. The encountered wave frequency is dependent on ship speed U and heading angle β. Hence, if a vessel is operating with ship speed U_i, heading angle β_i, in a sea state with significant wave height H_{si}, the fatigue damage during such a sea state (30-minute intervals), is then estimated by Eq. (13) as follows:

$$D_i \approx \frac{0.47TC_i^3}{\alpha} \left(\frac{H_{si}^{2.5}}{3.75} + \frac{2\pi U_i \cos\beta_i H_{si}^2}{3.75^2 g} \right), \tag{13}$$

where T is the time period of one sea state (1800 seconds here), C_i is the constant relation between ship response h_{si} and H_{si} for the sea state discussed above, Eq. (10).

3.4. Fatigue Model for Estimating Damage during One Voyage

The model in Eq. (13) for estimating fatigue damage during a sea state depends on ship speed, heading angle and wave height. Besides that, the constant C_i as Eq. (10) is also dependent on the detailed loading condition and wave period T_z. However, when estimating the fatigue damage accumulated during one voyage, the loading condition of the vessel can be considered to be constant. The wave period T_z (4 to 20 seconds) during the voyage can also be assumed to follow a fixed distribution, based on the long-term wave statistics [16]. For simplification, the distribution of U_i in Eq. (10) is also fixed as the ship service speed, U_0 (reasonably based on the economical operation), thus the constant C of one voyage is only expressed in terms of the distribution of β_i. The zero up-crossing response frequency f_z is less important when estimating fatigue damage in the whole voyage. For f_z expression in Eq. (11), U_i is also assumed to be the ship service speed, U_0 (reasonably based on the economical operation), and β_i is further simplified equal to 0° (head sea), which may be a little conservative. Finally, the estimation model of fatigue during one voyage becomes as described in Eq. (14):

$$D_{voy} \approx \frac{0.47TC^3}{\alpha} \cdot \sum_i \left(\frac{H_{si}^{2.5}}{3.75} + \frac{2\pi U_0 H_{si}^2}{3.75^2 g} \right), \tag{14}$$

where C is the constant relation for the whole voyage mentioned above and dependent on the distribution of β_i. It can be calculated by a least square method based on the measurement of h_{si} and H_{si} in this voyage. Furthermore, if there are no measurements available, it can also be predicted by software, such as Waveship [17].

4. VALIDATION OF THE PROPOSED FATIGUE MODEL

A 2800 TEU container vessel operating between the EU and Canada is chosen for our application. Detailed dimensions and measurement locations are described in [1, 12]. An onboard hull monitoring system has been installed to measure the time series of stress and encountered wave heights along the operation routes. The measurement place chosen in this paper is approximately located amidships, and the stress is mainly caused due to vertical bending measured by a strain sensor, see [1]. The measurement considered is taken from the first half-year of 2008, shown in the first and third columns of Table 2.

In this paper, the numerical hydrodynamic simulation is performed by a linear strip theory program, Waveship [17], and the stress is based on vertical bending and is estimated by a simple ship beam model with SCF = 2. The rainflow analysis is carried out by WAFO [18, 19]. Note that the calculations do not include horizontal bending and axial stress, which are present in the measurements as well as warping stress from torsion distribution. Vertical bending is however dominating.

4.1. Calculation and Validation of the Constant C by Two Approaches

The constant C_i of one sea state, denoted as the linear relation between h_{si} and H_{si}, is calculated directly by Waveship [17] shown in Fig. 3. For the calculation of the constant C_i in Eq. (10), ship speed is assumed to be the ship service speed of 10 m/s. The encountered sea state is, respectively, modelled as JONSWAP with $\gamma = 3.3$ and $\gamma = 5.0$ for steep sea state, and Pierson-Moskowitz spectrum with spreading functions of $\mathrm{Cos}^2\alpha$ and $\mathrm{Cos}^8\alpha$ for the short-crested sea. Although for engineering applications, the $\mathrm{Cos}^2\alpha$ spreading function is often applied [15, 16], one should observe that the constant C_i changes greatly due to different wave spectrum models and spreading functions, see Fig. 3, but reflects that the expectations, i.e. P-M with $\cos^2\alpha$, give less variations since it is more "smeared out".

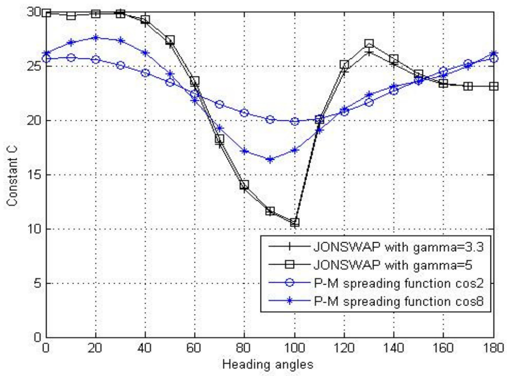

Fig. 3: The constant C_i in terms of heading angle with ship service speed $V = 10$ m/s, under sea states modelled as JONSWAP with $\gamma = 3.3$ and 5.0 for steep sea state (line with pluses and squares, respectively), and P-M spectrum with spreading functions of $\mathrm{Cos}^2\alpha$ and $\mathrm{Cos}^8\alpha$ for the short-crested sea (line with circles and asterisks, respectively).

After getting the constant C_i for different heading angles of all encountered sea states during one voyage, we can use them to compute the constant C of the whole voyage based on the heading angle distribution of that voyage. Furthermore, the constant C of the whole voyage can also be calculated by statistical analysis of the time series of stress. First, we compute the significant response height h_{si} for all sea states with the significant wave height H_{si} during one voyage (h_{si}, H_{si}), and then we employ the least square method to calculate the constant C for this voyage, which is listed in Table 2. For most voyages C is around 17 to 19, which is less than the one calculated by Waveship. The difference may be caused by an overestimation of the wave height measurement by onboard wave radar [12]. This will be further discussed in Section 5.1.

Table 2: Constant C calculated by least square method based on measured time series of stress for different voyages.

Voyage date	Constant C	Voyage date	Constant C
080106	18.4	080321	19.1
080117	13.9	080401	18.0
080129	17.2	080411	19.0
080209	13.2	080424	19.4
080218	20.2	080504	17.8
080301	13.8	080603	17.3
080312	16.7	080613	19.1

Note that the constant C in Table 2 for the voyages 080117, 080209 and 080301 is less than 19, approximately 13.5, which may be caused by a different heading angle distribution, obtained by measured directional wave spectrum for each sea state. If we assume the loading condition for all voyages as being fixed, the heading angle distribution of all voyages and sea states is as shown in Fig. 4a, and in Fig. 4b, the heading angle distribution for sea states $H_s \geq 5$ m is presented. The pluses represent the three special voyages with the small constant C and the dots represent all other voyages. The three special voyages are approximately operated in stern quartering, and the other voyages are bow quartering. Thus, from a statistical point of view, the constant C for a stern quartering voyage can be taken as 13.5, whereas 18.5 is a suitable value for others. This can be used for simple estimation of fatigue damage accumulated in one voyage for this vessel.

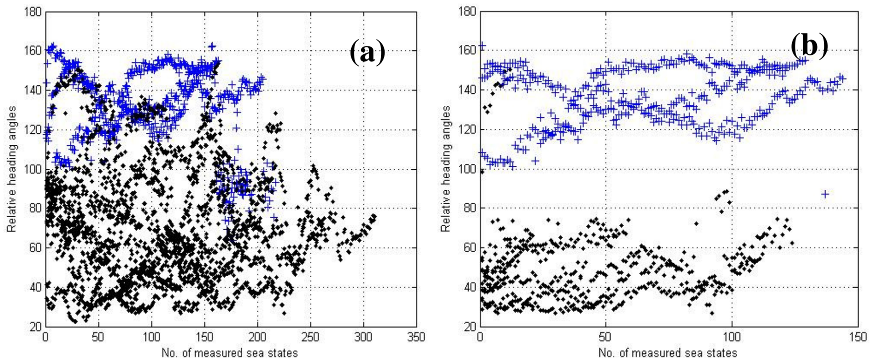

Fig. 4: (**a**) Heading angles for all sea states of different voyages; (**b**) heading angles for sea states $H_s \geq 5$ m of different voyages.

The comparison of the significant response height h_s from a statistical time series of stress analysis as the real response (x-axis) and our proposed model $C_i{\cdot}H_{sij}$ is shown in Fig. 5, where the constant C_i is constant for the same voyage, but different for different voyages, based on Table 2. In Fig. 5, h_s calculated by our model works quite well with real response results, but there are still some special cases, where the calm sea states (small measured H_s) caused a big vessel response, and measured moderate sea states caused a small response, which may come from the error of wave height measurement.

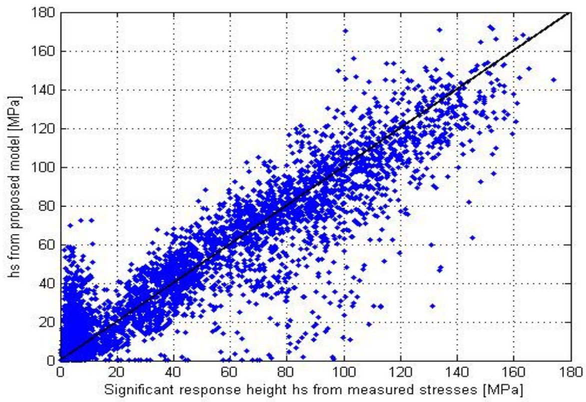

Fig. 5: Significant response height h_s calculated by statistical analysis of time series of stress (x-axis) and our proposed model (y-axis) for all measured sea states.

4.2. Investigation of the f_z Assumption

In the proposed model, the zero up-crossing frequency f_z is expressed by Eqs (11) and (12), where the ship speed U and the heading angle β are further simplified to be the ship service speed 10 m/s and 0°, respectively. In Fig. 6, the dots represent f_z for all measured sea states, where the x-axis represents the observed $f_z=N^+(0)$ (real value) and the y-axis is calculated by the model. The f_z expression in the model is a little rough for the real conditions. However, it is also somewhat reasonable for fatigue damage estimation, since their magnitude is satisfactory for the big sea states represented by the circles in the figure, and most of the fatigue damage in one voyage is accumulated during the period with big sea states. It is also shown in Fig. 7, where Fig. 7a is the comparison of $1/f_z$ for voyages from the EU to Canada, and Fig. 7b is for voyages in the opposite direction. The f_z expression works well for voyages from the EU to Canada. But for the voyages in the opposite direction, in particular the first three voyages, i.e. voyage 080117, 080209 and 080301 mentioned above, there has been much overestimation. This may be caused by the simplification of the heading angle (i.e. 0º) in the model, since for these voyages are following sea during most of the operating time.

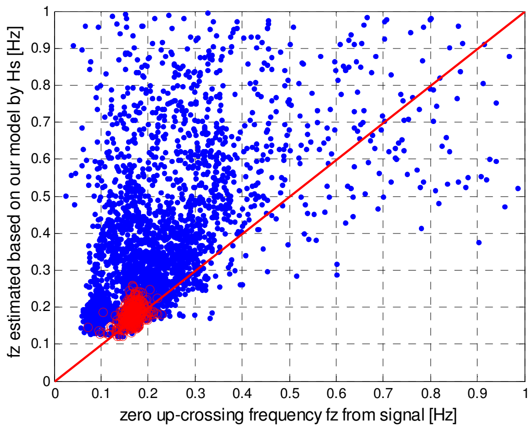

Fig. 6: Zero-crossing response frequency f_z comparison (real on the x-axis and our model on the y-axis) for all measured sea states from all voyages.

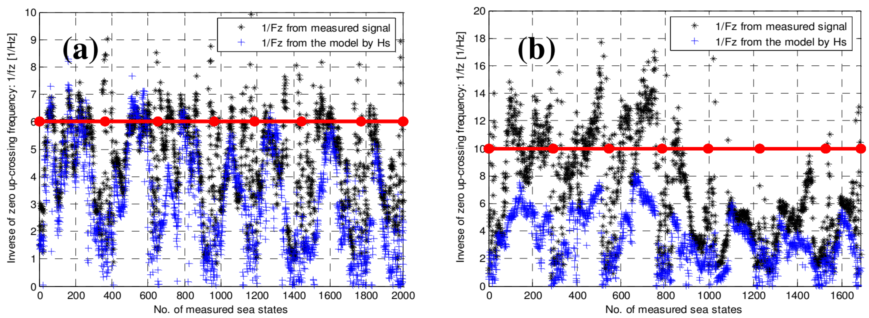

Fig. 7: Zero-crossing response frequency f_z respectively estimated by our model in terms of Hs (pluses) and directly calculated from time series of stress (asterisks). (**a**) $1/f_z$ comparison for all measured sea states of voyages from the EU to Canada; (**b**) $1/f_z$ of voyages from Canada to the EU.

4.3. Estimation of the Fatigue Damage Accumulated Per Voyage

As mentioned above, the heading angle distribution during one voyage is a main factor of our proposed model. In this section, all the measured voyages are divided into two parts: one is made up of the voyages from the EU to Canada; the other refers to the opposite direction. The fatigue damage is estimated by rainflow analysis, Waveship and the proposed fatigue model, respectively, and the results are shown in Fig. 8 (close to shore the navigational radar is used for navigation instead of wave measurements). Different voyages are separated by diamonds on a thick line, and only the sea states with both time series of stress and wave spectrum measurement are presented in Fig. 8. The fatigue damage distribution of voyages from the EU to Canada is shown in Fig. 8a, where asterisks, pluses and dots represent the three methods. Fig. 8b presents the same results as Fig. 8a, but for voyages from Canada to the EU. The detailed estimation values of fatigue damage accumulated during each voyage is listed in Tables 3 and 4. Table 3 shows the results for the voyages going from the EU to Canada, and Table 4 is for the voyages going in the opposite direction. In order to compare different estimation approaches, we only take into account the sea states with wave spectra measurements for each voyage.

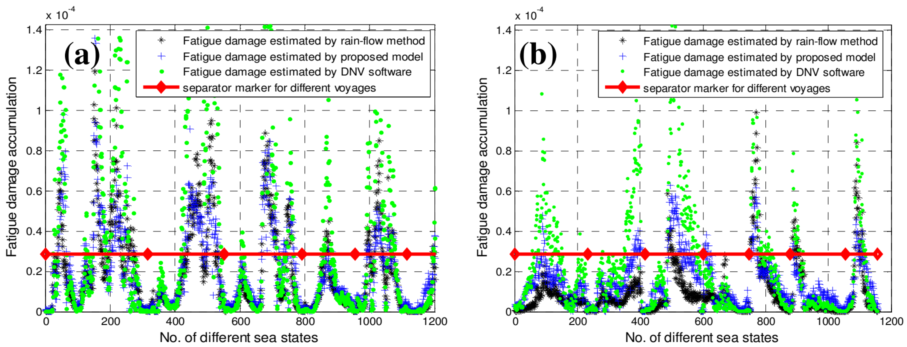

Fig. 8: (**a**) Fatigue damage distribution of all measured voyages (the EU to Canada) estimated by the rainflow method, Waveship and the preliminarily proposed model, respectively; **(b)** the same results as the upper figure for voyages in the opposite direction.

The estimation made using the proposed fatigue model is satisfactory for the voyages from the EU to Canada. The pluses are close to the "accurate" evaluation represented by asterisks in the upper figure of Fig. 8. The error of the proposed model is about 10% for the accumulated fatigue damage caused by all voyages (from the EU to Canada, see Table 3). However, the results are less satisfactory for the estimations of voyages from Canada to the EU. The errors of the first three voyages in Table 4 may result from the f_z assumption, which is not precise for the following sea with the constant C being approximately 13.5. There are also large errors in the fourth voyage in Table 4 (denoted as 080321). An investigation of this voyage showed that this is caused by the wave measurement, since the measurement of H_s almost equals to 0 during the "storm" period with a "big" response and fatigue damage, possibly from swell. But, for the last three voyages, their estimations also agree well with the rainflow analysis, and it is observed that the heading angle distribution of these voyages is approximately head sea with the constant C of 18 to 20.

Table 3: Total fatigue damage accumulated for different voyages (the EU to Canada).

Voyage date	RFC	Our model	Waveship
080106	0.0080	0.0083	0.0143
080129	0.0057	0.0059	0.0184
080218	0.0045	0.0052	0.0079
080312	0.0015	0.0015	0.0023
080401	0.0033	0.0031	0.0059
080424	0.0027	0.0034	0.0055
080603	0.0008	0.0009	0.0014

Table 4: Total fatigue damage accumulated for different voyages (Canada to the EU).

Voyage date	RFC	Our model	Waveship
080117	0.0014	0.0030	0.0051
080209	0.0011	0.0025	0.0047
080301	0.0020	0.0039	0.0078
080321	0.0009	0.0013	0.0008
080411	0.0025	0.0024	0.0044
080504	0.0012	0.0012	0.0015
080613	0.0015	0.0015	0.0025

5. FURTHER DISCUSSION AND IMPROVEMENT OF THE MODEL

Although the proposed fatigue model works well for the head sea voyages, there is still room for improvement for following sea. The parameter f_z may not be good enough as seen in Figs 7 and 8, especially for the following sea. In this section, we will investigate the model thoroughly in order to make it more suitable for the ship engineering application. Further, some possible applications of this model are also introduced at the end of the current study.

5.1. Calibration of Onboard Wave Measurement

The proposed fatigue model is strongly dependent on the significant wave height. For example, the constant C, estimated by measurement and predicted by Waveship, may be different due to the overestimation of wave heights measurements by onboard wave radar [12]. This overestimation will also influence the f_z assumption in the model. Storhaug and Heggelund [12] indicate a factor of 0.7 based on a comparison with buoys for the moderate sea states. In the following, we will compare the onboard wave measurement with the satellite wave height measurement. While buoys is regarded as better than satellite measurements, the buoys are located close to shore and often measure smaller sea states, the satellites cover the open ocean with higher sea states. This is then a good addition in the calibration process.

The fourteen measured passages of the 2800 TEU container vessel operations during the first half-year 2008 are shown in Fig. 9a as the thin curves crossing North Atlantic. They have already been chosen for the validation in Section 4. In the figure, the thick curves describe the tracks of satellite measurement. It is observed that there are several crossing points between these two types of passages. However, since the speed of a satellite is much faster than the ship speed, it is not so practical to find such a crossing point that two measurements are carried out at the same time. In order to calibrate the onboard wave radar by satellite measurement, we first assume that the area with a spatial distance of less than 50 km and a temporal interval smaller than 30 minutes has the same sea state. Hence, for each ship location with onboard wave measurement, we can search the corresponding satellite measurements, located in the above spatial and temporal area corresponding to this location. If there are more than one satellite measurements found inside this area, the one closest to the ship location is taken for comparison (the asterisk with circle in Fig. 9b). There may be only a few satellite measurements available for comparison for all the measured voyages. However, the temporal difference between the ship location and the closest available satellite measurement may be maximum 30 minutes. It means that the measurement before or after the closest position (asterisk with circle in Fig. 9b) along the satellite track may reflect the real sea state of ship location by satellite. Also, to decrease the possible casual “error” by satellite measurement, 20 satellite measurements along the same track as the selected closest one, see Fig. 9b, are used, and the mean value of their measurements is used in the calibration.

The wave height measurement from three different satellites, i.e. GFO-1, JASON-1 and ERS-2, are taken for our investigation. All the measurements coincident with the above description are shown in Fig. 10. The dots, asterisks and pluses are for the comparison between onboard wave measurement (x-axis) and three types of satellite measurements, respectively (y-axis). The factor of 0.8 for measurements between wave radar and satellite is shown as the thick line. The lower wave heights measurements have already been compared with buoys by Storhaug and Heggelund [12], indicating a factor of 0.7. Since here we are interested in the higher sea states, which contribute significantly to fatigue (>5m H_s), we choose the factor of 0.8 to represent the overestimation of onboard wave measurement.

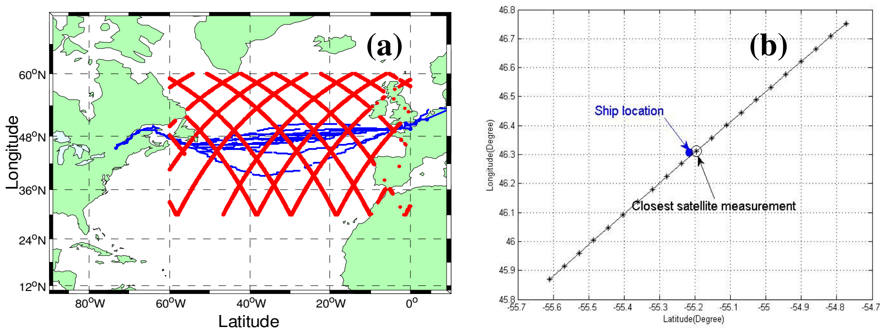

Fig. 9: (a) The fourteen measured passages taken for validation in this paper of the 2800 TEU container ship (thin curves), and satellite tracks (thick curves) in the North Atlantic; **(b)** the satellite measurement closest to ship location (marked by the circle) and 20 additional measurements along the same satellite track.

The overestimation of onboard wave heights measurements could cause big gaps for the application of the initially proposed model. For example, the constant *C* for different voyages in Table 2 is quite different from the one predicted by Waveship shown in Fig. 3. Further, fatigue damage estimated by the accurate rainflow method differs greatly from the estimation by Waveship, see Fig. 8 and Tables 3 and 4.

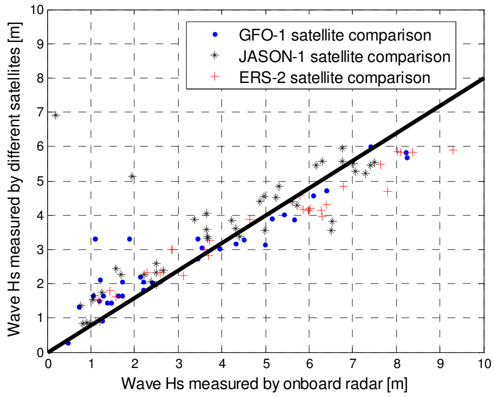

Fig. 10: Significant wave height H_s measured by onboard radar, comparing with H_s measured by three different satellite measurements.

It may be noted that there is a difference in the estimation of fatigue between the proposed fatigue model and Waveship. In the proposed fatigue model, the used least square method eliminates the influence of wave height overestimation in the fatigue estimation. In Waveship, however, C is independent of H_s. As a consequence, the overestimation of wave height measurements yields that the fatigue estimation of Waveship is larger in contrast to the initial model. All the above gaps are related to onboard wave measurements. Another reason for the overestimation of fatigue damage may come from f_z, which is used in Waveship, assuming ship response as a stationary Gaussian process; for a detailed discussion, see appendix B.

If we use the factor 0.8 as indicated and validated from satellites measurement above, the significant wave height H_{si} will change to $0.8{\cdot}H_{si}$, and the significant response height h_{si} from the time series of stress remains constant. Hence, the constant C_i in Table 2 calculated by the least square method increases to $C_i/0.8$. These "new constants" agree well with the Waveship predicted values in Fig. 3 for the 2800 TEU container vessel. During bow quartering operations (i.e. the heading angle being between 30º and 60º), the estimated value of C using Waveship is between 22.5 and 26.5 for a P-M spectrum with $\mathrm{Cos}^2\alpha$ spreading. However, for a stern quartering operation (i.e. the heading angle being between 100º and 140º) it is between 17 and 24, see Fig. 3.

5.2. Improvement of the Proposed Fatigue Model

For the application of the proposed fatigue model, one should use the wave height measurement calibrated by satellite. To predict the fatigue damage of a vessel without a time series of stress measurement, the constant C in the model can first be calculated by some hydrodynamic code, such as Waveship. But, the zero up-crossing frequency f_z should also be improved based on the calibration of wave measurement. Hence, taking into account the indication factor of 0.8 for the onboard wave height measurement, one can replace $H_s = H_{s,real}/0.8$ inside the fatigue model in Section 3, where H_s is measured onboard and $H_{s,real}$ is the accurate wave measurement corresponding to satellite calibration, thus f_z becomes as follows:

$$T_z = 3.75\sqrt{H_{s,real}/0.8}\ . \tag{15}$$

It was discussed in Section 4 that there is a huge influence of the f_z assumption due to different heading angles, such as head sea and following sea operation. Here, Eq. (11) has to be divided to be able to be applied on the following two cases: bow quartering and stern quartering operation. For the bow quartering operation, the value of β in Eq. (11) is set to 0º. However, for the stern quartering operation, the "real" heading angle observed during higher sea states is between 100º and 150º, see Fig. 4b. However, if β is set to 180º in Eq. (11) for stern quartering operation, the fatigue damage rate predicted by the model is underestimated; note that β equals to 0º results in an overestimation of the accumulated fatigue damage. As a result, β equals to 90º is used instead and the reasons to this are twofold: it shows a better agreement with the current fatigue measurements for stern quartering operation, and it gives an “acceptable” conservative estimation of the accumulated fatigue damage. Finally, based on the “accurate” wave height measurement calibrated by satellite, the proposed model for estimation of the fatigue damage during one voyage becomes:

$$D(T) \approx \frac{0.47TC^3}{\alpha}\sum_i\left(\frac{H_{si,real}^{2.5}}{4.2}+\frac{2\pi U_0 H_{si,real}^{2}}{17.6g}\right), \tag{16}$$

$$D(T) \approx \frac{0.47TC^3}{\alpha}\sum_i\frac{H_{si,real}^{2.5}}{4.2}, \tag{17}$$

where Eq. (16) is used for the fatigue estimation of head sea operations and Eq. (17) is used for the other operation conditions, $H_{si,real}$ is referred to as the significant wave height with accurate measurement and U_0 is the corresponding service speed for the voyage.

The fatigue damage accumulated during different voyages using the revised fatigue model is shown in Fig. 11. It is observed that the fatigue estimated by the revised model agrees well with the rainflow analysis, not only for the severe voyages with large fatigue damage accumulation, but also for the relative calm voyages. The errors using the model appear to be less than 10-20%.

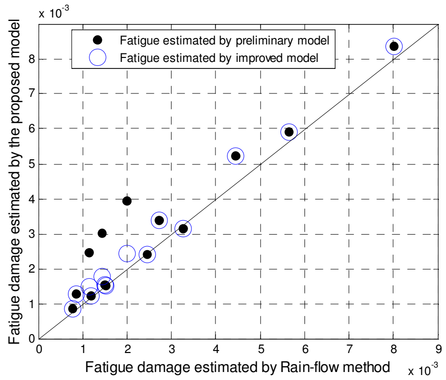

Fig. 11: Fatigue damage estimated by the proposed fatigue model Eq. (14) (dots) and the improved model Eqs (16) and (17) (circles) in the *y*-axis, compared to accurate rainflow estimation in the *x*-axis.

It is observed that the proposed fatigue model works well for the chosen container vessel in this paper. However, this model should be validated by more vessels for it to be applicable as the general methodology and more crossings for the same vessel. Also, the f_z assumption in the model should also be investigated carefully through analysing different types of vessels. Furthermore, as reported in some of the literature about the non-Gaussian influence on fatigue, such as whipping [1, 2, 12], one should work more on the detailed contributions to the fatigue damage from these aspects and improve the proposed fatigue model more precisely.

5.3. Application of the Proposed Fatigue Model

5.3.1 A Decision Support System for Fatigue

The initial purpose to develop the fatigue model is to apply it for the scheduling of a ship's route with minimum fatigue damage, i.e. a ship routing design related to fatigue influence. There are already some routing tools commercially available. For example, WRI fleet routing is targeted to provide the time-optimized route [20]. SeaWare routing aims at predicting an intended route with minimum fuel consumption and accurate ETA (estimated time of arrival) [21], and Amarcon OCTOPUS intends to supply the response-based route by installing an onboard hull monitoring and decision support system [22], etc. Most of these routing tools are based on the weather forecast information updated every 6 to 24 hours, but fatigue problems have so far not been considered. It is known that most fatigue damage in one voyage is accumulated during storms (H_s>5m) with a short duration, in which situation the vessel should be operated around a safe heading angle and the forward speed is also decreased involuntarily and voluntarily. Hence, the routing tool is needed to help vessels operate with a minimum of fatigue damage and still arrive port on time. The proposed model characterized as Eqs (2), (10) and (11) can be used to estimate fatigue damage in each sea state, which is mainly dependent on the constant C. During the storm sailing period, this constant C is strongly dependent on the ship speed and heading angle, shown in Fig. 12. The figure can help the captain to choose suitable operation parameters with less fatigue damage (small C) under each sea state.

When designing routing for the whole voyage with minimum fatigue damage, we assume that a vessel is sailing in one sea state with significant wave height H_{si}. Under such a sea state, ship speed, heading angle and operation distance of the vessel is, respectively, equal to U_i, β_i and L_i. The constant C_i in the fatigue model is then determined by the operation parameters (U_i, β_i). For one sea state in a calm sea it may be large, although it can be controlled to be of relatively small value in severe sea states. Finally, the total fatigue damage for the voyage, estimated and based on Eq. (13), is then proportional to $\Sigma_i(C_i^3(H_{si}^{2.5}+H_{si}^2)L_i/U_i)$, which can be optimized to determine the route with a minimum of fatigue damage.

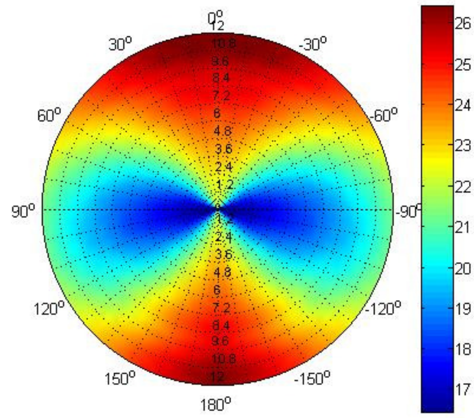

Fig. 12: Polar diagram of the constant C (linear relation between h_s and H_s) in terms of ship speed U (radial direction) and heading angle β (circular direction), calculated by Waveship.

5.3.2 Simple Estimation of Fatigue Damage during Ship's Voyages

As discussed in the previous sections, the fatigue estimation by the model works well compared with the "accurate" rainflow analysis. Hence, it can also be employed to design the ship structure considering fatigue influence. Firstly, the constant C is computed by some general engineering software, based on the preliminary designed ship structure model. Secondly, the encountered wave height scatter diagram corresponding to the vessel operation region is also known [16]. Hence they are combined to obtain the fatigue status during some design period for further improvement of structure design.

5.3.3 Fatigue Reliability Analysis for a Large Amount of Locations in the Ship Structure

However, the fatigue estimations, even for the relatively "accurate" rainflow analysis, contain a number of uncertainties. These "errors" may come from variable amplitude fatigue tests for the *S-N* curve, or may be caused by possible modelling errors, for example, using the Palmgren-Miner rule, neglecting sequential effects between voyages, using stress concentration factors and other simplifications, etc. One alternative way to evaluate ship fatigue characters is to use the so-called fatigue reliability analysis. It can be carried out by combining the proposed model with the constant C, calculated by some engineering software such as Waveship, and the encountered wave height model. One of its detailed applications is shown in Mao et al. [23].

The model is also applicable when estimating the fatigue reliability coefficient for a large number of locations in a ship, mainly through the analysis of the constant C in the model. Thus we can get to know the fatigue safety properties of the whole ship. It can be used as input to inspections and maintenance planning of the ship structure. For example, if a fatigue crack is found in one place at the ship structure, we can predict the probability of the existence of fatigue cracks in the vicinity through the estimated fatigue reliability correlated coefficient of the whole ship. In practice, however, this is somewhat cumbersome since there are quite many critical details in a ship.

6. CONCLUSIONS

A simple model for estimating specific voyage fatigue damage is proposed based on the theory of narrow-band approximation and linear structure response. It is expressed only in terms of significant wave height H_s and agrees well with the "accurate" rainflow estimation. Inside the model, a constant C describes the relation between the significant response height h_s and H_s, and it is mainly based on the vessel's heading angle distribution during a voyage. This works satisfactorily and is validated against measurements from a 2800 TEU North Atlantic sailing container vessel. Due to the large influence of heading angle, the zero up-crossing response frequency f_z is improved in two different cases: one is for a bow quartering operation, and one for other conditions. Further, the proposed fatigue model is presented based on the wave height measurements calibrated with satellite measurements. The model works well with an "error" of less than 10-20% for voyages of both bow and stern quartering operations through a comparison with rainflow analysis for a 2800 TEU container vessel.

The proposed fatigue model seems to be good enough for one voyage, and hence, it may be good enough also for a routing tool. For a routing tool application, it can be combined with other parameters such as a ship's speed and course, in order to optimize a route for minimizing the fatigue damage. Additionally, the model can be used for simple estimation of fatigue damages caused during one voyage. As a more general methodology, this model is also suitable for fatigue reliability analysis for both a special ship structural detail and for the whole ship structure. However, more investigation should be carried out for more general application in marine engineering. For example, the zero up-crossing frequency assumption in the model should be validated thoroughly for different types of vessels. Also, some non-Gaussian response with high frequency, such as whipping, should also be taken into account for more precise estimation.

ACKNOWLEDGEMENTS

The authors acknowledge the support from the EU project SEAMOCS (Applied Stochastic Models for Ocean Engineering, Climate and Safe Transportation) and Gothenburg Stochastic Center and the Swedish foundation for Strategic Research through GMMC, Gothenburg Mathematical Modeling Center. Also many thanks to DNV, crews, the management company and the ship owner for providing data.

REFERENCES

[1] Storhaug, G., Moe, E., and Piedras Lopes, T.A., 2007, "Whipping Measurements Onboard a Midsize Container Vessel Operating in the North Atlantic", Marintec China Proceedings (RINA, CMP and SNAME), International Symposium on Ship Design and Construction, 28-29th of November, Shanghai, China, pp. 55-70.

[2] Moe, E., Holtsmark, G., and Storhaug, G., 2005, "Full Scale Measurements of the Wave Induced Hull Girder Vibrations of an Ore Carrier Trading in the North Atlantic", RINA, International Conference on Design and Operation of Bulk Carriers, 18-19th of October 2005, London, UK, pp. 57-85.

[3] Matsuishi, M., and Endo, T., 1968, "Fatigue of Metals Subjected to Varying Stress", Proceedings of the Kyushu Branch of Japan Society of Mechanics Engineering, Fukuoka, Japan, pp. 37-40.

[4] Rychlik, I., 1987, "A New Definition of the Rainflow Cycle Counting Method", International Journal of Fatigue, 9(2), pp. 119-121.

[5] ASTM E1049-85, 2005, "Standard Practices for Cycle Counting in Fatigue Analysis", ASTM International.

[6] Bendat, J.S., 1964, "Probability Functions for Random Responses: Prediction of Peaks", Fatigue Damage and Catastrophic Failures, NASA technical report 1964.

[7] Rychlik, I., 1993, "On the "Narrow-band" Approximation for Expected Fatigue Damage", Probabilistic Engineering Mechanics, 8, pp. 1-4.

[8] Benasciutti, D., and Tova, R., 2005, "Comparison of Spectral Methods for Fatigue Damage Assessment in Bimodal Random Process", Proceedings of the 9th International Conference on Structural Safety and Reliability, Rome, Italy, pp. 3181-3188.

[9] Det Norske Veritas, 2005, “Fatigue Assessment of Ship Structure”, Classification Note No.30.7, July 2005.

[10] Gao, Z., and Moan, T., 2007, “Fatigue Damage Induced by non Gaussian Bimodal Wave Loading in Mooring Lines”, Applied Ocean Research, 29, pp. 45-54.

[11] Bogsjö, K., and Rychlik, I., 2007, “Vehicle Fatigue Damage Caused by Road Irregularities”, Fatigue and Fracture of Engineering Materials & Structures, In Press (LUTFMS-5067-2007).

[12] Storhaug, G., and Heggelund, S.E., 2008, “Measurements of Wave Induced Vibrations and Fatigue Loading Onboard Two Container Vessels Operating in Harsh Wave Environment”, RINA, Proceedings of the International Conference on Design and Operation of Container Ships, 3-4th of July 2008, London, UK, pp. 81-100.

[13] Rychlik, I., 1993, “Note on Cycle Counts in Irregular Loads”. Fatigue and Fracture of Engineering Materials & Structures, 16, pp. 377-390.

[14] Bengtsson, A.K., and Rychlik, I., 2008, “Uncertainty in Fatigue Life Prediction of Structures Subject to Gaussian Loads”, Probabilistic Engineering Mechanics, In Press.

[15] Lewis, E.V., 1989, Principles of Naval Architecture: Volume III - Motions in Waves and Controllability, Society of Naval Architects and Marine Engineers, Jersey City, NJ, USA.

[16] Det Norske Veritas, 2007, “Environmental Conditions and Environmental Loads”, Recommended practice DNV-RP-C205, April 2007.

[17] Det Norske Veritas, 1993, “Sesam User’s Manual Waveship”, DNV Sesam Report No.:93-7080/Rev.1, October 1993.

[18] Brodtkorb, P.A., Johannesson, P., Lindgren, G., Rychlik, I., Rydén, J., and Sjö, E., 2000, “WAFO - a Matlab Toolbox for Analysis of Random Waves and Loads”, Proceedings of the 10th International Offshore and Polar Engineering Conference, Seattle, USA, Vol III, pp. 343-350.

[19] WAFO-group, 2000, “WAFO - a Matlab Toolbox for Analysis of Random Waves and Loads - A Tutorial”. Department of Mathematical Statistics, Centre for Mathematical Sciences, Lund University, Lund, Sweden, 2008-11-24, URL: http://www.maths.lth.se/matstat/wafo.

[20] WRI Fleet Routing,
2009-01-04, URL: http://www.wriwx.com/fleet_ routing.html.

[21] SeaWare Routing,
2009-01-04, URL: http://www.seaware.se/Routing.aspx.

[22] Amarcon Octopus,
2009-01-04, URL: http://www.amarcon.com/products/index.html.

[23] Mao, W., Rychlik, I. and Storhaug, G., 2008, "Safety index of fatigue failure for ship structural details", Math. Statistics Preprint, 2008:40, 1-12.

[24] Rychlik, I., 2000, "On Some Reliability Applications of Rice's Formula for the Intensity of Level Crossings", Extremes, 3:4, 331-348.

Appendix A: Rainflow counting definition

The rainflow counting method is used in the analysis of fatigue data in order to reduce a time series of varying stress into a set of simple stress reversals. It is applicable to be combined with some fatigue accumulation law, e.g. linear Palmgren-Miner law, to estimate the fatigue damage of a structure subject to complex loading. A mathematical definition of the rainflow counting method given by Rychlik [4] is employed here and described as follows. It is able to consider closed-form computations from the statistical properties of the load signal.

For the random stress (measured time series of stress), each maximum of the stress signal, v_i, is paired with one particular local minimum u_i^{rfc}. The pair, (u_i^{rfc}, v_i), is called the rainflow cycle, and the cycle stress range, $S_i = v_i - u_i^{\mathrm{rfc}}$, is then applicable for fatigue analysis. The corresponding minimum of the cycle, u_i^{rfc}, is determined as follows, detailed discussion see [4]:

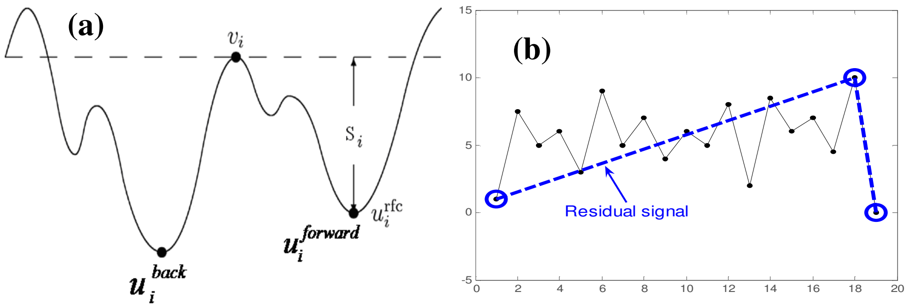

Fig. 13: **(a)** Definition of a rainflow cycle, **(b)** residual signal after rainflow counting

- From the i-th local maximum v_i, one determines the lowest values, u_i^{back} and $u_i^{forward}$ respectively in backward and forward directions between the time point of local maximum v_i, and the nearest crossing points of level v_i along the time series of stress in Fig. 13a.
- The larger value of those two points, denoted by u_i^{rfc}, is the rainflow minimum paired with v_i, i.e. u_i^{rfc} is the least drop before reaching the value v_i again between both sides. In the situation of Fig. 12, $u_i^{rfc} = u_i^{forward}$.
- Thus, the i-th rainflow pair is (u_i^{rfc}, v_i), and S_i is the stress range of this rainflow cycle.

Note that for some local maxima (outside the end of the signal), the corresponding rainflow minima could lie outside the measured or caring load sequence. In such situations, the incomplete rainflow cycles constitute the so called residual (see the thick dashed line in Fig. 13b) and have to be handled separately. In this approach, we assume that, in the residual, maxima form cycles with the preceding minima.

Appendix B: Generalized narrow-band approximation

For a stress $x(t)$, $t \in [0, T]$, one can define the number of up-crossings of the level u by $x(t)$ as:

$$N_t^+(u) = \#\{\tau \in [0,t] : x(\tau) = u, \quad \dot{x}(\tau) > 0\}, \tag{18}$$

where $\#\{\bullet\}$ means the number of elements in a set $\{\bullet\}$. If $x(t)$ is a stationary random stress, the expected number of up-crossings can be computed by means of up-crossing intensity, i.e. the expected number of up-crossings in unit time $E[N^+(u)]$, say, viz.

$$E[N_t^+(u)] = t \cdot E[N^+(u)]. \tag{19}$$

In the following, for simplification of formulas only, we assume that the random stress has mean zero. In a special case when up-crossing intensity is unimodal and symmetrical $E[N^+(u)] = E[N^+(-u)]$, one can approximate the expected damage by the so-called narrow-band approximation, first proposed by Bendat [6], as follows:

$$E[D^{nb}(t)] = \frac{t}{\alpha} \int_0^{+\infty} 2k(2u)^{k-1} E[N^+(u)] dz, \tag{20}$$

where α, k are parameters of the S-N curve. Note that for a stationary stress $x(t)$, the expected rainflow damage is $E[D^{rfc}(t)] < E[D^{nb}(t)]$, see [7] for the proof.

Example: Suppose that expected up-crossing intensity of $x(t)$ is expressed by Eq. (21):

$$E[N^+(u)] = f_z e^{-\frac{u^2}{2\sigma^2}}, \tag{21}$$

where $f_z = E[N^+(0)]$ is the corresponding zero up-crossing frequency. Now the narrow-band approximation in Eq. (20) is given by:

$$E[D^{nb}(t)] = t f_z h_s^k 2^{-k/2} \Gamma(1 + k/2) / \alpha, \tag{22}$$

where $h_s = 4\sigma$ and $\Gamma(x)$ is the gamma function.

Narrow-band Approximation for a Stationary Gaussian Process

If the stress $x(t)$ is a stationary Gaussian process then by Rice's formula [24]:

$$E\left[N^{+}(u)\right]=\frac{1}{2\pi}\sqrt{\frac{\mathrm{Var}(\dot{x}(0))}{\mathrm{Var}(x(0))}}\exp\left[-\frac{u^{2}}{2\mathrm{Var}(x(0))}\right]=\frac{1}{2\pi}\sqrt{\lambda_2/\lambda_0}\,e^{-\frac{u^2}{2\lambda_0}} \tag{23}$$

Further, let $S(\omega)$ be the power spectral density of $x(t)$. Using spectral moments $\lambda_i=\int\omega^i S(\omega)d\omega$, $\mathrm{Var}(x(0))=\lambda_0$, $\mathrm{Var}(\dot{x}(0))=\lambda_2$. Now, Eq. (23) coincides with Eq. (21) if:

$$f_z=\frac{1}{2\pi}\sqrt{\lambda_2/\lambda_0},\quad h_s=4\sqrt{\lambda_0}\ . \tag{24}$$

Hence, we derive the well-known narrow-band approximation in Eq. (22) for Gaussian loads.

Generalized Narrow-Band Approximation for Measured Ship Response

In our studies of the measured stresses we found that the observed up-crossing intensity can be sufficiently well approximated by Eq. (21). Here, the zero up-crossing frequency f_z was estimated from the measured signal:

$$f_z=N_t^{+}(0)/t\,, \tag{25}$$

while σ^2 in Eq. (21) is taken to be equal to λ_0 of the stress $x(0)$ with $\lambda_0=\mathrm{Var}(x(0))$. This is illustrated by plots of up-crossing intensities, shown in Fig.14, for four stress responses $x(t)$ of typical sea states (H_s is equal to 1.1, 3.3, 4.9 and 7.7 m, respectively), for the voyage denoted as "080106" in Table 1. (The stresses have zero mean.) In the figure, the irregular line represents the observed $N_t^+(u)$ while the dashed line is an estimate of the $t\cdot E[N^+(u)]$, by means of Eq. (21), where f_z is given in Eq. (25). We can see that the agreement is quite good, which motivates the accuracy of damage-prediction methods used in this investigation. For comparison we also give the estimate of $t\cdot E[N^+(u)]$, where f_z is replaced by Eq. (24), i.e. under the assumption that the stress is a Gaussian process. It can be seen in Fig. 14 (dash-dotted line) that the measured stresses are non-Gaussian and that using narrow-band approximation with f_z and h_s defined in Eq. (24) give 20% higher values of narrow-band approximation.

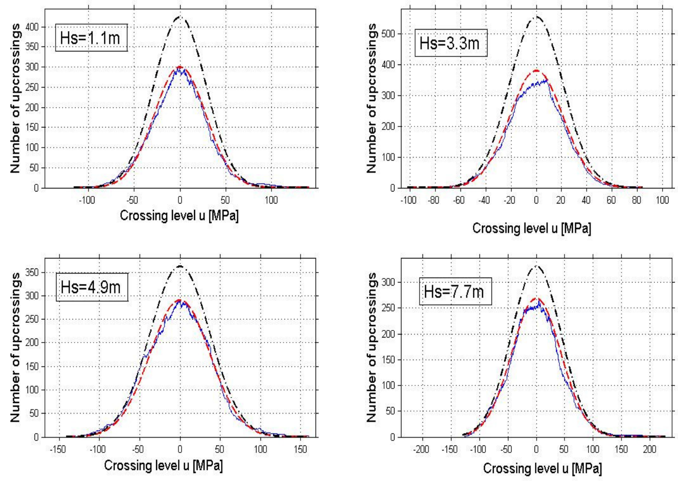

Fig. 14: Crossing spectrum of the response (transformed to zero mean) for the four typical sea states in the voyage "080106" (the time interval of each sea state is 30 minutes).

In the following example we illustrate the difference between the measured stress and the Gaussian model.

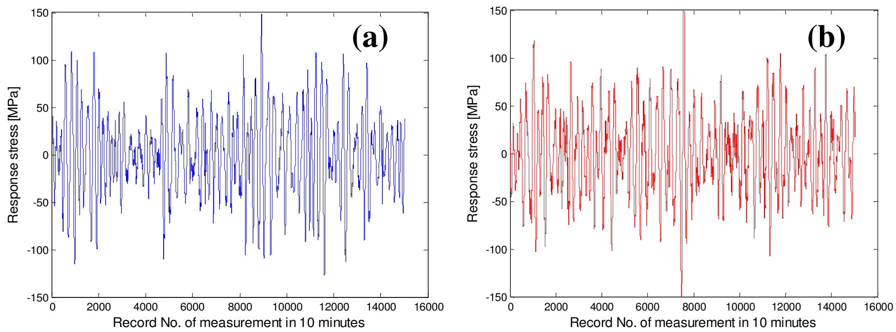

Fig. 15: **(a)** Time series of stress $x(t)$ measured in one sea state with H_s = 7.7 m; **(b)** Simulated stationary Gaussian stress $y(t)$ with the same spectrum of $x(t)$.

Example: Let us consider a measured stress $x(t)$, say, during a 10-minute period (H_s = 7.7 m); see Fig. 15a. We estimate the spectrum $S(\omega)$ for the stress $x(t)$. Further, let $y(t)$ be a simulation of a Gaussian process having the same spectrum; see Fig. 15b. (Note that the spectrum defines uniquely all properties of $y(t)$). It can be seen that the time series of stresses, from measurement $x(t)$, and simulation $y(t)$, are quite different, although both signals have the same spectrum. Next, in Fig. 16, we compare the observed up-crossings in signals presented in Fig. 15. The observed up-crossings in the measured signal is below the one found in the simulated $y(t)$. The difference is significant. The thick dash-dotted line is the theoretical expected number of up-crossings (under a Gaussian assumption), given by Eq. (23), while the dashed line is defined by Eqs (21) and (25).

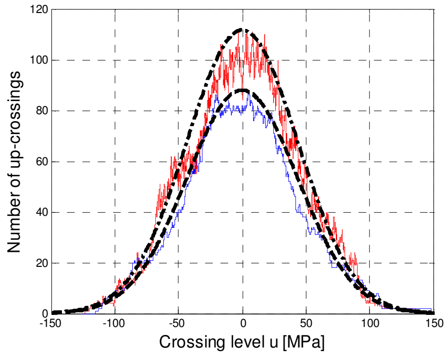

Fig.16: Crossing spectrum for the measured stress $x(t)$ and simulated stress $y(t)$ calculated by different approaches.

We conclude that the measured stress is not well modelled through a Gaussian process. This is somewhat surprising because the marginal distribution of the measured stress is Gaussian; see Fig. 17a. In Fig. 17b, the derivative of the measured stress is presented and we can see that it is slightly non-Gaussian.

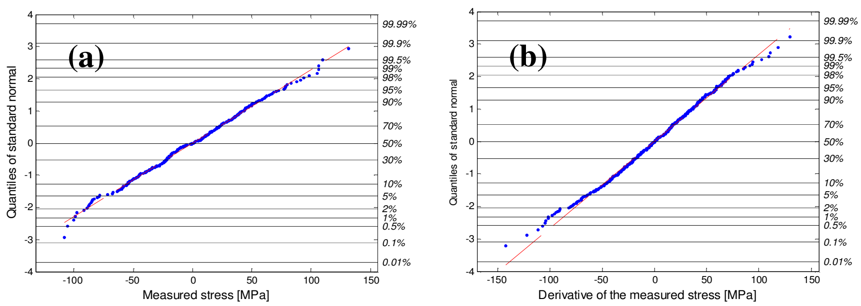

Fig. 17: **(a)** Normal plots of measured stress $x(t)$ in one sea state with $H_s = 7.7$ m; **(b)** normal plots of a derivative of the measured stress $x(t)$.

Paper III

Safety Index of Fatigue Failure for Ship Structure Details

Wengang Mao,[*] **Igor Rychlik**,[*] and **Gaute Storhaug**[†]

[*]Department of Mathematical Sciences, Chalmers University of Technology, SE-412 96, Gothenburg, Sweden

[†]Det Norske Veritas, Maritime Technical Consultancy, 1322 Hovik, Norway

Abstract

One way to assess the uncertainty in fatigue damage analysis is to use a so-called safety index. In the computation of such an index the variation coefficient for the accumulated damage is required. In this paper the expected fatigue damage and its coefficient of variation is firstly estimated from measured stress. Secondly, when suitable stress measurements are not available these are computed from models for damage accumulation and sea states variability. Stresses during ship sailing period are known as the non-stationary, slowly changing, Gaussian processes and hence damage accumulation, during encountered sea state, can be approximated by an algebraic function of significant wave height, ship speed and heading angle; Further the space time variability of significant wave height is modeled as a lognormal field with parameters estimated from the satellite measurements. The proposed methods to estimate uncertainties in the damage accumulation process are validated using full scale measurements carried out for a container vessel operating in the North Atlantic.

Keywords: Rainflow damage, fatigue risk of ship structure detail, safety index, damage variability.

1 Introduction

Material fatigue is one of the most important safety issues for structures subject to cyclic loads and the cause of failure in a majority of cases. Fatigue life of a structural detail is greatly influenced by a number of components and material dependent factors, such as geometry, size of the structure, surface smoothness, surface coating, residual stress, material grain size and defects. Further, the nature of the load process is important. The complex dependence between these factors and fatigue life makes predictions uncertain and even for controlled laboratory experiments the results from fatigue life tests exhibit a considerable scatter.

In this paper we present a simplified safety analysis showing how the different sources of uncertainties can be combined into a safety index using a Bayesian approach with material and structure detail dependent parameters modeled as random variables. We will particularly focus on the variability of the loads a ship may encounter in a specified period of time.

When studying a variable environment, the average damage growth rate may not be sufficient to properly estimate the risk for fatigue failure. For example, the fatigue crack risk of a ship structure detail during one year depends on the age of such detail, and can be high during a year if a vessel encounters an extreme storm. The probability of meeting such a storm can be very small but may still influence the value of the estimated risk. Consequently the uncertainties in long term variability of load properties should be included in the risk analysis.

In this paper methods to estimate the fatigue risk of ship structure details will be presented. Data from an extensive measurement campaign will be used to validate the proposed methodology. The paper is organized as follows. In Section 2 some basic definitions of rainflow damage are given and in Section 2.1 variable amplitude tests are discussed. Safety index is introduced in Section 2.2. The computation of such index is illustrated in Section 3 where the measured stresses during half a year are used to compute the safety index of trade in different numbers of years. An important case of computation of the safety index when no stress measurements are available is discussed in Section 4. In this section the safety index will be estimated, by means of a model for the sea state variability estimated using the satellite data. The model is presented in the appendix. Some further mathematical details about computing the coefficient of variation of the accumulated damage are moved to the appendix. Finally, a numerical example is given in Section 5.

2 Fatigue review

Fatigue testing of structural details has traditionally been carried out using constant amplitude stress cycles. In these experiments the stress oscillates between the minimum and maximum value until fatigue failure occurs. Repeating the experiments for different amplitudes, keeping the ratio, R, between minimum and maximum load constant, result in what is known as a Wöhler curve, also called S-N curve, with a log-linear dependence between the number of cycles to failure, N, and the stress cycle range, h,

$$\log(N) = \alpha - k\log(h) + e \ , \tag{1}$$

where parameters $\alpha > 0$ and $k \geq 1$ depend on material and structural detail properties and the stress ratio R. When studying fatigue of welded ship structures, the parameters α, k are usually categorized into different types based on the properties of structural details. In this paper, we will use the simple one slope S-N curve with $k = 3$ and $\alpha = 12.76$, where the unit of stress cycle range h should be "MPa", detailed description see *DNV (2005)*.

For random stresses the stress cycles and cycle ranges need to be defined using some cycle count procedure. In fatigue analysis the "rainflow" method, see Appendix A, has been shown to give the most accurate results. The method was originally introduced by Endo: The first paper in English is *Matsuishi and Endo (1968)*. Here we shall use the alternative definition given in *Rychlik (1987)*, which is more suitable for statistical analysis.

Fatigue damage from variable amplitude (random) stresses is commonly regarded as a cumulative process. Let h_i be the ranges of the rainflow cycles, see Fig. 5, found in the stress then using the linear Palmgren-Miner damage accumulation rule (*Palmgren, 1924, Miner, 1945*) one defines the pseudo rainflow damage $D^{rfc}(t)$ at time t as

$$D^{rfc}(t) = \sum_i h_i^k \quad . \tag{2}$$

Finally, it is assumed that fatigue failure occurs when $\log(D^{rfc}(t)) > \alpha$ (Note that h_i should have the same unit as the stress cycle range h in Eq. (1)). In practice one is observing failures when $\log(D^{rfc}(t)) > \alpha - 0.5$ due to variability of material properties and other factors, relevant for fatigue accumulation, see *Johannesson et al. (2005a)* for detailed discussion. A possible solution to incorporate these factors in the model is to estimate the parameters α and k of the S-N curve using tests with variable amplitude loads similar to the real load processes. We will discuss this issue further in the next section.

2.1 Variable amplitude S-N curve

Let us introduce the equivalent cycle range defined as

$$h^{eq}(n) = \left(\frac{1}{n}\sum_{i=1}^{n} h_i^k\right)^{1/k}, \tag{3}$$

where $\{h_i\}_1^n$ are stress ranges of rainflow cycles. Usually the stress signal is rainflow filtered, i.e. small cycles, with range smaller than some chosen threshold relative to the fatigue limits, are removed before computation of the equivalent range. Consequently n in (3) is the number of remaining rainflow cycles used in the blocked test load. For stationary (ergodic) Gaussian loads $h^{eq}(n)$ fast approaches a limit h^{eq}, say,

$$h^{eq} = \lim_{n\to\infty} h^{eq}(n), \tag{4}$$

which can be computed from a single long measurement of the load. Empirical tests, see *Agerskov (2000)* and Fig. 1, have shown that the S-N curve (1) is valid also for

Gaussian random loads if the constant stress range s is replaced by h^{eq},

$$\log(N) = \alpha - k\log(h^{eq}) + e\,. \qquad (5)$$

The S-N curve (5) tells us that, if an undamaged structure details loaded by a stationary Gaussian stress under time t, then the load is safe for this structure detail if

$$\alpha - \log(D^{rfc}(t)) + e > 0\,. \qquad (6)$$

In Fig. 1 the results of constant amplitude experiments are marked by pluses and one can see that the S-N relation for the constant amplitude load would give the same k but also a higher value of the parameter α. It indicates that using α in Eq. (6) from the constant amplitude experiments will give some (non-conservative) bias.

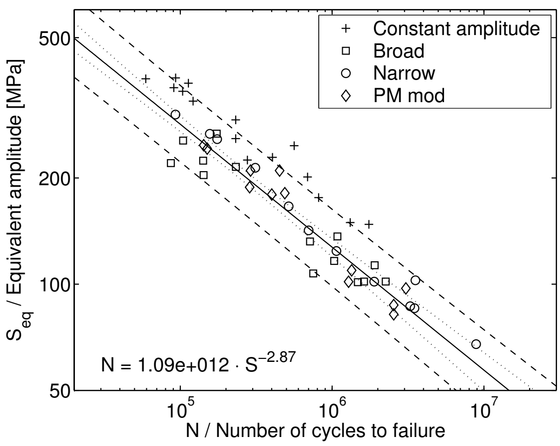

Fig. 1 S-N curve estimated from variable amplitude tests using broad-banded, narrow-banded and Pierson-Moskowitz spectra compared with constant amplitude tests *(Agerskov, 2000)*.

2.2 Fatigue in variable environment

Measurements show that the Gaussian processes are often good models for variability of the wave induced stresses to ship structure details under stationary sea conditions, from about 30 minutes to several hours. However the sea-states vary along the route and hence the stress is in fact a non-stationary Gaussian process. Since the fatigue tests leading to S-N curve Eq. (5) were performed under stationary conditions and hence it is not obvious that one can again use the S-N based criterion Eq. (6) to estimate the risk of fatigue failure. In fact some additional assumptions are needed to extend applicability of the criterion from stationary to non-stationary loading. For example one needs to neglect the possible sequential effects and then use the S-N curve obtained for stationary Gaussian loads.

More precisely, suppose that during period *T, M* voyages were undertaken. Further, assume that the damage accumulated in harbors during loading and unloading operations can be neglected. If the stresses are known during the voyages then the pseudo rainflow damage D_j^{rfc}, during *j*th voyage and defined by Eq. (2), can be evaluated and the total pseudo damage defined by

$$D^{rfc}(T) = \sum_{j=1}^{M} D_j^{rfc} \ . \tag{7}$$

Now the Palmgren-Miner hypothesis is equivalent to the criterion that the stress history is safe for fatigue if

$$\alpha - \log(D^{rfc}(T)) + e + \tilde{e} > 0 \,, \tag{8}$$

where α and e are taken from variable amplitude fatigue tests. Further, the additional error term $\tilde{e}$ represents the uncertainties caused by possible modeling errors, e.g. using Palmgren-Miner rule, neglecting sequential effects between voyages, using stress concentration factor and other simplifications. (The mean of $\tilde{e}$ is often assumed to be zero while the variance of $\tilde{e}$ needs to be determined by means of experience.)

The total accumulated pseudo damage $D^{rfc}(T)$, defined in Eq. (7), is a function of the magnitudes of stresses experienced by structure details during the period *T*. However, most often the stresses are unknown. In such situation one can model the uncertain value of the damage $D^{rfc}(T)$ by a distribution of the possible values it can take, in other words $D^{rfc}(T)$ is a random variable. And then one is interested in the failure probability $P_f = P(a - \log(D^{rfc}(T)) + e + \tilde{e} \le 0)$.

Here, using the Bayesian ideas α, $D^{rfc}(T)$, e and $\tilde{e}$ are random variables. If

$G = \alpha - \log(D_{rfc}(T)) + e + \tilde{e}$,

is normally distributed then the probability of cracking occurrences for the structural detail $P_f=1-\Phi(I_C)$, where Φ is the cumulative distribution function (cdf) of a standard normal variable, while I_C is the so called Corell's safety index defined as follows

$$I_C = \frac{E[G]}{\sqrt{Var(G)}} = \frac{E[a - \log(D_{rfc}(T)) + e + \tilde{e}]}{\sqrt{Var(a - \log(D_{rfc}(T)) + e + \tilde{e})}} . \tag{9}$$

Most often G is not normally distributed and hence $P_f \neq 1 - \Phi(I_C)$ but the index is still a useful measure for the risk of cracking for the structure detail.

In the case when the distributions of α, $D^{rfc}(T)$, e and $\tilde{e}$ are not well known one is further simplifying the safety index (assuming independence and employing Gauss formulas) by

$$I_C = \frac{E[a] - \log(E[D^{rfc}(T)])}{\sqrt{Var(a) + Var(\log(D^{rfc}(T))) + Var(e) + Var(\tilde{e})}} . \tag{10}$$

In the following examples we shall use $k = 3$ and $E[\alpha] = 12.76$ as mentioned before. The value of variance of a (and the two other variances as well) is not available and we shall use typical values taken from literature. The variability of a, and e were studied in *Johannesson et al. (2005a)*, typical values are $Var(a) = 0.005$, $Var(e) = 0.14$ while $Var(\tilde{e}) = 0.1$. Further, $Var(log(D^{rfc}(T)))$ can be approximated by $CoV(D^{rfc}(T))^2 = \frac{Var(D^{rfc}(T))}{E[D^{rfc}(T)]^2}$, coefficient of variation of pseudo damage. Then the safety index is approximated as

$$I_C \approx \frac{E[a] - \log(E[D^{rfc}(T)])}{\sqrt{Var(a) + CoV(D^{rfc}(T))^2 + Var(e) + Var(\tilde{e})}} . \tag{11}$$

Hence only the orders of $E[D^{rfc}(T)]$ and $CoV(D^{rfc}(T))^2$, have to be estimated. In what follows two simplifying assumptions, both realistic, are employed to estimate the order of $CoV(D^{rfc}(T))^2$: firstly, if routes i, j and their starting dates are known then D_i^{rfc}, D_j^{rfc} are independent; and secondly, the errors of time series of stress measurement can be neglected. Suppose that one wishes to compute variation coefficient after M voyages for which routes are known then

$$CoV(D^{rfc}(T))^2 = CoV(\sum_{j=1}^{M} D_j^{rfc})^2 = \frac{\sum_{j=1}^{M} Var(D_j^{rfc})}{(\sum_{j=1}^{M} E[D_j^{rfc}])^2} . \tag{12}$$

We shall use Eq. (12) in the following situations. Suppose that a ship will operate in similar conditions for T years, and that we found a way to estimate the variation coefficient for T_0 period, such as 0.5 or 1 year, then

$$CoV(Drfc(T))^2 = \frac{T_0}{T} CoV(D^{rfc}(T_0))^2 . \tag{13}$$

There is a vast literature proposing different means for estimating of $E[D^{rfc}(T)]$ and one is often assuming that the uncertainty in the damage, i.e. $CoV(D^{rfc}(T))^2$, is negligible relatively to other uncertainties. Formula (13) could be used to motivate this practice. However sometimes the shipping for an old vessel can be drastically changed and then the $CoV(D^{rfc}(T))^2$ for short time period T is not negligible and should be included in evaluation of the safety index.

Two principally different approaches to estimate $E[D^{rfc}(T)]$ and $Var(D^{rfc}(T))$ will be presented in the following sections. The first one is the statistical (nonparametric) approach when the information from historical data (measured stresses) will be used and the second, parametric one, is when a model for the stress variability will be employed to compute $E[D^{rfc}(T)]$ and $Var(D^{rfc}(T))$. (Obviously one needs data to estimate the parameters in the model.)

3 Safety index, extrapolation of measurement to longer periods

Often in practice when long time series of stresses have been measured one may assume that the future damage increase is stationary, i.e. varies in the same way as during the measured period, e.g. when a vessel is operated in the similar routes. In what follows we shall denote the observed rainflow pseudo damages during jth voyage by d_j^{rfc}. We assume that measurement errors are negligible and denote as $d^{rfc} = \sum d_j^{rfc}$ the rainflow pseudo damage computed from the measured stresses during a period T_0, e.g. a year. If one is planning to use a vessel for T-years on similar transports (routes, cargo) as during the measured period T_0 $(T \geq T_0)$ then, as will be shown in Appendix B, the safety index can be evaluated according to the following formula

$$I_C \approx \frac{E[a] - \log(T/T_0) - \log(d^{rfc})}{\sqrt{Var(a) + K\dfrac{Var(D^{rfc}(T_0))}{(d^{rfc})^2} + Var(e) + Var(\tilde{e})}}, \quad K = \frac{T - T_0}{T}. \tag{14}$$

(Obviously K grows from zero to one as extrapolation period increases.) In order to evaluate I_C one still needs to estimate $Var(D^{rfc}(T_0))$. Since damages accumulated during individual voyages are independent the variance can be estimated by means of standard statistical method if there are voyages that have the same expectation. For example voyages on similar routes undertaken at the same month should have the same mean and can be used to estimate both mean and variance, see the following example.

(a) Measured locations at the 2800 TEU vessel

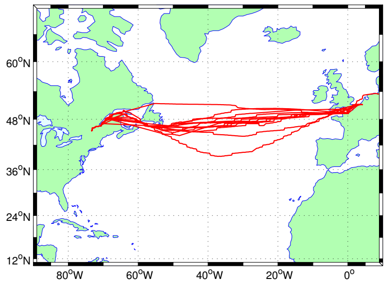

(b) Measured courses in the North Atlantic

Fig. 2 The locations and detailed routes of 15 measured voyages for the 2800TEU container ship operating in the North Atlantic during the first half of year 2008.

Example 1: One container vessel is now operating in the North Atlantic between EU and Canada. The time series of stress were measured at 2 critical locations at this vessel, shown in Fig. 2(a), during the first half of year 2008 (detailed description about the measurement see Storhaug et al. (2007)). There are 15 voyages measured during this period, and the detailed courses are shown in Fig. 2(b). The rainflow estimated pseudo damages during different voyages are provided in Fig. 3, where (a) presents the observed pseudo damage d_j^{rfc} of the structure detail in the midship, while (b) shows d_j^{rfc} of the other structure detail in the aftership. In Fig. 3 the stars represent the pseudo damages d_j^{rfc} measured on voyages from Canada to EU while dots are pseudo damages d_j^{rfc} when sailing from EU to Canada. For the structure detail in the midship, the accumulated damage $d_{mid}^{rfc} = 23.3\times 10^{10}$, for the one in the aftership, the corresponding damage $d_{aft}^{rfc} = 2.44\times 10^{10}$. In both cases the measuring period T_0 = *0.5* year. The variances of $Var(D_{mid}^{rfc}(T_0))$ and $Var(D_{aft}^{rfc}(T_0))$ will be estimated next.

The data consists of 15 passages over North Atlantic and the measured d_j^{rfc} are presented in Fig. 3. Inspired by the figure, we split the voyages into two groups: three most damaging winter passages from EU to Canada and the remaining 12 less damaging passages. For structure detail in the midship, variance of a winter passage from EU to Canada is estimated to be 1.08×10^{20}, while the less damaging type passage has variance 2.82×10^{19}. Consequently the variance $Var(D_{mid}^{rfc}(T_0)) \approx 6.62\times 10^{20}$, and hence $Var(D_{mid}^{rfc}(T_0))/(d_{mid}^{rfc})^2 \approx 0.012$. Meanwhile for the aftership detail, taking the same approach, variance of a winter passage from EU to Canada is estimated to be 3.78×10^{18} while the less damaging type passage has variance 2.85×10^{17}, thus $Var(D_{aft}^{rfc}(T_0)) \approx 1.48\times 10^{19}$ and $Var(D_{aft}^{rfc}(T_0))/(d_{aft}^{rfc})^2 \approx 0.025$.

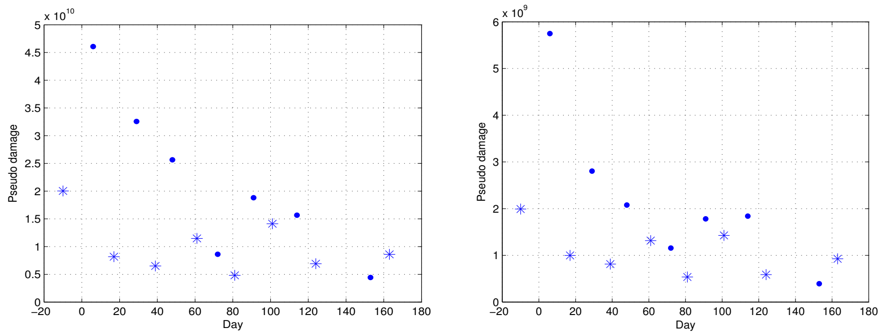

(a) d_j^{rfc} of midship position (b) d_j^{rfc} of aftership position

Fig. 3 The observed pseudo damages d_j^{rfc} for a container ship: stars are the passages from Canada to EU while dots are passages from EU to Canada. The x axis gives the day of the year when trips are finished.

Now for any $T \geq 0.5$ the safety indexes of structure details in midship and aftership are respectively computed as follows:

$$I_{C\_mid} \approx \frac{12.76 - \log(d_{mid}^{rfc}) - \log(T/T_0)}{\sqrt{0.005 + 0.012K + 0.14 + 0.1}},$$

$$I_{C\_aft} \approx \frac{12.76 - \log(d_{aft}^{rfc}) - \log(T/T_0)}{\sqrt{0.005 + 0.025K + 0.14 + 0.1}},$$

where $K = (T - T_0)/T$.

In the following Table 1, we will give the safety indexes for different periods T.

Table 1 Column 1 - time period T; Column 2 - safety index for midship position; Column 3 - nominal probability of fatigue failure (crack) for structure detail in the midship; Column 4 - safety index for aftership position; Column 5 - nominal probability of fatigue failure for aftership structure detail.

T	I_{C_mid}	$1-\Phi(I_C)$	I_{C_aft}	$1-\Phi(I_C)$
0.5	2.81	0.002	4.79	$8 \cdot 10^{-7}$
1	2.18	0.015	4.08	0.00002
2	1.57	0.06	3.45	0.0002
3	1.22	0.11	3.09	0.001
5	0.78	0.22	2.65	0.004

Base on this simplified analysis, we conclude that the risk of fatigue cracking for the structure detail in midship is not negligible even for the time period of 1 year; and that the safety of aftership detail is also low for the time period exceeding 5 years, in the sense of possibility of crack development. However it has to be noted that the consequence of existence of a crack may not affect the hull integrity. (Cracks are often accepted after 20 years of age.)

4 Safety index, parametric approach

In the previous section we derived the safety index by means of the extrapolation of the measured damage during a period of time T_0. Here we will consider the case when one cannot use the extrapolation approach because either measured stresses are not representative for the future loads or there are no measurements of stresses at all. In such situation one needs to estimate $E[D^{rfc}(T)]$ and $CoV(D^{rfc}(T))^2$ by proposing a model for the distribution of $D^{rfc}(T)$. The following properties of the wave induced stresses are basis of our model:

(a) The waves are built up from rather long period, about 30 minutes, when the loading conditions can be assumed to be stationary.

(b) The mean stress remains almost constant over long time period, i.e. for a voyage between two harbors.

(c) Wave load has short memory, i.e. load process becomes independent after couple of minutes.

Properties (a-b) allow us to approximate the damage accumulated during a voyage by the sum of damages caused by loads during the stationary periods, see *Bogsjö and Rychlik (2007)*, *Bengtsson et al. (2008)* for more detailed discussion. In *Mao et al. (2008)* it is shown that the error of such an approximation was less than 1% for stresses measured during 15 voyages over North Atlantic.

Although cycles vary in unpredictable manner during the stationary periods the variability of the pseudo damage $D^{rfc}(T)$ is still negligible, because of (c), in comparison with other sources of uncertainties, see *Bengtsson and Rychlik (2008)*. Consequently, as it is often done in practice, one can approximate the damage increments during stationary periods by their expected values. The expectations can then be bounded by means of the narrow-band approximation, reviewed next.

4.1 Narrow-band bound

Let $Y(t)$ be a Gaussian stress, and $h_s = 4\sqrt{Var(Y(0))}$ be the significant stress range while $f_z = \frac{1}{2\pi}\sqrt{\frac{Var(\dot{Y}(0))}{Var(Y(0))}}$, the apparent frequency (the intensity of mean stress level up-crossings by Y), then the expected pseudo rainflow damage in the period t is bounded by

$$E\left[D^{rfc}(t)\right] \leq 0.5 t f_z h_s^k \ , \tag{15}$$

for $2 \leq k \leq 4$, see *Rychlik (1993)* for the proof. (This is the so called narrow-band approximation introduced by *Bendat (1964).*) Furthermore, as it was reported in *Bengtsson and Rychlik (2008)*, the coefficient of variation of $D^{rfc}(t)$ converges fast to zero as t increases and, for typical wave spectra, one can assume that even $D^{rfc}(t) \leq 0.5 t f_z h_s^k$. During a voyage if the stress properties change slowly (conditions (a-c) are valid) then, approximately, the accumulated pseudo damage:

$$D_j^{rfc} \leq 0.5 \Delta t \sum f_z(i) h_s^k(i) = D_j^{nb} \ . \tag{16}$$

Here D_j^{rfc} is the increase of the rainflow pseudo damage during jth voyage, Δt is the common length of stationary period, usually 1800 seconds, $h_s(i)$ and $f_z(i)$ are the significant stress range and apparent frequency estimated from ith stationary period in the jth voyage. In the previous work Mao et al. (2008) it was demonstrated that $(d_j^{nb} - d_j^{rfc}) / d_j^{rfc}$ was less than 0.3. As before we denote by d_j^{nb}, d_j^{rfc} the measured damages estimated by narrow-band approximation and rainflow analysis, respectively. (In addition Eq. (16) is used in many dedicated software to estimate the damage accumulation during a sea state.) What remains is to find a model for variability of significant stress range h_s and apparent frequencies f_z, which is done in the following subsections.

4.1.1 Model for f_z

Suppose that the sea contains only one cosine wave with period T. For a vessel sailing with heading angle β and speed v, then the encountered frequency is

$$f^e = \left| \frac{1}{T} + \frac{2\pi v \cos(\beta)}{g T^2} \right| = f_z \ , \tag{17}$$

by assumed linear relation between stresses and encountered waves. Since the sea is composed of many waves having different periods and since the heading angle, to these waves, may also vary hence we propose to replace T and β in Eq. (17) by the peak period T_p and the average heading angle $\overline{\beta}$, respectively, giving the following approximation of f_z

$$f_z = \left| \frac{1}{T_p} + \frac{2\pi v_s \cos(\overline{\beta})}{g {T_p}^2} \right| . \tag{18}$$

Here it is assumed that main wave period does not deviate much from main response spectrum, but this can happen for "narrow" band transfer function $S_R(\omega) = |H(\omega)|^2 S(\omega)$, where $S(\omega)$ is the encountered wave spectrum.

Both the average heading angle and the peak period have to be estimated onboard of the vessel. Finally we also propose to estimate as follows $T_p = 4.9\sqrt{H_s}$, approximately valid for fully developed sea, see *DNV (2005)* now replaced by new recommendation in *DNV (2007)*, giving

$$f_z = \left| \frac{1}{4.9\sqrt{H_s}} + \frac{2\pi v_s \cos(\overline{\beta})}{24 g H_s} \right|. \tag{19}$$

Example 1 cntd.: For a container ship the directional spectrum $S_i(\omega,\alpha)$ were measured by means of a radar and hence one can estimate the average heading angle $\overline{\beta}_i$, during stationary periods, by means of

$$\overline{\beta}_i = \frac{\int_0^{180}\int_0^{\infty} \alpha S_i(\omega,\alpha) d\omega d\alpha}{\int_0^{180}\int_0^{\infty} S_i(\omega,\alpha) d\omega d\alpha}. \tag{20}$$

(Note that we defined directional spectrum only for angles *[0, 180]*, instead for more commonly used *[0, 360]*.)

4.1.2 Model for h_s

Suppose that we use a linear wave model then sea state, under stationary condition, is defined by a directional spectrum $S(\omega,\alpha)$. A typical model for $S(\omega,\alpha)$, is obtained by combining Piearson - Moskowitz spectrum $S(\omega)$ and $cos^2\alpha$ spreading function. Such a directional spectrum is characterized by significant wave height H_s and T_z only. The linear transfer function, estimated by means of dedicated software, give a relation

$$h_s = C(T_z, \beta, v) H_s ,$$

where as before, β is the heading angle, while v is the ship speed. Next, for fixed v, the constant $C(\beta)$ is defined as the average $C(\beta) = E[C(T_z, \beta)]$ where T_z has a long term distribution that ship would encountered in the particular route. Here a simplification is done by choosing the T_z-distribution used by DNV for the North Atlantic scatter diagram which does not reflect the seasonal variability, detailed discussion see *DNV (2007)*.

For the particular details, respectively located in the midship and aftership of investigated container vessel, the constant $C(\beta)$ is computed using the linear strip software Waveship (see *Waveship User's Manual (1993)*) and given in the Table 2, where $C_{mid}(\beta)$ is for midship detail and $C_{aft}(\beta)$ is for aftership detail. (We have assumed that the ship is sailing with the constant service speed 10 [m/s]).

Combining the proposed model the following approximation, say the new narrow band approximation, for the increase of the pseudo damage during the *j*th voyage is proposed

$$D_j^{nb} \approx \Delta t \sum_i C(\overline{\beta}_i)^3 \left| \frac{1}{9.8} H_s(i)^{2.5} + \frac{\pi v_s \cos(\overline{\beta}_i)}{24g} H_s(i)^2 \right|, \quad D^{nb}(T) = \sum_{j=1}^{M} D_j^{nb}, \tag{21}$$

where Δt is the common length of the stationary period taken to be 1800 seconds here. Obviously the values of significant wave height encountered during a voyage, as well as heading angles are not known in advance and hence D_j^{nb} is a random variable. For a specific voyage, i.e. when starting date, ship speed and the route is defined, then one could bound D^{nb} by taking heading angle $\beta = 0$. Then what remains is to model the variability of encountered significant wave height H_s along the route. Using model for H_s variability, presented in Appendix C, one can simulate the sequence of $H_s(i)$ and then compute values of D_j^{nb}. Repeating independently the simulations one can obtain the distribution D^{nb} by a standard statistical method.

Table 2 The constant $C(\beta)$ computed using linear strip software Waveship and to be used in Eq. (21) to approximate the increment of pseudo damage during a voyage.

β	0	10	20	30	40	50	60	70	80
$C_{mid}(\beta)$	25.66	25.77	25.58	25.10	24.37	23.47	22.47	21.48	20.65
$C_{aft}(\beta)$	12.73	12.76	12.62	12.35	11.96	11.46	10.99	10.51	10.13
β	90	100	110	120	130	140	150	160	170
$C_{mid}(\beta)$	20.10	19.92	20.16	20.77	21.65	22.66	23.67	24.56	25.24
$C_{aft}(\beta)$	9.89	9.84	9.99	10.32	10.78	11.29	11.79	12.23	12.55

4.2 Estimation of safety index Ic

Let T be the computed period, usually measured in years, the safety index $I_C(T)$, given by (11), can be now estimated by replacing $D^{rfc}(T)$ by $D^{nb}(T)$. (Note that this is a conservative approximation and hence we do not add any additional uncertainty into denominator of the index). Now the safety index based on the proposed model becomes

$$I_C \approx \frac{E[a] - \log(E[D^{nb}(T)])}{\sqrt{Var(a) + CoV(D^{nb}(T))^2 + Var(e) + Var(\tilde{e})}}. \tag{22}$$

Hence only the orders of $E[D^{nb}(T)]$ and $CoV(D^{nb}(T))^2$, have to be estimated. Consequently by Eq. (21) one needs to have a model for variability of encountered significant wave height H_s and heading angle β.

Finally in order to easy comparison between non-parametric and parametric approaches to estimate the index we will now give a parametric version of formula (14). Suppose that there is a period T_0, for example one year, and that the similar shipping is planned for the whole period of T years then

$$I_C \approx \frac{E[a] - \log(T/T_0) - \log(E[D^{nb}(T_0)])}{\sqrt{Var(a) + KCoV(D^{nb}(T_0)) + Var(e) + Var(\tilde{e})}}, \quad K = \frac{T_0}{T}. \tag{23}$$

5 Validation of the proposed approach

We say that operation schedule of a vessel is specified if: a number of voyages are given together with planned time of the year when voyage starts; positions in latitude, longitude and ship velocity for the routes are chosen. In such situation uncertainties in values of accumulated damages are results of "lack of knowledge" of the significant wave heights and heading angles which will be encountered during the planned voyages. The heading angles can be taken to zero giving the conservative estimates of damages and what remains is finding a statistical model for H_s variability. Such a model has been proposed in *Baxevani et al. (2005)* and *Baxevani et al. (2009)*. The parameters of the model, estimated from the satellite measurements of Hs, are presented in *Baxevani et al. (2008)* and hence one can find the distribution of D_j^{nb} for almost any route.

Since in this section we are primarily interested in checking the accuracy of the proposed approach by validating it against the measured data the distribution of D_j^{nb} will be found only for the 15 routes for which measured values of d_j^{rfc} are available. In order to increase precision we also assume that heading angle β_i on that 15 routes are known, i.e. the same as measured (each half hour) on that voyages (the speed is kept constant 9 [m/s] for the whole voyage). Two types of checks will be performed. The first one is to compute probability that, for a voyage indexed by $j = 1, ..., 15$, D_j^{nb} is smaller than the observed damage d_j^{rfc}. Values below 0.01 and above 0.99 would indicate a significant difference between the observed damages and the variability of D_j^{nb}. The results are presented in Table 3, third and seventh columns respectively for locations in midship and aftership. (In second and sixth columns of this table we have $d_j^{rfc} \times 10^{-10}$.) Results presented in the table show that observed variability of rainflow damages is well modeled by D_j^{nb} in Eq. (21).

Table 3 Column 1 - day the voyage ends; Columns 2 to 5 list the results of structure detail located in the midship: Column 2 - the observed pseudo damage $10^{-10} \cdot d_j^{rfc}$ computed using the measured stresses (stress concentration factor 2), Column 3 - a

Monte Carlo estimation of the probability $P(D_j^{nb} \le d_j^{rfc})$, Column 4,5 - the expected accumulated damage $10^{-10} \cdot E[D_j^{nb}]$ and the standard deviation $10^{-10} \cdot \sqrt{D_j^{nb}}$, where D_j^{nb} defined as in (21), and the model for Hs variability estimated using satellite measurements of significant wave height presented in Appendix C. Columns 6 to 9 are the results for aftership structure detail with the same meaning as column 2 to 5.

Voyage Date	MidSect				AftSect			
2007-12-20	2.00	(0.40)	2.53	2.03	0.20	(0.34)	0.30	0.24
2008-01-06	4.61	(0.44)	4.85	1.76	0.57	(0.48)	0.59	0.21
2008-01-17	0.82	(0.27)	1.86	1.73	0.10	(0.28)	0.22	0.21
2008-01-29	3.26	(0.28)	4.46	2.06	0.28	(0.14)	0.54	0.24
2008-02-09	0.65	(0.30)	1.42	1.42	0.08	(0.30)	0.17	0.17
2008-02-18	2.56	(0.22)	3.83	1.64	0.21	(0.10)	0.46	0.20
2008-03-01	1.15	(0.76)	0.63	0.72	0.13	(0.75)	0.07	0.08
2008-03-12	0.86	(0.12)	2.04	1.02	0.12	(0.15)	0.25	0.13
2008-03-21	0.48	(0.23)	1.40	1.24	0.05	(0.23)	0.17	0.15
2008-04-01	1.88	(0.58)	1.74	0.75	0.18	(0.36)	0.21	0.09
2008-04-11	1.41	(0.50)	1.42	1.05	0.14	(0.41)	0.17	0.12
2008-04-24	1.57	(0.72)	1.24	0.56	0.18	(0.70)	0.15	0.07
2008-05-04	0.69	(0.53)	0.66	0.42	0.06	(0.34)	0.08	0.05
2008-06-03	0.44	(0.44)	0.47	0.20	0.04	(0.23)	0.06	0.03
2008-06-13	0.86	(1.00)	0.24	0.20	0.09	(1.00)	0.03	0.02

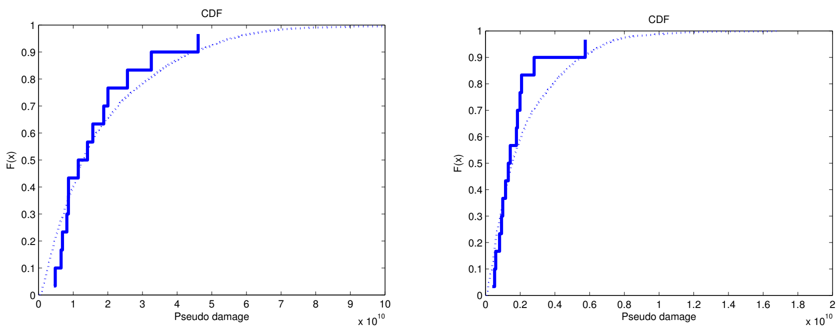

(a) Result of location at Midship

(b) Result of location at Aftership

Fig. 4 Comparison between empirical cumulative distributions of the observed rainflow pseudo damages $d_{rfc\,j}$ for the 15 voyages and the cumulative distribution of D_j^{nb} (dotted line) defined by means of (21), for structure details respectively in the midship and aftership. (The distributions describe variability of pseudo damages on a route taken at random from the 15 passages.)

The second comparison is presented in Fig. 4, where (a) is for midship location and (b) is for the aftership location. The solid line is the cumulative distribution function (cdf) of the observed values of d_j^{rfc}. Such cdf describes variability of rainflow damages that are selected at random from the second column (for midship) or seventh column (for aftership) in Table 3. The dotted cdf describes variability of the corresponding random experiment for the damages D_j^{nb}, i.e. drawing at random one of the 15 routes and simulating the value of D_j^{nb}. Two distributions agree surprisingly well for both of the structure details in the midship and aftership. Hence we conclude that D_j^{nb} seems to be a very good approximation for drfc j and one can compute the safety index I_C for the 15 voyages by replacing $D^{rfc}(T)$ with $D^{nb}(T) = \sum_{j=1}^{15} D_j^{nb}$.

In order to compute safety index I_C, for extension in sailing for additional $T = 0.5$ year, one needs $E[D_j^{nb}]$ and $Var(D_j^{nb})$. Those are given in columns 4, 5 (for midship detail) and column 8, 9 (for aftership detail) in Table 3, respectively. (The details of the computations of $E[D_j^{nb}]$, $Var(D_j^{nb})$ are given in Appendix C). Finally the safety indexes of locations in midship and aftership are respectively given by

$$I_{C\_mid} = \frac{12.76 - \log(2.88) - \log(T/T_0) - 11}{\sqrt{0.005 + 0.0295 \cdot (T/T_0) + 0.14 + 0.1}} ,$$

$$I_{C\_aft} = \frac{12.76 - \log(3.46) - \log(T/T_0) - 10}{\sqrt{0.005 + 0.0291 \cdot (T/T_0) + 0.14 + 0.1}} .$$

In the following Table 4, we will give the safety indexes for different periods T.

Table 4 Column 1 - time period *T*; Column 2 - safety index for midship location; Column 3 - nominal probability of failure for midship location; Column 4 - safety index for aftership location; Column 5 - nominal probability of failure for aftership location.

T	I_{C_mid}	$1-\Phi(I_C)$	I_{C_aft}	$1-\Phi(I_C)$
0.5	2.48	0.006	4.24	$2\cdot10^{-5}$
1	1.96	0.025	3.77	0.00008
2	1.39	0.08	3.22	0.0007
3	1.05	0.15	2.89	0.002
5	0.60	0.27	2.45	0.007

Comparing the results presented in Table 1, we conclude that derived indexes obtained by the methods are equivalent. However applying both methods we neglected some uncertainties, statistical errors when estimating $Var(D^{rfc}(T_0))$ (this error can be large due to crudeness of our estimation method) while for the parametric method we neglected the possibility of modeling errors.

6 Conclusions

In this paper nonparametric (extrapolation of measured damages) and parametric (based on a model for significant wave height variable along a route) were presented and validated. The application of the nonparametric approach is limited to the case of stationary shipping.

The second approach, defined in (21), seems to provide with a very accurate approximation of the damage accumulation process. It has a clear advantage that no measurements of stresses or significant wave height are explicitly needed and could be applied to any route and ship. However the deficiency of this approach is possibility of "modeling errors", i.e. that the linear transfer function is too simple model to describe relation between waves and stresses. Further the transfer function itself may be not estimated accurately enough. There could be similar uncertainty in the modeled wave environment (e.g. by assuming Pierson-Moskowitz spectrum and $cos^2\alpha$ spreading function). Consequently measurements of stresses could still be needed to validate the results of numerical computations.

The safety index indicate that the current ship has relatively good fatigue strength, but that fatigue cracks may be anticipated before ending of the ships life. The method does not yet reflect the possibility to reduce the fatigue damage risk and corresponding safety index, but this is subject of future work.

Acknowledgements

Prof. Jonas Ringsberg had provided valuable discussions. The research is supported in part by EU project SEAMOCS and the Gothenburg Stochastic Center and the Swedish foundation for Strategic Research through GMMC, Gothenburg Mathematical Modeling Center. We are also grateful for DNV, crew, management company and owner for providing measurement data.

References

Agerskov, H. 2000, Fatigue in steel structures under random loading, *Journal of Constructional Steel Research*, **53,** 283–305.

Baxevani, A., Rychlik, I., and Wilsson, R. 2005, A new method for modelling the space variability of significant wave height, *Extremes*, **8,** 267–294.

Baxevani, A., and Rychlik, I. 2007, Fatigue Life Prediction for a Vessel Sailing the North Atlantic Route, Probabilistic Engineering Mechanics, **22,** 159–169.

Baxevani, A., Borget, C., and Rychlik, I. 2008, Spatial Models for the Variability of the Significant Wave Height on the World Oceans, International Journal of Offshore and Polar Engineering (ISSN 1053-5381) Vol. 18, No. 1, 1–7.

Baxevani, A., Caires, S., and Rychlik, I. 2009, Spatio-temporal statistical modelling of significant wave heigth, Environmetrics 2009; 20: 14–31.

DNV 2005, Fatigue Assessment of Ship Structures, Classification Note 30.7, July.

DNV 2007, Environmental conditions and environmental loads, Recommended Practice, April.

DNV 1993, Sesam user's manual waveship, DNV Sesam Report No.:93-7080/Rev.1, 15 Oct.

Bendat., J.S. 1964, Probability functions for random responses: Predictions of peaks, fatigue damage and catastrophic failures, Technical report, NASA.

Bengtsson, A., and Rychlik, I. 2008, Uncertainty in fatigue life prediction of structures subject to Gaussian loads, *Probabilistic Engineering Mechanics*.

Bengtsson, A., Bogsjö, K., and Rychlik, I. 2008, Uncertainty of estimated rainflow damage for random loads, *Marine Structures*.

Bogsjö, K., and Rychlik, I. 2007, Vehicle fatigue damage caused by road irregularities, Fatigue and Fracture of Engineering Materials and Structures, to appear. LUTFMS-5067.

Johannesson, P., Svensson, T. and Maré, J. de. 2005a, Fatigue life prediction based on variable amplitude tests - methodology, *International Journal of Fatigue*, **27,** 954–965.

Johannesson, P., Svensson, T. and Maré. J. de. 2005b, Fatigue life prediction based on variable amplitude tests - specific applications, *International Journal of Fatigue*, **27,** 966–973.

Mao, W., Ringsberg, J.W., Rychlik, I. and Storhaug, G. 2008, Comparison between a fatigue model for voyage planning and measurements of a container vessel, to be presented at OMAE 2009, 1–13.

Matsuishi, M. and Endo, T. 1968, Fatigue of metals subject to varying stress. *Paper presented to Japan Society of Mechanical Engineers, Fukuoka, Japan*.

Miner, M.A. 1945, Cumulative damage in fatigue, *Journal of Applied Mechanics*, **12,** A159–A164.

Palmgren, A. 1924, Die lebensdauer von kugellagern, *Zeitschrift des Vereins Deutscher Ingenieure*, **68,** 339–341.

Rychlik, I. 1987, A new definition of the rainflow cycle counting method, *Int. J. Fatigue*, **9, 10,** 119–121.

Rychlik, I. 1993b, On the "narrow-band" approximation for expected fatigue damage, *Probabilistic Engineering Mechanics*, **8,** 1–4.

Storhaug, G., Moe, E., and Piedras Lopes, T.A. 2007, Whipping Measurements Onboard a Midsize Container Vessel Operating in the North Atlantic, RINA, 28-29th of November, Shanghai, China, 55-70.

Storhaug, G. and Heggelund, S.E. 2008, Measurements of wave induced vibrations and fatigue loading onboard two container vessels operating in harsh wave environment, Proc. Intern. Conference, Design and Operation of container ships, 3-4th of July, London, UK, 81-100.

Appendix A: Rainflow definition

In the rainflow cycle count each local maximum of the load process is paired with one particular local minimum, determined as follows:

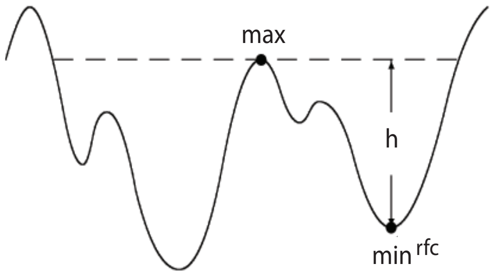

Fig. 5 A rainflow pair

· From the local maximum one determines the lowest values in forward and backward directions between the time point of the local maximum and the nearest points at which the load exceeds the value of the local maximum.

· The larger of those two values is the rainflow minimum paired with that specific local maximum, i.e. the rainflow minimum is the least drop before reaching the value of the local maximum again on either side.

· The cycle range, *h*, is the difference between the local maximum and the paired rainflow minimum.

Note that for some local maxima, the corresponding rainflow minimum could lie outside the measured load sequence. In such situations, the incomplete rainflow cycle constitutes the so called residual and has to be handled separately. In this approach, we assume that, in the residual, the maxima form cycles with the preceding minima.

Appendix B: Safety index estimation

In this appendix we shall motivate the approximation (14). Suppose that one has measured stresses during a period T_0, and let denote the accumulated pseudo damage by d^{rfc}. (We assume that measurements errors are negligible.) Obviously $d^{rfc} \neq E[D^{rfc}(T_0)]$ and let e_{T_0} be the error

$$e_{T_0} = E\left[D^{rfc}(T_{0)}\right] - d^{rfc}, \quad E\left[e_{T_0}\right] = 0, \quad Var(e_{T_0}) = Var(D^{rfc}(T_0)).$$

The safety index for *T* years of trade, given by (11), is equal to

$$I_C \approx \frac{E[a] - \log(E[D^{rfc}(T)])}{\sqrt{Var(a) + CoV(D^{rfc}(T))^2 + Var(e) + Var(\tilde{e})}} \;.$$

If one is planning similar trade (routes, cargo) for T years as during the measured period T_0 then I_C can be computed as follows. From stationarity of damage accumulation process and independence of D_i, D_j it follows that

$$E[D^{rfc}(T)] = \frac{T}{T_0} d^{rfc} + \frac{T - T_0}{T_0} e_{T_0} \,, \qquad Var(D^{rfc}(T)) = \frac{T - T_0}{T_0} Var(D^{rfc}(T_0)) \,.$$

Next, using $log(a + x) \approx log(a) + x/a$,

$$\log(E[D^{rfc}(T)]) \approx \log(d^{rfc}) + \log(T/T_0) + \frac{T - T_0}{T} \frac{e_{T_0}}{d^{rfc}}$$

Since $E[e_{T_0}/d^{rfc}] = 0$ we further approximate the index as follows

$$T_C \approx \frac{E[a] - \log(d^{rfc}) - \log(T/T_0)}{\sqrt{Var(a) + CoV(D^{rfc}(T))^2 + Var(e) + Var(\tilde{e}) + Var(X)}} \;.$$

Where $X = \frac{T - T_0}{T^2} \frac{e_{T_0}}{d^{rfc}}$. Since $E[D^{rfc}(T_0)] \approx d^{rfc}$, we obtain

$$CoV(D^{rfc}(T))^2 = \frac{(T - T_0)T_0}{T^2} \frac{Var(D^{rfc}(T_0))}{(d^{rfc})^2}$$

and hence

$$CoV(D^{rfc}(T))^2 + Var(X) = \frac{(T - T_0)}{T^2} \frac{Var(D^{rfc}(T_0))}{(d^{rfc})^2}$$

giving Eq. (14).

Appendix C: Spatio-temporal wave model

As reported in *Baxevani et al. (2005)* the significant wave height at position $\boldsymbol{p}$ and time t is accurately model by means of lognormal cdf. Let $X(\boldsymbol{p}, t) = ln(H_s(\boldsymbol{p}, t))$ denote a field of logarithms of significant wave height that evolves in time. Suppose t_0 be the starting date of a voyage, $\boldsymbol{p}(t) = (x(t), y(t))$, $[t_0, t_1]$, the planned route, while $v(t) = (v_x(t), v_y(t))$ a velocity a ship will move with. For a route let $z(t) = X(\boldsymbol{p}(t), t)$ be the encountered logarithms of the significant wave heights. (The encountered significant wave heights are $H_s(t) = exp(z(t))$.) The $z(t)$ is a non stationary Gaussian process and in this appendix we give a model for the covariance function $r_z(t_1, t_2) = C(z(t_1), z(t_2))$.

Locally stationary field: Suppose that for a fixed geographical region and season (e.g. January) X is a stationary Gaussian field with mean m, variance σ^2 and separable correlation structure. We also assume that the field is drifting (moving) with a constant velocity $V = (V_x, V_y)$, say. By this we mean that there are two autocorrelation functions ρ_S correlation between $logH_s$ at two positions at the same time and ρ_T the correlation of $logH_s$ at the same location but different time instances that defines the covariance between $logH_s$ at different locations and time instances, viz.

$$C(X(\mathrm{P}_1,t_1),X(\mathrm{P}_2,t_2)) = \sigma^2 \rho_S(x_2 - x_1 - V_x(t_2 - t_1), y_2 - y_1 - V_y(t_2 - t_1)) \cdot \rho_T(t_2 - t_1) .$$

(The correlation ρ_S could be estimated from a map of H_s derived by means of Hindcast data (ERA40) or satellite measurements while ρ_T comes from the buoy measurements.)

Now suppose that a vessel is sailing with constant velocity (v_x, v_y) and let $z(t)$ be encountered $log(H_s)$ at time t. If variability in time and space of $logH_s$ is modeled by the stationary Gaussian field X then z is also stationary Gaussian process with mean m and the covariance function

$$C(z(t_1), z(t_2)) = \sigma^2 \rho_S(v_1(t_2 - t_1), v_2(t_2 - t_1)) \cdot \rho_T(t_2 - t_1) = r_z(t_2 - t_1) , \tag{24}$$

where $v_1 = v_x - V_x$ and $v_2 = v_y - V_y$. In *Baxevani et al. (2009)* one used, in Eq. (24),

$$\rho_S(x, y) = \exp(-(x^2 + y^2)/2L^2) , \quad \rho_T(t) = \exp(-\lambda\,|\,t\,|) , \tag{25}$$

t in hours, where parameters L and λ are slowly varying over oceans and seasons.

Since z is a stationary process it has power spectral density (psd) $S(\omega)$, say. Here the psd depends on parameters σ^2, L, λ and the relative ship velocity $v = (v_1, v_2)$. (The parameters σ^2, L were estimated by means of satellite observation while λ is estimated using H_s measured by buoys, see *Baxevani et al. (2008)* where the variability of the parameters in season and geographical location over the globe is presented.)

We have assumed that the process z is stationary however in practice the assumption may be valid for short period of time because the statistical properties of sea changes with the geographical locations. Consequently, as has been observed in data, parameters m, σ^2, L, λ and velocity v varies between different geographical locations on the oceans. Hence the encountered $logH_s$ process, i.e. $z(t)$, cannot be stationary for the whole voyage. Since the properties of z changes slowly we shall model it by means of locally stationary processes defined next.

Let $S_t(\omega)$ be the spectrum of a stationary process z with covariance function defined by formulas (24-25) where the parameters $\sigma^2(t)$, $L(t)$, $\lambda(t)$ and $v(t)$ are functions of position of a ship $\boldsymbol{p}(t)$. If St is known for all $t \in [t_0, t_1]$ then a "locally stationary" process z can be defined, by means of spectral representation and moving averages construction, as follows

$$z(t) = \int \exp(-it\omega)\sqrt{S_t(\omega)}dB(\omega) \,, \qquad (26)$$

where $B(\omega)$ is a Brownian motion. This is somewhat technical construction which results in a non-stationary Gaussian model for z, with $E[z(t)] = m(t)$ and

$$C(z(t_1), z(t_2)) = \int \exp(-i(t_2 - t_1)\omega)\sqrt{S_{t_1}(\omega)S_{t_2}(\omega)}d\omega = r_z(t_1, t_2)\,. \qquad (27)$$

Since the Gaussian process z is uniquely defined by its mean $m(t)$ and covariance function $r_z(t_1, t_2)$ hence also $H_s(t) = exp(z(t))$ is uniquely defined when the encountered local spectra $S_t(\omega)$ and means $m(t)$ are known. Here it means that one have to estimate parameters defining spectra for geographical locations and time of the year of interest for shipping, see *Baxevani et al. (2008)*.

Having r_z and m then, by means of methods presented in Baxevani and Rychlik (2007), one can compute $E[D_j]$ and variance $Var(D_j)$ if the heading angles $\beta(t)$ and speed of the vessel are known. However in order to estimate the distribution of damage D_j a Monte Carlo approach is the most convenient. Simply one can generate sequences of $H_s(i)$ of possible values of significant wave heights along routes and then compute the damage D_j .

More precisely, let times t_i, $i = 0, \ldots, n$, with $t_{i+1} - t_i = \Delta t$ equal 30 minutes, be the times a vessel is passing positions $(x_i, y_i) = (x(t_i), y(t_i))$ and the values of significant wave height at the position $H_s(i) = exp(z_i)$, where $z_i = z(t_i)$ are correlated normal variables. It is a simple task to generate a sequence of z_i when the vector of means $\boldsymbol{m} = [m_i]$, $m_i = m(t_i)$, and the covariance matrix $\Sigma = [r_{ij}]$, where $r_{ij} = r_z(t_i, t_j)$ are known.

However in order to make computation fast one would like to have explicit formula for covariance r_z instead of the integral (27) that has to be evaluated numerically. In addition for the particular choice of the autocorrelations ρ_S and ρ_T, given in (25), even spectrum $S_t(\omega)$ has to be computed by means of numerical procedure. e.g. FFT transform, for all t values. In the following subsection we shall modify the autocorrelation function ρ_T in such a way that covariance r_z will be given by an explicit algebraic expression depending only on easily interpretable parameters.

Approximation of $r_z(t_1, t_2)$

In previous work we have used (24) with $\rho_T(t) = exp(-\lambda|t|)$ to define time correlation structure of the significant wave field at a fixed position. A typical value for parameter λ estimated from buoys is 0.0125, which means that correlation length τ_T , say, is about 40 hours. (Here we define correlation length as a time lag the correlation drops to 0.6.) In order to simplify computation we propose to approximate the covariance $\rho_T\,(t) = exp(-0.0125\ |t|)$, where t is defined in hours, by the Gaussian covariance with the same correlation length, viz.

$\rho\,(t) = exp(-0.5(t/\tau_T\,)^2), \quad \tau_T = 2/\lambda.$

Using (24), some simple algebra gives

$$r_z(t) = \sigma^2 \exp(-0.5t^2 / C^2)\ , \quad C = \frac{\tau_T \tau_S}{\sqrt{\tau_T^2 + \tau_S^2}}\ , \quad \tau_S = \sqrt{v_1^2 + v_2^2}\,/\,L\ . \tag{28}$$

Note that τ_S is the space related correlation length and has interpretation as the time it takes for a vessel to move between two positions $\boldsymbol{p}_1$ and $\boldsymbol{p}_2$ for which the log of significant wave heights spatial correlation drops to 0.6. Parameters τ_T and τ_S characterize the spatial and time sizes of storms, respectively. The covariance (28) is particularly convenient since the power spectrum S_t, used in (26), can be given in an explicit way

$$S_t(\omega) = \sigma^2 \frac{C}{\sqrt{2\pi}} \exp(-\omega^2 C^2 / 2)\ .$$

The spectrum depends on t because the values of parameters σ^2 and C are changing along the route $\boldsymbol{p}(t)$. Knowing $\sigma(t)$ and $C(t)$ the integral in (27) can be computed giving

$$r_z(t,s) = 2\sigma(t)\sigma(s)\frac{C(t)C(s)}{C(t)^2 + C(2)^2} e^{-(t-s)^2 /(C(s)^2 + C(t)^2)}\ .$$